Student Poster Session

2021 IEEE PES General Meeting

Virtual Conference
July 26-29, 2021

Poster Categories:

- Advanced Computational Methods for Power System Planning, Operation, and Control
- Asset Management
- Communication & Control in Energy Systems
- Cyber and Physical Security of the Smart Grid
- Dynamic Performance and Control of Power Systems
- Electric Machines and Drives
- Emerging Software Needs for the Restructured Grid
- Flexible AC Transmission Systems
- Integrating Renewable Energy into the Grid
- Intelligent Monitoring and Outage Management
- Market Interactions in Power Systems
- Power Electronics
- Power System Modeling and Simulation
- Smart Cities
- Smart Grid Technology
- Smart Sensors, Communication and Control in Energy Systems
- Substation and Distribution Automation
- System-Wide Events and Analysis Methods

IEEE PES Student Activities Subcommittee
Dr. Valentina Cecchi, Dr. Sridhar Chouhan, Dr. Anthony Deese, Dr. Paras Mandal, Dr. Luke Dosiek

Advanced Computational Methods for Power System Planning, Operation, and Control

No.	Poster Title	Student Name (Last, First)	UG/Grad
21STUGM001	Sizing Energy Storage System for Energy Arbitrage in Extreme Fast Charging Station	Rehman, Waqas Ur	GRAD
21STUGM002	A Distributionally Robust Optimization Approach to Unit Commitment in Microgrids	Yurdakul, Ogün	GRAD
21STUGM003	Novel Protection Method for Fully Inverter-Based Distribution System Connected Microgrid	Banu, Bilkis	GRAD
21STUGM004	Optimization-based Voltage and Frequency Dynamics Estimation and Control of Microgrids	Bhujel, Niranjan	GRAD
21STUGM005	Reinforcement Learning Based Optimal Battery Control Under Cycle-based Degradation Cost	Kwon, Kyung-bin	GRAD
21STUGM006	The Impact of Different Control Strategies on Residential Battery Degradation	Mohamed, Ahmed	GRAD
21STUGM007	Guaranteeing a physically realizable battery dispatch without charge-discharge complementarity constraints	Nazir, Nawaf	GRAD
21STUGM008	LSTM-based short-term electrical load forecasting framework with improved input feature space	Sharma, Abhishek	GRAD

Cyber and Physical Security of the Smart Grid

No.	Poster Title	Student Name (Last First)	UG/Grad
21STUGM009	Targeted False Data Injection Attack against DC State Estimation without Line Parameters	Du, Mingqiu	GRAD
21STUGM010	Cyberattack Resilient Control of Microgrids Equipped with Renewable Energy	Tabassum, Tambiara	GRAD
21STUGM011	Cyber-Physical Energy Systems: The Need for Security Evaluation	Zografopoulos, Ioannis	GRAD

Dynamic Performance and Control of Power Systems

No.	Poster Title	Student Name (Last First)	UG/Grad
21STUGM012	Data Anomaly Detection, Classification, and True Data Recovery in Real-time Wide-area Monitoring Applications	Chatterjee, Kaustav	GRAD
21STUGM013	A Cooperative Game Theory-based Approach to Under-frequency Load Shedding Control	Gautam, Mukesh	GRAD
21STUGM014	Impact of Phase-Lock-Loop Controller on the Small-signal Stability of Grid-connected Droop-controller Microgrid Connected to RL Load	Hurayb, Khalid	GRAD
21STUGM015	A Feasible Region Analysis Method for Continuous Commutation Failure in HVDC	Li, Yang	UG
21STUGM016	Synergistic Frequency Regulation Control Mechanism for DFIG Wind Turbines With Optimal Pitch Dynamics	Prasad, Rashmi	GRAD
21STUGM017	A Moving Horizon Parameter Estimation and Model Validation of Diesel Generators	Rauniyar, Manisha	GRAD

Integrating Renewable Energy into the Grid

No.	Poster Title	Student Name (Last First)	UG/Grad
21STUGM018	Investigation of Fast Frequency Contingency Reserve with Large-Scale Renewable Integration	Alcaide, Indira	GRAD
21STUGM019	Large-Scale Solar PV and Battery Energy Storage Model Study on a Proposed Benchmark Transmission System	Bankes, Gerald	GRAD

21STUGM020	GIS-Based Distribution System Planning for New PV Installations	Bunme, Pawita	GRAD
21STUGM021	Impacts of Effective Grid Impedance on Inverter Based Resources Plant	Das, Himadry Shekhar	GRAD
21STUGM022	DC Fault Analysis and Transient Average Current based Fault Detection for Radial MTDC System	Li, Jiapeng	GRAD
21STUGM023	Optimal Sizing and Techno-Economic Analysis of a Grid-Connected Solar Photovoltaic System	Manzoor, Taniya	GRAD
21STUGM024	Stakeholder Decision Tool for University Campus Microgrid with Solar Farm Integration	Wilk, Patrick	GRAD
21STUGM025	Data-driven Global Sensitivity Analysis of Three-Phase Distribution System with PVs	Ye, Ketian	GRAD

Intelligent Monitoring and Outage Management

No.	Poster Title	Student Name (Last First)	UG/Grad
21STUGM026	An Intelligent Event Detection Framework To Improve Situational Awareness In Large PMU Power Distribution Networks.	Amoateng, David	GRAD
21STUGM027	Prescriptive Service Restoration for Improved Distribution System Outage Management	Lawanson, Tumininu	GRAD
21STUGM028	Event Identification Framework Based on Modal Analysis of Phasor Measurement Unit Data	TaghipourBazargani, Nima	GRAD

Market Interactions in Power Systems

No.	Poster Title	Student Name (Last First)	UG/Grad
21STUGM029	Community Pool-Based Active-Hour Appliance Management Model	Dash, Shitikantha	GRAD
21STUGM030	A Reinforcement Learning Method for Power Suppliers' Strategic Bidding with Insufficient Information	Jia, Qiangang	GRAD
21STUGM031	Market-Based Volt-Var Optimization and Its Applications on Bottom-Up Load Modeling Method	Li, Ang	GRAD
21STUGM032	Joint Offering Strategy of Strategic GenCo in FTR Auction and Day-Ahead Market Considering Virtual Bidding	Mehdipourpicha, Hossein	GRAD

Power Electronics

No.	Poster Title	Student Name (Last First)	UG/Grad
21STUGM033	Estimating PV Plants Dynamic Model Parameters	Ishaq, Saima	GRAD
21STUGM034	Voltage Unbalance Mitigation in Distribution Networks Using Single-Phase BESS Inverters	Mexis, Ioannis	GRAD

Power System Modeling and Simulation

No.	Poster Title	Student Name (Last First)	UG/Grad
21STUGM035	Impact of Electric Vehicle Charging Schemes on the Performance of Distribution Grid	Ahmed, Sina Ibne	GRAD
21STUGM036	Improvement of Load Scheduling Utilizing AMI Measurements	Atchison, Forest	UG
21STUGM037	Comparison of Linearized Three-Phase Unbalanced Power Flow Models	Bertcher, Catherine	UG
21STUGM038	Data-driven Modeling of Power Electronic Converters with Grid Support Functions	Guruwacharya, Nischal	GRAD
21STUGM039	Detection of Small Changes in Power Systems with Hardware-in-Loop Testing	Hosur, Sanjay	GRAD
21STUGM040	Co-simulation of Electric Power Distribution and Buildings with EnergyPlus and OpenDSS	Jones, Stewart	GRAD
21STUGM041	Analysis of Diverse and Dynamic Effects of DERs in Residential Microgrid Using RAPSim Software	Newbolt, Travis	UG
21STUGM042	Optimal Power Flow Analysis Using Power World Simulator: Enhancing Power Engineering Education at Undergraduate Level	Newbolt, Travis	UG
21STUGM043	Machine Learning Applications for Photovoltaic Power Forecasting	Perez, Arturo	UG
21STUGM044	Unsupervised Hybrid Deep Generative Models for Photovoltaic Synthetic Data Generation	Rosa de Jesus, Dan	GRAD
21STUGM045	Machine Learning Based Utility Measure for Expected Value of Sensed Information in the Context of Renewable Energy Prediction	Rosa de Jesus, Dan	GRAD
21STUGM046	Partitioned Dynamic Modeling of Inverter with Grid Support Functions	Subedi, Sunil	GRAD
21STUGM047	Voltage Control for Three-phase Battery Inverter Connected to Unbalanced Distribution Networks	Xu, Bei	GRAD
21STUGM048	A Smart Meter Measurement Time Error Identification and Correction Method based on TESM and Correlation Analysis	Zhang, Xiaopeng	GRAD

Smart Grid Technology

No.	Poster Title	Student Name (Last First)	UG/Grad
21STUGM049	Artificial Intelligence-based Short-term Electric Load Forecasts for Experimental Smart Homes including HVAC, EWH, and PV Components	Alden, Rosemary	UG
21STUGM050	Stochastic assessment of PV hosting capacity under coordinated voltage regulation strategy in active distribution networks	Chang Hee, Han	GRAD
21STUGM051	Home Energy Management System for Coordinated PV and HVAC Controls based on AI Forecasting	Gong, Huangjie	GRAD
21STUGM052	Low-order Dynamic Virtual Battery Model for a fleet of DERs under Packetized Energy Management	Khurram, Adil	GRAD
21STUGM053	Grid-Edge Spatio-temporal Learning for Behind-the-Meter Solar Disaggregation	Lin, Shanny	GRAD
21STUGM054	Fast Frequency Response Using Packet-based Coordination and Control	Mavalizadeh, Hani	GRAD
21STUGM055	A Resilience Quantification Framework and Enhancement Scheme for Active Distribution Networks	Mishra, Dillip	GRAD
21STUGM056	IoT-based Building Energy Management System for Advanced Grid Services	Nezampasandarbabi, Farinaz	GRAD
21STUGM057	Electric Vehicles for Residential Emergency Response During Power Outages	Quezada Simental, Orlando	GRAD
21STUGM058	A Deep Learning Approach to Model Pseudo-Measurements in Active Distribution Power Networks	Radhoush, Sepideh	GRAD
21STUGM059	Hierarchical Multi-timescale Framework For Operation of Dynamic Community Microgrid	Shirsat, Ashwin	GRAD

21STUGM060	An Enhanced Solar Irradiance Forecasting Model Based on Deep Reinforcement Learning	Lyu, Cheng	GRAD

Substation and Distribution Automation

No.	Poster Title	Student Name (Last First)	UG/Grad
21STUGM061	i-Autonomous: Standardization and integration of modular and autonomous components in intelligent local substations	Palaniappan, Rajkumar	GRAD
21STUGM062	Reliability Analysis of the Control and Automation Systems in Electrical Substations	Tarquinio, Joao	UG

System-Wide Events and Analysis Methods

No.	Poster Title	Student Name (Last First)	UG/Grad
21STUGM063	Critical Risk Analysis and Price Effects of Texas Power Outage	Owolabi, Olukunle	GRAD
21STUGM064	A Novel Assessment Method of Resilient Power System Using Stochastic Geometry	Ren, Chenhao	GRAD
21STUGM065	Data Generation for Transient Stability Assessment to Address Lack of Training Data	Ma, Rui	GRAD
21STUGM066	Impact of the Inertia Constant of Synchronous Condenser to Nadir Frequency in HVDC interconnected Jeju Power System	Park, Jeonghoo	GRAD

Impact of Electric Vehicle Charging Schemes on the Performance of Distribution Grid

Sina Ibne Ahmed
Hossein Salehfar
School of Electrical Engineering and Computer Science
University of North Dakota
Grand Forks, USA
sina.ahmed@und.edu, h.salehfar@und.edu

Daisy Flora Selvaraj
Energy & Environmental Research Center
University of North Dakota
Grand Forks, USA
dselvaraj@undeerc.org

***Abstract*— The expected continuous growth of the electric vehicles (EVs) market will eventually expedite the development of their charging infrastructure. However, the integration of EVs into the power grid poses significant power quality and system stability challenges. Expansion of the charging infrastructure will necessitate in-depth analyses and assessment of the existing power grid. Studies of vehicle use and charging patterns in various geographic areas can provide actual estimates of the charging effects on the distribution systems. The substantial growth of charging infrastructure also necessitates the optimal location placement of charging stations. This study evaluates the impact of EV charging on distribution feeders using three types of EV charging techniques and varying EV penetration levels. Both graphical and real-time simulation studies have been conducted to evaluate the impact of EV charging schemes on power distribution systems. Further analysis of this project has considered the user charging patterns and optimal location of charging facilities.**

Keywords—electric vehicles, EV charging, distribution feeder.

I. INTRODUCTION

The landscape of the transportation ecosystem has been changing rapidly in recent years. Electric vehicles (EVs) are being considered a promising solution to global carbon emissions and climate change. However, mass integration of EV to the electric grid poses significant grid challenges; therefore, there is a pressing need for modeling and assessing the impacts of EV charging on the grid. This study examines the effect of EV charging on the residential distribution grid in terms of voltage deviation and harmonic distortion. A model of residential distribution grid along with electric vehicles is developed and simulated within the OPAL-RT's real-time digital simulator. Multiple scenarios of coordinated and uncoordinated charging of EVs have been simulated at peak and off-peak demand. Level 1 (L1) and Level 2 (L2) charging mechanisms have been employed at diverse penetration levels ranging from 20% to 60%. A Simulink model of a DC fast-charging station is also developed. The impact of a combination of all three different charging mechanisms on residential distribution networks has been further observed.

II. SIMULATION MODEL

A hypothetical distribution system is used to investigate the impacts of Level 1, Level 2, and DC fast charging of EVs on the residential feeder. The system used in this study is a 22.9 kV radial distribution system, a representative residential network shown in Fig. 1. There is a total of 50 customers connected with the system. A synthetic dataset of the electricity demand profile of 200 households generated by the National Renewable Energy Laboratory (NREL) is used for this study. The load profiles of 50 randomly selected houses for one day with a 10-minute resolution are used in this study.

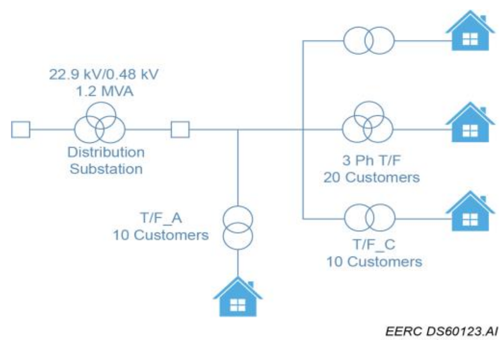

Fig. 1. One-line diagram of a residential distribution network under study

L1 and L2 chargers are modeled in the Simulink. Two MOSFET switches are used to build a bidirectional DC-DC converter system. The switches are operated by complementary control signals. For L2 chargers, a single-phase transformer has been used to raise the charging voltage to 240-V AC. The DC charging station supplies DC power directly to the battery, thus nullifying the charging constraints of an onboard EV-charging system. A multistage constant current charging method is applied to determine the optimal charging pattern in the DC fast-charging technique.

III. CONCLUSIONS SUMMARY

The results indicate a higher THD of voltage and large per unit voltage deviations during peak hours. Phase voltages show a momentary dip for the initial incursion of L1 chargers and warrant mandatory voltage compensation in the distribution feeder. The voltage, current, and maximum power level of L2 chargers are significantly higher than L1 chargers, which tends to overload the distribution transformers. The study further investigates the effect of uncontrolled charging schemes by incorporating all three types of chargers using real-world EV charging demands.

Investigation of Fast Frequency Contingency Reserve with Large-Scale Renewable Integration

Indira Alcaide-Godinez, Student Member, IEEE,
School of Information Technology and Electrical Engineering, The University of Queensland, Australia

***Abstract*—The fast frequency response service provided by battery energy storage systems is an option to mitigate a sudden loss of a big generator. The requirement of the fast frequency contingency reserve of a BESS is crucial because an overestimated reserve increases the grid operation cost. Conversely, an underestimation of the reserve is a hazard for the grid. System operators usually employ a huge amount of time and resources for modelling, tuning of control parameters and testing a variety of control strategies to assess the fast frequency response and its contingency reserve. This proposed method determines the fast frequency contingency requirement of a large-scale power grid from a broader and simpler premise. Results are validated via a realistic grid under the largest loss of generation. These provide relevant insights regarding how to assess the fast frequency response requirements for planning and day-ahead dispatch.**

***Keywords*— Fast frequency response (FFR), fast contingency reserve, under-frequency load shedding.**

I. Methodology for Contingency FFR of a BESS

The methodology is depicted in Fig. 1 where P_{ffr_res} is the FFR power reserve, $T_{trig} \in \varphi_{trig}$ is the trigger time, $T_{fact} \in \varphi_{fact}$ is the fully-activated time, f_{nad} is the frequency nadir and f_{ufls} is the under-frequency load shedding limit. Firstly, selected power reserves and typical time-response capabilities of a BESS are used to emulate the FFR service by using a negative load [1]. Results in Fig. 2 can be organised into non-sufficient ($f_{nad}<f_{ufls}$), sufficient ($f_{nad}\approx f_{ufls}$) and over-estimated ($f_{nad}>f_{ufls}$). The sufficient and over-estimated reserves are validated by using a BESS model (Fig. 3).

II. Conclusions

The proposed method identifies the fast frequency contingency requirement of a battery from a broader and simpler approach. The features of power and time-response capabilities can be directly identified graphically. Results prove that an extensive study can be effectively made by using a negative load to emulate a sustained FFR before reaching the frequency nadir. This allows determining the fast frequency contingency requirement in a simple way.

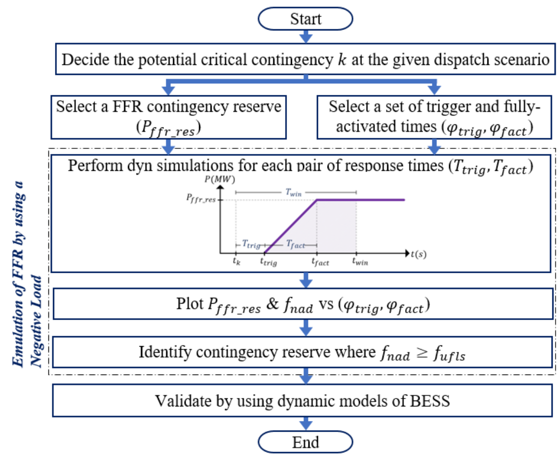

Fig. 1. The proposed method to determine the FFR contingency reserve.

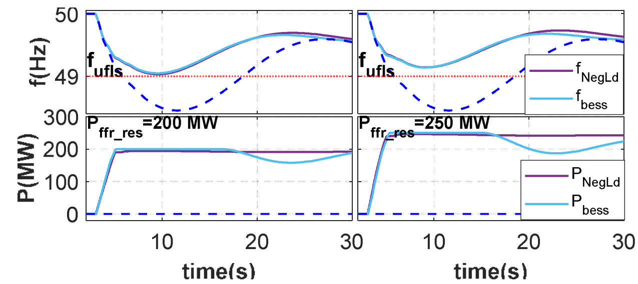

Fig. 3. Validation by using a BESS model with (T_{trig}=0.05, T_{fact}=2) s.

References

[1] P. V. Brogan, R. J. Best, D. J. Morrow, K. McKinley, and M. L. Kubik, "Effect of BESS Response on Frequency and RoCoF During Underfrequency Transients," *IEEE Transactions on Power Systems,* vol. 34, no. 1, pp. 575-583, 2019.

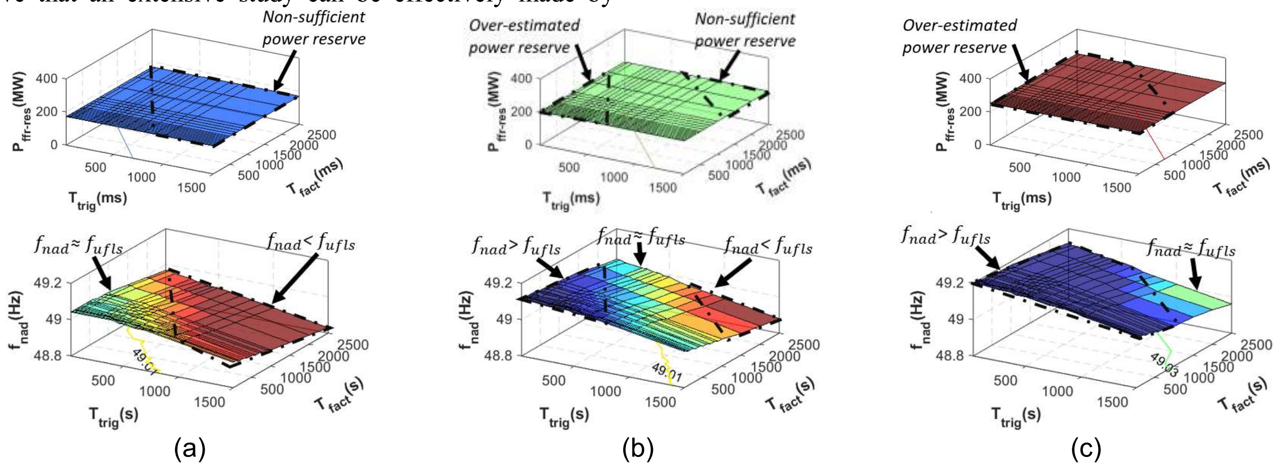

Fig. 2. FFR contingency reserve of a BESS and frequency nadir values for: (a) 170 MW reserve, (b) 200 MW reserve and (c) 250 MW reserve.

Artificial Intelligence-based Short-term Electric Load Forecasts for Experimental Smart Homes including HVAC, EWH, and PV Components

Rosemary E. Alden, *Student Member, IEEE*, Cristinel Ababei, *Senior Member, IEEE*, Dan M. Ionel, *Fellow, IEEE*

***Abstract*—Individual residence load profiles are the most difficult to predict due to high variability of appliances and randomness introduced by human behavior. Within this poster, the SHINES residential field demonstration site in Pensacola, FL managed by the Electric Power Research Institute (EPRI), is used to compare the performance of the same deep learning Long Short Term Memory (LSTM) model on predicting the total, HVAC, WH, and solar power usage or generation between two homes. This comparison will highlight the influence of the owners and appliance type on demand profile and the challenges with using machine learning to predict the main loads and generation of the future Smart Homes. A second approach to forecast the difference between a home and a desired load profile will be introduced. The value of these predictions lies in that they can be used to assess variability in model accuracy and to inform optimizations at HEMs level with the goal to reduce energy usage, peak load stress on utilities, and overall costs.**

***Index Terms*—Big data, EnergyPlus, variable loads, machine learning, residential**

I. Smart Grid Application of AI-Based Electric Load Forecasts

Within the future smart grid, new configurations for coordinating distributed energy resources are needed and frameworks proposed for the inclusion of prosumers would benefit from improved electric load forecasting for pricing and generation planning. Artificial-intelligence based electric load forecasting has proven potential for community level predictions in academia. Newer models such as the Long Short Term Memory (LSTM) Model, a Recurrent Neural Network, are able to learn long term patterns more effectively, and, thus, are used for residential load forecasting applications.

II. Experimental Data Driven LSTM Encoder Decoder Model

Electric load forecasting studies have been conducted to assess the difference of performance in predicting total, HVAC, PV, and EWH load between two residencies from the SHINES field demonstration. All data was pre-processed to isolate the daytime only from 6am to 9pm during the summer months of June 1st to September 15th for 2018 - 2020. For example, measured data for HVAC predictions is shown in Fig.1. The LSTM model used was trained on the first two summers of 2018 and 2019. The summer of 2020 was used as the test set.

Rosemary E. Alden and Dan M. Ionel are with SPARK Laboratory, Electrical and Computer Engineering Dept., University of Kentucky, Lexington, KY. Cristinel Ababei is with the Electrical and Computer Engineering Dept., Marquette University, Milwaukee, WI.

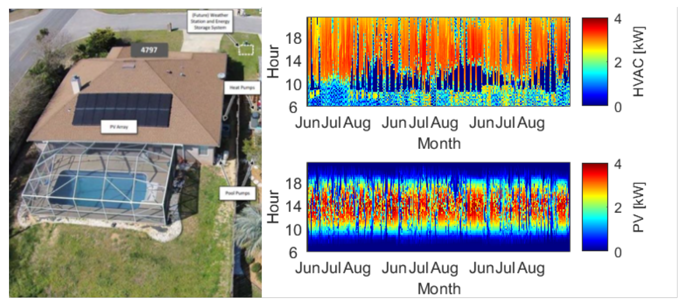

(a)

Figure 1. The power usage over the summer months of 2018 - 2020 by the HVAC system in the H1 SHINES house (top) is higher than the H2 SHINES house (bottom) with H2 being more variable and intermittent.

All day-ahead predictions were made based on a sliding window three days in length of previously measured average power as well as two days of prior and one day of weather parameters as a "perfect forecast". Influential weather parameters identified include irradiance, outdoor temperature, and temperature difference from internal set point. The utilization of a "perfect forecast" serves as an optimal case to demonstrate the capability of the LSTM model.

The comparison from Fig.2 demonstrates favorable performance in predicting HVAC for both houses. Further results for the additional smart home variables will be presented and error distribution analysis described. An additional prediction for the difference between a home's usage and a desired profile will be introduced. This approach offers another source of guidance for HEMS control schemes and would show a user how their usage could change to accomplish either economic or environmental goals.

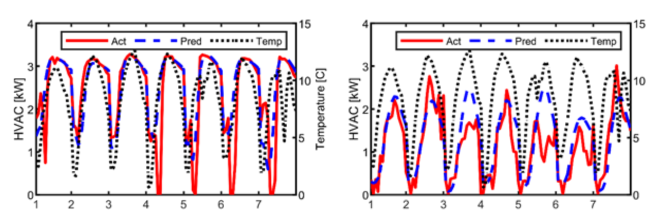

(a) (b)

Figure 2. (a) HVAC predictions for SHINES Homes H1 and (b) H2 for the week of July 31st to Aug 6, 2020. The LSTM followed the trends of HVAC power over the day better in H1 than in H2 with less error.

An Intelligent Event Detection Framework To Improve Situational Awareness In Large PMU Power Distribution Networks.

David Ofosu Amoateng, *Student Member, IEEE*, Ruifeng Yan, *Member, IEEE*, Tapan Kumar Saha, *Fellow, IEEE*

***Abstract*—With PMUs, network operators are able observe events which are unobservable using SCADA. Large PMU networks generate vast amounts of data, span large geographical areas and cover different load profiles, with varying dynamic system responses across PMUs. The challenge is to analyse these enormous amounts of information and to set suitable threshold levels for all PMUs in the network. Care must be taken when choosing thresholds as the region between missing events and near constant triggering may be small leading to false positives. In this regard, we propose a novel intelligent deep autoencoder based PMU event detector, which learns a representation of the normal operating state of the distribution network and outputs a high prediction error when an event occurs. The event detector is trained using 8 days of real data (12 billion measurement points) from a 28 PMU distribution network located in Queensland, Australia. The result is an event detector which uses a single threshold value for all PMU measurements in the network irrespective of their location and dynamic response and can be used post hoc or in realtime PMU streams. Different useful cases are presented and the effectiveness of the proposed framework is verified using data from the 28 PMU distribution network.**

***Index Terms*—Event detection, event categorisation, deep learning, phasor measurement units, distribution network.**

I. Introduction

Advancing technology has diversified the conventional electric power system, adding new sources of distributed energy resources (DERs) in order to address environmental concerns and sustainability . Advanced sensor networks and monitoring systems using phasor measurement units (PMUs) have granted system operators access to information that would be unobservable using traditional measurement units. Deploying PMUs on distribution grids, enables the power system operator to detect anomalies and events in real time which may help avoid disruptions.

Most event detection schemes are based on a premise: An event detector uses statistical or signal processing technique, to identify PMU data points that are significantly different from others and labels them as outliers. The challenge is to analyse these enormous amounts of information and to set suitable threshold levels for all PMUs in the network. Care must be taken when choosing thresholds as the region between missing events and near constant triggering may be small leading to false positives.

D. O. Amoateng, R. Yan and T. K. Saha are with the School of Information Technology and Electrical Engineering, The University of Queensland, Brisbane, Australia.

This Activity received funding from the Australian Renewable Energy Agency (ARENA) as part of ARENA's advancing renewables programme.

II. Recurrent Autoencoder Based Event Detection Framework

Using recorded PMU data, the goal is to construct a model using current and previous data window samples. The model reconstructs the error difference between the two windows and outputs its own prediction. An event is said to be detected if the prediction error is greater than a threshold. To achieve this, we assume the PMU dataset for building the model is unbalanced where the number of non event data is orders of magnitude greater than the event data points. As such the model is biased towards recognising and reconstructing normal error data points, such that an item wise error difference e will yield a high reconstruction or prediction error if the current window contains an event. A deep recurrent autoencoder is utilised to learn these normal error differences between data windows.

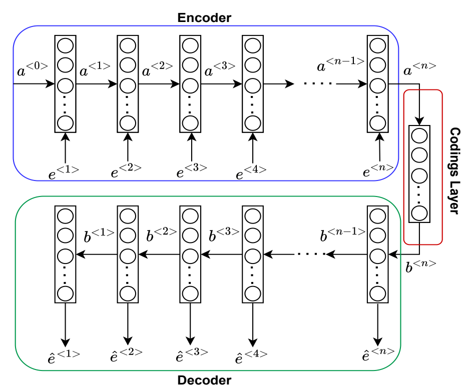

Fig. 1: Recurrent Autoencoder For Event Detection

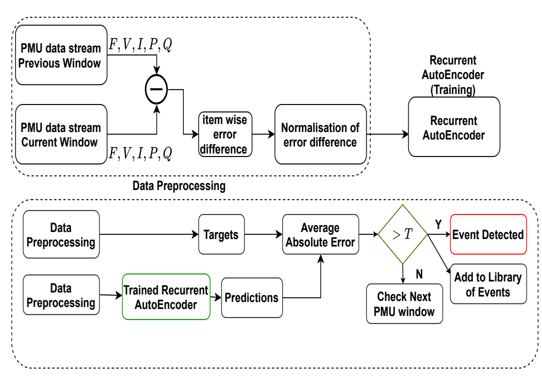

Fig. 2: Event Detection Framework

Improvement of Load Scheduling Utilizing AMI Measurements

Forest Atchison, Valentina Cecchi, Sukumar Kamalasadan
University of North Carolina at Charlotte
Charlotte, NC USA

***Abstract*—The customer class load schedules traditionally used by electric utility distribution management systems (DMS) inform system-level modeling, including distribution power flow, which in turn dictates decision making at the most foundational levels. These load schedules vary based on the customer's load category (e.g., residential, commercial, and industrial), season, and type of day (e.g., weekend or weekday). In the absence of detailed customer data, load schedules have conventionally been derived from heuristic techniques, assumptions, and examples, and in some cases have remained static as the modern power grid has evolved to contain more modern load types such as LED lighting fixtures, smart appliances, and household electric vehicle charging stations. Due to the advent of more readily-available data due to advanced metering infrastructure (AMI), this work provides data-driven improved customer class load schedules that decrease average error across a particular load category. Additionally, the improved schedules will be shown to decrease error in the aggregate when viewed from the level of a distribution feeder.**

I. Poster Overview

As a crucial input to DMS-performed distribution power flow, scheduled load for a given point in time is of fundamental importance in ensuring that grid management decisions are timely and correct. As such, the accuracy of average customer load schedules that serve as estimates for customer usage are critical to effective operation of distribution management system practices. Among utility companies there is a recognized need, as the loading characteristics at the customer level and the access to customer usage information have changed, to revisit the conventional assumptions of loading patterns represented by customer class load schedules.

A customer class load schedule can be defined as the combination of load category, season, and type of day that serve to categorize a particular load at a particular time. For example, considering five load categories (residential, industrial, and small, mid, and large commercial), forty unique customer class load schedules can be defined over the course of a year. Traditionally, each of these schedules can be represented as a normalized base value at regular time intervals that is scaled by some nominal factor to represent the estimated load at a certain time. Often dating from before the widespread availability of large amounts of detailed customer usage data, the schedules can contain antiquated assumptions of loading characteristics.

Using customer usage information provided by Duke Energy, this work provides updated and improved customer class load schedules that more accurately represent current customer usage. This analysis used the 15 to 30-minute increment kWh measurements from 2020 of more than 4000 meters existing on a certain feeder in the Duke Energy network to develop average load schedules that were typical of each customer class. The developed schedules were then tested on an unbiased second feeder of more than 2500 meters to determine to what extent the improved schedules decrease error when compared to the original schedules. As indicated in Table I, the aggregation of the improved schedules across the test feeder, as developed from the AMI data, were shown to decrease the error across the year as compared to the original schedules both in magnitude (mean absolute percent error, mean squared error) and in the shape of the curve (cosine similarity). Fig. 1 allows the visualization from the perspective of the feeder of the original and improved estimates of an average summer weekday as compared to the AMI profile.

Table I: Original and improved load schedule error

		MAPE (%)	MSE (kWh^2)	COS
Fall Weekday	Improved	8.1	39036	0.9998
	Original	11.7	87615	0.9936
Fall Weekend	Improved	12.2	89389	0.9995
	Original	12.4	91130	0.9915
Spring Weekday	Improved	7.5	35247	0.9996
	Original	18.2	243863	0.9913
Spring Weekend	Improved	10.5	84438	0.9994
	Original	22.4	435539	0.9886
Summer Weekday	Improved	7.1	84867	0.9999
	Original	24.5	929961	0.9970
Summer Weekend	Improved	9.5	148309	0.9998
	Original	27.3	1147757	0.9959
Winter Weekday	Improved	9.0	48485	0.9990
	Original	26.8	724667	0.9908
Winter Weekend	Improved	13.4	118680	0.9994
	Original	26.3	690484	0.9933

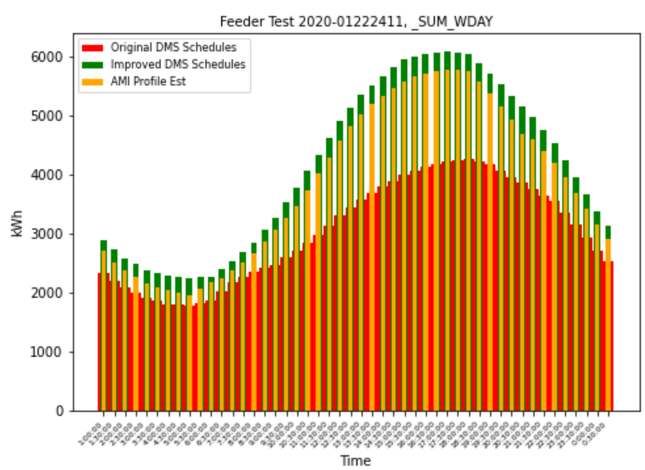

Figure 1: Comparison of schedules vs. AMI, summer weekday

Large-Scale Solar PV and Battery Energy Storage Model Study on a Proposed Benchmark Transmission System

Gerald W. Bankes, *Student Member, IEEE*, Oluwaseun Akeyo, *Member, IEEE*, Dan M. Ionel, *Fellow, IEEE*

***Abstract*—This study evaluates through computer simulation and analysis both the impact of large-scale PV and BESS connection to a test transmission circuit and the benefits of BESS during conditions of sudden PV shading and transient fault. Contrary to conventional approaches, this study proposes an improved dynamic model for inverter-based resources (IBR) that captures the modelling of high-frequency power electronics to be suitable for simulating unbalanced transient conditions such as single-phase to ground faults. The performance of the proposed models was studied and simulated in PSCAD/EMTDC on a modified IEEE 12 bus transmission system. The results of the study demonstrate that in addition to reducing PV power plant intermittency, BESS may be employed to support grid voltage and avoid equipment failure during fault conditions.**

***Index Terms*—Solar, PV, battery energy storage, hosting capacity, dynamic PV, PSCAD, Volt-VAR, inverter, MPPT.**

I. Dynamic PV and Battery Module in PSCAD/EMTDC

This study proposes a dynamic IBR module with variable capacity which can be employed for various energy systems including solar PV, wind, and BES systems. The proposed module combines the benefits of detailed inverter-based models with the reduced computational requirement of average models. In this approach, the output of a three-phase controlled current source is proportional to the output current of a representative detailed inverter-based model, which includes modelling of high-frequency power electronics and their associated controls.

The proposed model for the PV system in this study includes a detailed 1MW solar PV plant connected to a controllable voltage source, whose magnitude, phase, and frequency matches those of the point of interconnection. The output current of the detailed model is then used to regulate the output current of the three-phase current source used to represent the dynamic model.

II. Transient Studies on the Modified Test System

The effect of sudden solar PV shading on the operation of the PV plant and BES system was simulated and analyzed using the IEEE 12 bus transmission system modified to include a 100MW PV and 100MW BESS connected to Bus 2 (Fig. 1). The irradiance of the solar PV array was set to decrease from 1000W/m^2 to 200W/m^2 for a duration of 2s at 2s simulation time.

Gerald W. Bankes and Dan M. Ionel are with the Spark Laboratory, Electrical and Computer Engineering Dept., University of Kentucky, Lexington, KY. Oluwaseun Akeyo was with the Spark Laboratory and is now with Sargent & Lundy, L.L.C.

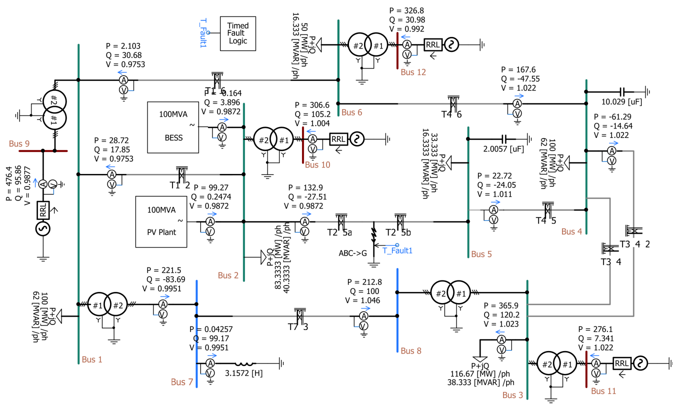

Figure 1. Single-line diagram of IEEE 12 bus system in PSCAD/EMTDC modified to include 100MW PV plant and 100MW battery energy storage system at bus 2.

The real power output of the BESS was configured to compensate for loss of PV generation. The simulation results demonstrated in Fig. 2a show that augmenting PV power output with BESS during shading provides bus voltage support. In this case study, the BESS was able to prevent a transient voltage drop of 0.07pu at the point of interconnection.

The BESS is also able to provide voltage support of the grid through operation in Volt-VAR mode, which varies reactive power output in response to voltage variation. The results, illustrated in Fig. 2b, of a transient study of a three-phase fault lasting 0.05s on the test system show that reactive support of the BESS was able to reduce the voltage drop during the fault when compared to cases without PV or with PV without BESS support.

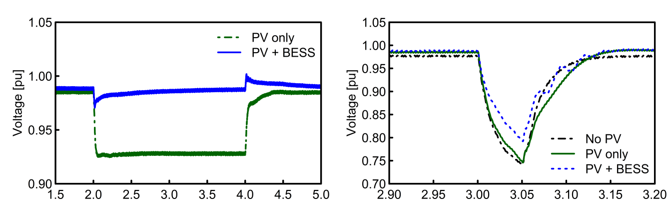

(a) (b)

Figure 2. Bus 2 point of interconnection voltage for (a) transient shading and (b) three-phase fault conditions.

Novel Protection Method for Fully Inverter-Based Distribution System Connected Microgrid

Bilkis Banu, *Student Member, IEEE*, Michael Smith, *Member, IEEE* and Sukumar Kamalasadan, *Senior Member, IEEE*

***Abstract*—Limited fault current from an inverter poses several protection challenges, such as fault detection, protection coordination for completely inverter-based microgrids. This paper studies the effect of inverter-based distributed generation on distribution protection device operation for different scenarios and proposes a novel method for detecting faults for inverter based distribution microgrid. Simulation results are performed on an IEEE 34 bus unbalanced test system using PSCAD and CYME to show the efficacy of proposed method.**

***Index Terms*—inverter, protection coordination, resiliency.**

I. Introduction

This paper studies the protection challenges associated with 100% inverter-based (IBG) medium voltage distribution connected microgrids. Several methods are shown in the literature for addressing the issues with IBG microgrid protection, but each method has limitations [1]. This paper proposes a novel protection method for detecting faults in IBG microgrids.

II. Proposed Protection Method

The IEEE 34 Bus test system is modified to add protective devices (i.e., relays, reclosers, fuses, and circuit breaker), as shown in Fig. 1. The IEEE standard for protective relay applications [2] is applied for the protection device (PD) settings and coordination. Then, the test system is modified to connect a utility scale Battery Energy Storage System (BESS) with a $2MVA$ rating at Node 826. An islanding recloser is located upstream to Node 826, which can operate to create a IBG based microgrid following an upstream outage. The proposed protection method uses a combination of several protection element to detect faults in the microgrid, where microprocessor-based PDs can implement Algorithm 1.

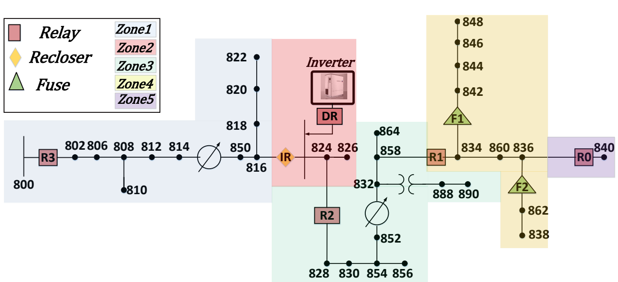

Fig. 1. IEEE 34 bus with protection devices.

III. Simulation Results and Discussion

Fig. 2 shows that for a fault at Node 860, the PD operates acceptably for both the "substation connected only" and the "substation and inverter connected" cases. However, when the islanding recloser is opened and a microgrid is created with the downstream section, the PDs do not detect the fault. Table I shows a comparison of proposed method with conventional overcurrent (OC) protection for the distribution network. The results show that the proposed method accurately detects faults faster for different fault locations.

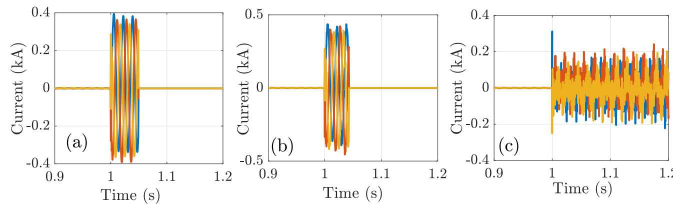

Fig. 2. (a) Fault current from substation only, (b) Fault current from both substation and inverter, (c) Fault current in microgrid from only inverter.

Algorithm 1 Proposed Microgrid Fault Detection Method

Step: 1 Calculate phase voltages (V_{abc}) and currents (I_{abc}) at protection device locations using CTs and PTs.

Step: 2 Calculate sequence voltages and currents.

Step: 3 Extract current harmonics components (I_n).

Step: 4 Determine thresholds for protection elements: $3I_2^{limit}, 3I_0^{limit}, 3V_0^{limit}, H^{limit}$.

Step: 5 Calculate $\frac{3I_2}{I_1}, \frac{3I_0}{I_1}, \frac{3V_2}{V_1}, I_H$ where $I_H = \frac{\sqrt{\sum_{n=1}^{7} I_n^2}}{n}$.

Step: 6 If $(\frac{3I_2}{I_1} \geq 3I_2^{limit}) \,||\, (\frac{3I_0}{I_1} \geq 3I_0^{limit}) \,||\, (\frac{3V_2}{V_1} \geq 3V_0^{limit}) \,||\, (I_H \geq H^{limit})$, $T_{Trip} = start$.

Step: 7 $\text{TRIP}=\begin{cases} 1, & \text{If } T_{Trip} > R_{TimeDelay}. \\ 0, & \text{otherwise.} \end{cases}$

TABLE I
Comparison of Proposed Method with Existing OC Method

Fault Location	Fault Type	PD	Conventional OC (s)	Proposed Method (s)
Node 840	LLLG	R0	$\geq$1s	0.003
	LG	R0	$\geq$1s	0.003
Node 846	LLLG	R1	$\geq$1s	0.001
	LG	R1	$\geq$1s	0.001
Node 854	LLLG	R2	$\geq$1s	0.221
	LG	R2	$\geq$1s	0.425
Node 826	LLLG	DR	$\geq$1s	0.181
	LG	DR	$\geq$1s	0.449

IV. Conclusion and Future Work

The proposed fault detection method (Algorithm 1) outperforms the conventional OC method (see Table I). Future work will use a real-time simulation platform to validate the performance of proposed method.

The authors are with the Energy Production Infrastructure Center (EPIC), Department of Electrical Engineering, and Department of Engineering Technology and Construction Management, University of North Carolina at Charlotte, Charlotte, NC 28223 USA. Corresponding Author: B. Banu (bbanu@uncc.edu).

References

[1] K. Lai, M. S. Illindala, and M. A. Haj-ahmed, "Comprehensive protection strategy for an islanded microgrid using intelligent relays," *IEEE Transactions on Industry Applications*, vol. 53, no. 1, pp. 47–55, 2017.

[2] "IEEE guide for protective relay applications to distribution lines," *IEEE Std C37.230-2007*, pp. 1–100, 2008.

Comparison of Linearized Three-Phase Unbalanced Power Flow Models

Catherine Bertcher, Anna Stuhlmacher, and Johanna L. Mathieu
Department of Electrical Engineering & Computer Science
University of Michigan, Ann Arbor, MI, USA
{kbertch, akstuhl, jlmath}@umich.edu

***Abstract*—It is critical to ensure safe operation of distribution networks as the level of distributed renewable energy resources increases. The power flow model is nonconvex, making it prohibitively time-intensive to include it in optimization problems for large networks. Several three-phase unbalanced linear approximations have been proposed for the radial power flow model to reduce the computational burden. However, it is unclear which model performs best given the network and application. To address this, we compare three variations of a linearized, three-phase unbalanced power flow model. We examine the impact of unbalance and reference power flows used to estimate losses on power flow and optimal power flow solution accuracy.**

***Index Terms*—Linear Power Flow Models, Multiphase Distribution Networks, Voltage Unbalance**

I. Motivation

Increasing levels of intermittent distributed energy resources in distribution networks can lead to larger voltage fluctuations and power quality issues. To ensure safe operation, it is becoming increasingly important to accurately model and optimize unbalanced distribution networks. The power flow model is in general nonconvex and challenging to solve at the scale and speed needed for real-time control and optimization. To address the computational burden of solving power flow, several three-phase unbalanced linear approximations of the power flow model have been proposed, e.g., [1]–[3]. These approximations assume the voltage unbalance at each bus is small. The formulation in [1], [2] is commonly referred to as 'Lin3DistFlow'. Ref. [3] also incorporates a reference power flow, or forecast, to approximate the loss terms as constants (which we will refer to as 'Lin3DistFlow + Losses') and to approximate the phase unbalance (which we will refer to as 'Lin3DistFlow + Losses + Voltage Ratios').

This work compares the performance of these three linear approximations to determine their accuracy under different conditions, e.g., varying levels of unbalance and forecast error. The goal is to identify the conditions under which a model performs better than others.

II. Model Comparisons

The approximated power flow results are assessed against the actual power flow using OpenDSS [4], and we test each model on several IEEE test networks.

As an illustrative example, Fig. 1 compares the average voltage magnitude error for 'Lin3DistFlow' and 'Lin3DistFlow + Losses' when the forecast error and voltage unbalance vary.

This project was funded by an REU Supplement to NSF Grant 1845093.

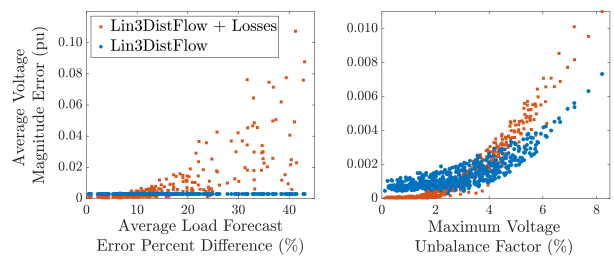

Fig. 1. Average voltage magnitude errors for 'Lin3DistFlow' and 'Lin3DistFlow + Losses' are evaluated when varying the average load forecast error percent difference (Left) and the maximum voltage unbalance factor (Right). A modified IEEE-13 test network is used. The IEEE definition of voltage unbalance factor is used.

The left plot depicts the impact of approximating the nonlinear loss terms from the forecast. We set the actual power demand and vary the power demand forecast by randomly generating 350 power demand forecast errors for each bus and phase from a Gaussian distribution. As expected, 'Lin3DistFlow + Losses' performs better than 'Lin3DistFlow' when the forecast error is small. However, as the forecast error increases, the approximated loss terms cause less accurate power flow results than simply neglecting the terms altogether. This represents a case where, depending on the expected accuracy of a forecast, it is beneficial to choose one model over the other.

The right plot evaluates how the level of unbalance in the test network impacts the accuracy of the approximations. We randomly generate the power demand at each bus and phase for 500 samples and plot the average voltage magnitude error against the maximum voltage unbalance factor. Here, the accuracy of both 'Lin3DistFlow' and 'Lin3DistFlow + Losses' generally degrades as the maximum voltage unbalance factor increases. This is because both approximations are based on the assumption that the voltages are nearly balanced.

Full results will include explorations over different networks, inclusion of 'Lin3DistFlow + Losses + Voltage Ratios', and an optimal power flow example to illustrate performance.

References

[1] D. B. Arnold, M. Sankur, R. Dobbe, K. Brady, D. S. Callaway, and A. Von Meier, "Optimal dispatch of reactive power for voltage regulation and balancing in unbalanced distribution systems," in *IEEE PES GM*, 2016.

[2] L. Gan and S. H. Low, "Convex relaxations and linear approximation for optimal power flow in multiphase radial networks," *Power Systems Computation Conference*, 2014.

[3] B. A. Robbins and A. D. Domínguez-García, "Optimal reactive power dispatch for voltage regulation in unbalanced distribution systems," *IEEE Trans. Power Syst.*, vol. 31, no. 4, pp. 2903–2913, 2016.

[4] R. C. Dugan and T. E. McDermott, "An open source platform for collaborating on smart grid research," in *IEEE PES GM*, 2011, pp. 1–7.

Optimization-based Voltage and Frequency Dynamics Estimation and Control of Microgrids

Niranjan Bhujel†, *Graduate Student Member, IEEE* and Reinaldo Tonkoski, *Senior Member, IEEE*
South Dakota State University, Brookings, South Dakota, USA
Email: †niranjan.bhujel@jacks.sdstate.edu

***Abstract*—Microgrid is generally characterized by a high R/X ratio which introduces higher cross-coupling between frequency and voltage dynamics. Further, microgrid costs are time-varying. Thus, optimal control approach is required. This optimal control approach is model-based which means it requires system information. Thus, an online estimation technique is required. In this paper, we present an integrated moving horizon estimation-model predictive control approach to provide voltage and frequency supports.**

***Index Terms*—Voltage support, frequency support, model predictive control, optimal control, microgrid.**

I. Key Equations

Benchmark, where the proposed MHE-MPC framework is implemented, is shown in Fig. 1. This system can be represented by state differential equations as

$$x_{k+1} = Ax_k + Bu_k \tag{1}$$

Let N be the horizon length in terms of sample length. Our objective is to support voltage and frequency. Then MPC formulation can be written as

$$\min_{i_{invd}, i_{invq}} J_\Gamma = \sum_{k=q}^{q+N-1} \left(||\Delta y_k||_Q + ||u_k||_S \right) \tag{2a}$$

subject to

$$x_{k+1} = F(x_k, u_k, \mathcal{P}) \ \forall\ k \in \Gamma \tag{3a}$$
$$|i_{invd_k}| \leq i_{d,max} \ \forall\ k \in \Gamma \tag{3b}$$
$$|i_{invq_k}| \leq i_{q,max} \ \forall\ k \in \Gamma \tag{3c}$$
$$|i_{invd_{k+1}} - i_{invd_k}| \leq S_d \ \forall\ k \in \Gamma \tag{3d}$$
$$|i_{invq_{k+1}} - i_{invq_k}| \leq S_q \ \forall\ k \in \Gamma \tag{3e}$$

where $\Delta y_k = [\Delta\omega_k \ \Delta\dot{\omega}_k \ \Delta v_{cdk}]^\top, i_{invdk}, i_{invqk}$, and J represents variables to be controlled, d, q component of inverter and cost function respectively. The above MPC formulation was implemented in CasADi. MHE can be formulated as:

$$\min_{x_k, u_{d,k}, \mathcal{P}} J_H = \left(\left\| \begin{matrix} x_L - \overline{x}_L \\ \mathcal{P} - \overline{\mathcal{P}}_L \end{matrix} \right\|^2_{V_L} + \sum_{k=q-L+1}^{q} ||y_k - h(x_k, \mathcal{P})||^2_V + \sum_{k=q-L+1}^{q-1} ||w_k||^2_W \right) \tag{4a}$$

subject to

$$x_{k+1} = F(x_k, u_k, \mathcal{P}) + w_k \quad \forall\ k \in \mathcal{H} - \{q\} \tag{5a}$$
$$\mathcal{P}_{min} \leq \mathcal{P} \leq \mathcal{P}_{max} \tag{5b}$$
$$u_{d,k+1} = u_{d,k} \quad \forall\ k \in \mathcal{H} - \{q\} \tag{5c}$$

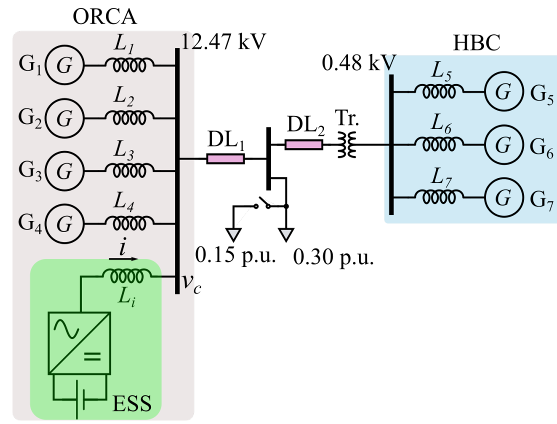

Fig. 1: Modified form of Cordova, Alaska, microgrid benchmark.

where L, V and W represents horizon length, inverse of measurement and process noise respectively.

II. Key Results

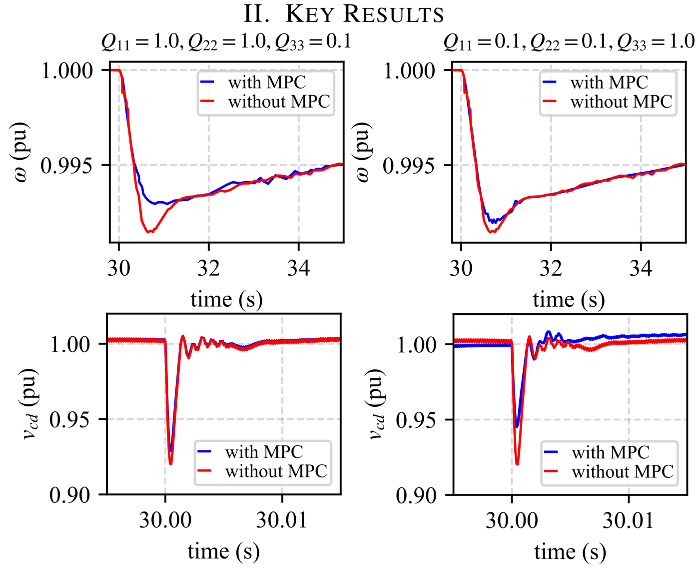

Fig. 2: Results showing performance of voltage and frequency support for two different cases.

Fig. 2 shows plots of ω and v_{cd} for two different cases (represented by column). In the first case, frequency support is prioritized whereas in the second case, voltage support is prioritized.

III. Future Work

In the future, we will implement multi-time scale control where two controllers at different time-scale are implemented without neglecting their coupling.

GIS-Based Distribution System Planning for New PV Installations

Pawita Bunme, *Student Member, IEEE*
Yasunori Mitani, *Senior Member, IEEE*
Department of Electrical and Electronics Engineering
Kyushu Institute of Technology
Kitakyushu, Japan
pawita.bunme589@mail.kyutech.jp

***Abstract*— Solar panel installations have increased significantly in Japan in recent decades. Due to this, world trends, such as clean/renewable energy, are being implemented in power systems all across Japan, particularly including installations of photovoltaic (PV) panels in general households. In this work, solar power was estimated using solar radiation data from Geographic Information System (GIS) technology. The solar power estimation was applied to the actual distribution system model of the Jono area in Kitakyushu City, Japan. In this work, real power consumption data was applied to a real-world distribution system model. We studied the impact of high installation rates of solar panels in Japanese residential areas. Additionally, we considered the voltage fluctuations in the distribution system model by assessing the impact of cloud shadows using a novel cloud movement simulation algorithm that uses real-world GIS data. The simulation results revealed that the shadow from the cloud movement process directly impacted the solar power generation in residential areas, which caused voltage fluctuations of the overall distribution system. Thus, we advocate distribution system planning with a large number of solar panels.**

Keywords*— Photovoltaic (PV); Solar Energy; Geographic Information System Technology; Digital Surface Model (DSM); Distribution System; Distribution System Planning)

I. Introduction

GIS programs are currently widely used in many fields, such as driving support systems for electric vehicles, estimating the amount of solar radiation on farmland for agriculture, and creating solar radiation maps for checking the solar radiation on an entire focus area. There are many merits when applying GIS technology together with solar energy, such as estimating the solar irradiance output or the potential of a roof surface for PV installation from a large-scale residential area. With the rapidly rising number of solar rooftops in the distribution system, there are impacts on the distribution system, because the panels are integrated by connecting them directly to the grids. The effects from a large number of solar panels on the power system include voltage or frequency fluctuations due to the shadow effects from trees, buildings, or the surrounding area.

To show a solar radiation map and the shadow covering the solar panels, a Digital Elevation Model (DEM), which represents the ground surface and the road network, from GIS technology was applied to create a landscape solar analysis. However, there are various methods to create solar radiation maps using a GIS program. As example is to apply a Digital Surface Model (DSM) representing the elevations of the trees and buildings together with GIS technology representing the solar radiation map to find efficient solar power placement. Thus, in this research, we created a solar radiation map using a GIS program and DSM layer to estimate the solar radiation map from the real-world residential area.

This research facilitates the distribution system with the solar panel high installation rate for future planning based on the Jono distribution area by simulating the solar radiation map with the distribution system. The real electricity consumption data from the households in the Jono distribution system were used in this research. Not only the consumption data but also the distribution model was adjusted to the existing residential area. With the GIS program, natural phenomena, such as the cloud movement process, were simulated in the solar installation map to consider the shadow's impact on the voltage fluctuations in the distribution system [1]. This work combines the actual distribution model together with the literal solar radiation output for the Jono research area, which was collected using the GIS technology to develop future distribution system planning. We focus on the voltage fluctuations considering the two scenarios of 50 and 100 percent of the maximum solar panel installation to the distribution system and comparing the results, and examining the amount of solar panel effects on the residential area. The results of this research accommodate the concepts of distribution system future planning. It is important to consider the impacts of the solar panel before PV rooftop installation.

II. Results

A. *The Simulation of 50% of Solar Panel Installation in the System with cloud movement process*

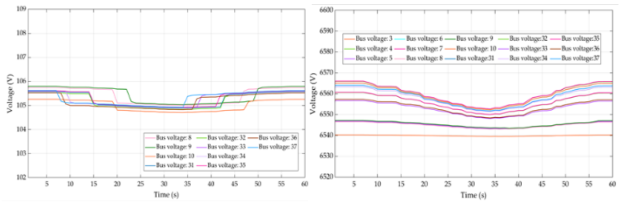

Fig. 1 Voltage fluctuation graphs of 50 percent solar panel installation in the system: (a) Low voltage (residential area side, 100 to 107 V); (b) High voltage side (between the distribution bus points, 6600 V)

B. *The Simulation of 100% of Solar Panels Installation in System with cloud movement process*

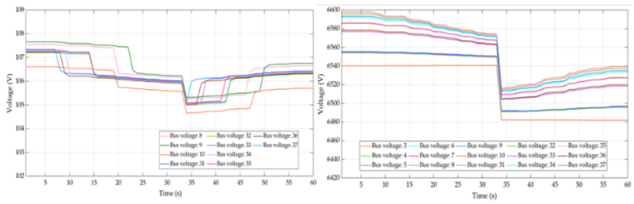

Fig. 2 Voltage fluctuation graphs of 100 percent solar panel installation in the system: (a) Low voltage (residential area side, 100 to 107 V); and (b) high voltage side (between the distribution bus points, 6600 V)

III. References

[1] P. Bunme, A. Shiota, and Y. Mitani, "Solar Power Estimation Using GIS Considering Shadow Effects for Distribution System Planning," *Proc. - 2020 IEEE Int. Conf. Environ. Electr. Eng. 2020 IEEE Ind. Commer. Power Syst. Eur. EEEIC / I CPS Eur. 2020*, pp. 6–10, 2020.

Stochastic assesment of PV hosting capacity under coordinated voltage regulation strategy in active distribution networks

Changhee Han
Department of Electrical Engineering
Korea University
Seoul, South Korea
hch0806@korea.ac.kr

Dongwon Lee
Department of Electrical Engineering
Korea University
Seoul, South Korea
dong951106@korea.ac.kr

Gilsoo Jang
Department of Electrical Engineering
Korea University
Seoul, South Korea
gjang@korea.ac.kr

***Abstract*—This paper proposes a two-stage optimization framework to estimate the maximum hosting capacity of PVs considering coordination between voltage regulation devices in distribution networks. A co-simulation environment is suggested using MATLAB and the OpenDSS. Through the mote-carlo simulation, the uncertainty in PV and load output over time is considered as random variables in stochastic assessment of hosting capacity. The proposed process can be applied to both three-phase balanced and unbalanced networks.**

Keywords—PV, Hosting Capacity, Active distribution network.

I. INTRODUCTION

In the process to estimate the HC of PVs, the impact of optimally coordinated management of control devices should be closely considered. Therefore, this paper proposes the framework to estimate the maximum HC of PVs considering coordinated optimal control of voltage regulation devices including smart inverters (SIs), OLTCs and SVCs. The constraints considered involves over-voltages, voltage unbalance limits, thermal capacity of lines, and substation capacity.

II. PROPOSED OPTIMIZATION FRAMEWORK

The framework is divided into two optimization problems. In the first stage, based on the predicted daily load profile and specified PV locations, the optimal base capacity combination of PVs that maximizes the total installed capacity is calculated for each time step. Consequently, a representative base capacity of each PV is determined. In the next stage, using the daily PV generation profile and base capacity determined in the previous step, the maximum HC of each PV can be calculated.

A. Optimal PV base capacity estimation

The decision variables in the proposed optimization expressed as (1) include the capacity of each PV at the pre-determined location, the volt-var curve parameter of the SI, tap position of transformer, and reactive power output of SVCs. The optimal PV base capacity (PVBC) is defined in (2) as the maximum PV capacity over time calculated by solving the proposed optimization problem.

$$max \sum_{i=1}^{n_{pv}} \sum_{p=a}^{c} S_{PV.t}^{i.p},\ \forall t \in n_t$$

$$\textit{s.t. voltage, thermal limit constraints} \tag{1}$$

$$\boldsymbol{S_{PV}^{rep}} = \max\{\boldsymbol{S_{PV.1}}, \boldsymbol{S_{PV.2}}, \cdots, \boldsymbol{S_{PV.n_t}}\} \tag{2}$$

Based on the representative PVBC, a generation profile variable σ_t^{rep} is defined to calculate how much power generation is possible for each time step during the entire time

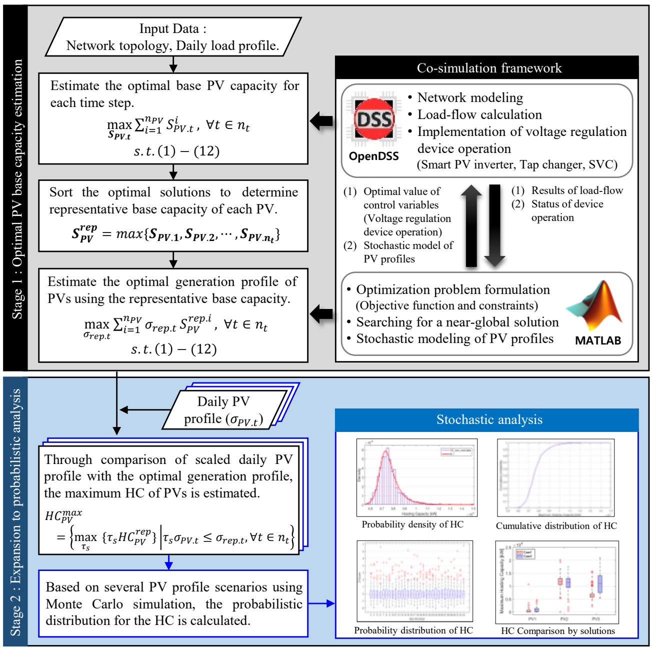

Fig. 1. Proposed two-stage optimization framework

horizon. The second optimization problem is formulated as (3) to estimate the maximum generation profile.

$$max \sum_{i=1}^{n_{pv}} \sum_{p=a}^{c} \sigma_t^{rep}\ S_{PV}^{rep.i.p},\ \ \forall t \in n_t$$

$$\textit{s.t. voltage, thermal limit constraints} \tag{3}$$

The graphical procedure and flow chart of proposed method are shown in Fig 1. To solve proposed optimization problems, a co-simulation environment is suggested using MATLAB with the OpenDSS.

B. Expansion to probabilistic analysis

Through the proposed process, one maximum HC of PVs is calculated for each actual PV profile curve. In this paper, based on the historical data for past years, numerous PV generation curves during the analysis time horizon (one day) following the probability distribution of actual irradiance records are generated. Then, the probabilistic HC of PVs is assessed through the repetition of the proposed method, reflecting the variability characteristic of PV.

III. FUTUREWORKS

The performance of the proposed calculation framework will be verified on the IEEE-123 test system. The sensitivity study on the various coordination strategy will be performed under proposed stochastic analysis on HC.

Data Anomaly Detection, Classification, and True Data Recovery in Real-time Wide-area Monitoring Applications

Kaustav Chatterjee, *Student Member, IEEE* and Nilanjan Ray Chaudhuri, *Senior Member, IEEE*
School of Electrical Engineering and Computer Science, Penn State University, USA

I. Problem Statement

High precision time-synchronized data from Phasor Measurement Units (PMUs) have enhanced situational awareness and real-time decision-making in modern power systems. However, owing to the chances of corruption in the measurements arising out of bad data outliers, missing data, and malicious injection of corruption samples due cyber attack, the accuracy of the monitoring algorithms may be compromised. Therefore, there is a need for development of online data preprocessing algorithms for detection of anomalous outliers and ensuring guaranteed data recovery following a successful detection. Further, the data streams may have outliers which appear similar to bad data but have origin in event-induced disturbances, and thus, contain useful monitoring information. Therefore, in addition, the data preprocessor should also be able to make a distinction between the nature of the outliers.

II. State-of-the-art Summary

Ideally, considering the underlying physics of the system, the measurement variables from multiple physical locations in the grid are expected to be spatio-temporally correlated. Building on this idea, several data-driven approaches have been proposed in literature which use low-rank matrix completion-like algorithms for outlier detection and correction. These methods, in general, assume that the data corruption to be sparse across PMU channels and/or time horizon. Leveraging on the sparsity of the outliers and low-rankness of the true measurements, first, the sources of bad data are identified and then, utilizing the correlated information from healthy PMUs, the true data from the corrupted PMU is recovered. However, with these, three major limitations have been identified: (1) these methods by themselves cannot differentiate between event-induced and bad data outliers, (2) the success of data recovery is dependent of the degree of correlation – and therefore, on the choice of PMU signals, and finally, (3) most of these being block-processing techniques are less suited to real-time applications. Going ahead, we propose a robust data recovery approach to address these challenges.

III. Proposed Approach

The contributions of this work are threefold. First, a clustering approach is proposed for grouping PMUs based on the relative modeshapes of the signal variables corresponding to the poorly-damped modes in the system. This is shown to increase the denseness of the individual signal groups and enhance data correlation for oscillatory transients, and therefore, improve the chances of guaranteeing data recovery using low-rank matrix completion methods. Second, a kernel principal component analysis (KPCA)-based unsupervised learning framework is adopted to classify between the nature of data outliers. It is shown that with suitable choice and tuning of kernel parameters, a linear separation between the bad data and event data outlier-classes can be obtained in a higher-dimensional feature space. This helps identifying the sources of bad data for further processing, while preserving the signatures of event-induced disturbances. And third, a sparse optimization-based vector processing approach is formulated (as shown in Fig. 1) for recovering true measurements data from bad data. Note that, the anomaly detection, classification, and data recovery is performed independently for each signal group, thereby, parallelizing the process across clusters.

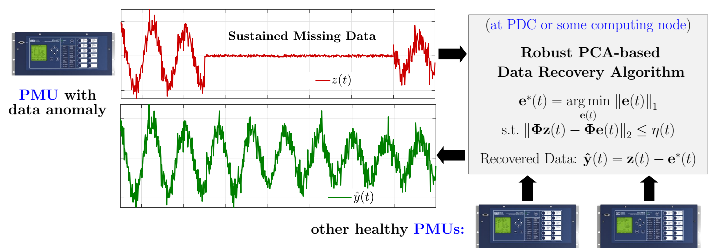

Fig. 1: Anomaly detection and data recovery in each signal cluster/group.

IV. Results

Bus voltage magnitude data from 40 different PMU locations in New York Power Authority (NYPA) are considered. Based on their modeshapes, the signals are clustered into two groups. $|V_6|$ and $|V_{27}|$ from group 1 and $|V_7|$ and $|V_{22}|$ from group 2 are artificially corrupted. Data recovery corresponding to two different types of corruption – sustained missing data and spurious outliers are studied, as shown in Fig. 2.

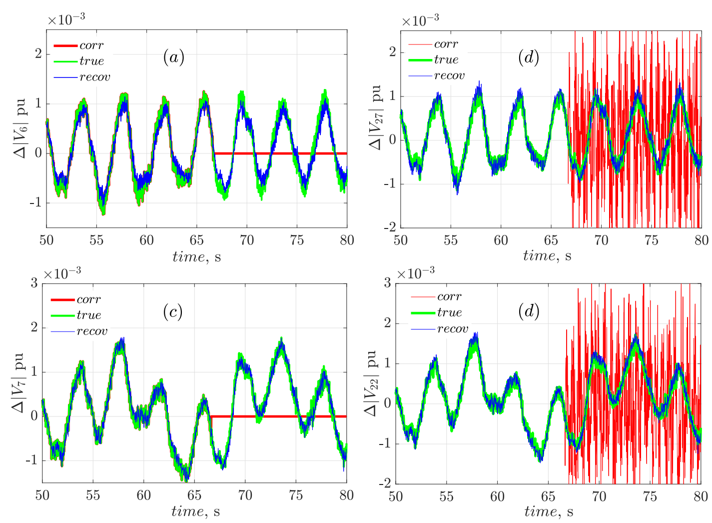

Fig. 2: Data recovery for signals in (a)-(b) group 1 and (c)-(d) group 2.

V. Conclusions

In this work, resilience of power system monitoring to spurious bad data and cyber attacks is studied. Robust algorithms are developed for real-time attack detection, classification, localization, and data recovery.

Impacts of Effective Grid Impedance on Inverter Based Resources Plant

Himadry Shekhar das, *Student Member, IEEE*, Shuhui Li, *Senior Member, IEEE*, and Bing Lu
Department of Electrical and Computer Engineering
The University of Alabama
Tuscaloosa - 35401, U.S.A.
hdas@crimson.ua.edu; sli@eng.ua.edu; blu2@crimson.ua.edu

***Abstract*— Nowadays a large number of inverter-based resources (IBRs) are integrated into the grid at a single connection point as an IBR plant. Due to the increase in number of IBRs in an IBR plant, the effect of IBRs on the grid impedance fluctuation as well as the effect of variation in grid impedance on the IBRs became significant. Several abnormal events have been reported due to this phenomenon. In this article, the reason of these abnormalities are analyzed from a novel point of view. The equivalent dynamic or effective grid impedance concept is developed and introduced to analyze the effect of multiple IBRs and their injected current into the grid. Also, the effects of the effective grid impedance on the IBR design, control, operation, and stability are analyzed. A frequency sweep simulation model is used to evaluate the impact of the effective grid impedance. The results show that the effective grid impedance, i.e. grid strength, changes with the number of IBRs added into an IBR plant. Conversely, the variation of the effective grid impedance has multiple effects on IBRs with different grid-connected filters, such as PCC voltage and harmonic stability and IBR controller stability.**

***Index Terms*-- inverter-based resources, vector control, grid-connected filters, effective grid impedance, stability, weak grid**

I. Introduction

The introduction of increased renewable energy sources, such as solar photovoltaic (PV) and wind power plants, is transforming the nature of modern electric power grid. These renewable energy sources are connected to the grid using power electronic converters and grid-connected filters, thus called inverter based resources (IBRs). Three most common grid-connected filtering topologies are L, LC and LCL filters. In most of the cases, IBRs are set up in multiple numbers to generate larger amount of power, which is called an IBR plant. Grid impedance is a crucial element of modern power system, as it governs the IBR system and controller design and operating performance. The dynamic nature of grid impedance in an IBR plant can lead to abnormal operations in power system. Various abnormal operation in IBR plants have been reported in recent years.

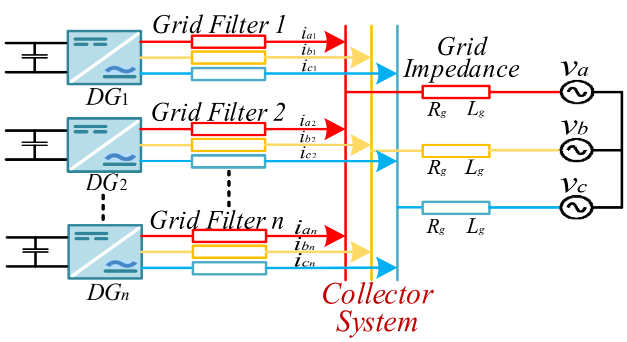

Fig. 1 Schematic of IBRs within an IBR plant connected to the grid

In this article, a novel equivalent dynamic grid impedance or effective grid impedance concept is developed and introduced for integration of an IBR plant with the grid. The effect on the effective grid impedance to the IBRs and IBR plant is analyzed by considering IBR control, filter design, the number of IBRs added in the plant, all of which affects the interconnection of the IBRs to the grid. The newly developed effective grid impedance concept is employed to evaluate previously reported IBR abnormal operation events based on theoretical and simulation studies presented in this paper.

II. Effective Grid Impedance of IBRs within an IBR Plant

Fig. 1 shows the equivalent circuit of the IBRs within an IBR plant connected to grid. Neglecting the impedance of the collector system, the voltage balance equation across the grid impedance is:

$$\left[v_{a,b,c\_PCC}\right] = R_g \sum_{k=1}^{n}\left[i_{a,b,c\_k}\right] + L_g \frac{d}{dt}\sum_{k=1}^{n}\left[i_{a,b,c\_k}\right] + \left[v_{a,b,c}\right] \quad (1)$$

If all the IBRs within the IBR plant produce the same current then,

$$\left[v_{a,b,c\_PCC}\right] = n \cdot R_g\left[i_{a,b,c}\right] + n \cdot L_g \frac{d}{dt}\left[i_{a,b,c}\right] + \left[v_{a,b,c}\right] \quad (2)$$

From (2), it can be seen that the grid impedance impact to the IBRs within an IBR plant depends not only on the grid but also on the number of the IBRs connected to the grid.

III. Impacts of Effective Grid Impedance

From the study it's found that the variation in effective grid impedance can heavily impact the operation and reliability of IBR based systems.

1) As the number of the IBRs connected to the grid increases, the PCC voltage impact becomes more evident for both weak and strong grid conditions.

2) For IBR with an L filter, the PCC voltage increases greatly at high order harmonics as the number of IBRs increases, although high order harmonic contents are typically small.

3) For LC or LCL filter, the PCC voltage impact becomes critical at and around the resonant frequencies that could be near the IBR current controller crossover frequency and thus affect the IBR control stability.

4) The IBR PCC voltage stability and harmonic stability depend not only the system strength but also are more importantly affected by the number of IBRs connected to the grid or the effective grid impedance.

Community Pool-Based Active-Hour Appliance Management Model

Shitikantha Dash, *Student Member, IEEE,* Ranjana Sodhi, *Member, IEEE,* and Balwinder Sodhi

***Abstract*—This paper proposes a model to cater the urgent energy requirement of an unscheduled active-hour (AH) appliance by curtailing or deferring other residences' AH appliances. A pool-based trading strategy is employed for the residences of an energy community to facilitate the decision-making in near real-time. Preliminary results reveal the effectiveness in supplying the energy need of AH appliances without violating the pre-committed total demand.**

***Index Terms*—Energy Management, Community, Aggregator**

I. Introduction

The prime goal of home energy management systems (HEMS) installed in smart residences (SR) is to control the appliances' energy consumption so as to minimise the total cost while maintaining end-users' comfort level above the desired limit. Every HEMS declares its day-ahead (DA) consumption based on the introductory price and receives a final price after the market clears [1]. This process is often brokered by an aggregator. Any additional purchase of energy may cost SRs higher depending on the real-time prices. Hence, HEMS prefers to reschedule or curtail the appliances instead of purchasing more energy. This rescheduling of appliances may end up with comfort limit violation or operating constraints violation [2]; because earlier, these appliances were scheduled by HEMS at optimal user comfort to minimise the consumption cost leaving little room for uncertainties. In this case, a trade-off is done to choose between purchasing more power or reducing consumption [3].

This paper proposes a pool-based local energy trading strategy within a community to address the energy need of an unscheduled active-hour (AH) appliance without violating the committed schedule. These AH appliances, traditionally considered as non-responsive, are the appliances that demand an active presence of end-user for its efficient operation *e.g.* a cooking top or a vacuum cleaner *etc.*, and it is primarily responsible for many unavoidable violations. The proposed strategy works by exploiting certainty associated with these appliances' operation to tackle total load demand uncertainty.

II. Methodology

In the proposed method, the community pool consists of potential sellers ($s \in \mathcal{S}$). It *clears* for each buyer ($b \in \mathcal{B}$) added in the pool to cater the energy need (E_b) of AH appliances as soon as possible. The process is also assisted by an *queue* that stores uncleared bs to be tried in next Δt; where t is the time instance when HEMS clears responsive loads. All demand bids and potential selling offers are converted into an effective price ($\zeta_{a,\Delta t}$) by taking comfort level ($\psi_{i,\Delta t}$), price sensitivity (α_i) end-users and their dearness ($\mu_{a,\Delta t}$) towards the appliance

Algorithm 1 Event-wise Pool clearing procedure

for each b added to the Pool **do**
  $\underset{f_{s,\Delta t}\ \forall s}{\text{Minimize}} \left|\zeta_{b,\Delta t} - \sum_{s=1}^{\mathcal{S}} (\zeta_{s,\Delta t} \times f_{s,\Delta t})\right|$
  Subject to:
    $E_{b,\Delta t} \leq \sum_{s=1}^{\mathcal{S}} (\zeta_{s,\Delta t} \times f_{s,\Delta t})$
$\zeta^{+}_{a,\Delta t} = \left(\alpha_i \times \sum_{s=1}^{\mathcal{S}} \left(\lambda^{offer}_{s,\Delta t} \times f_{s,\Delta t}\right)\right)$
return min.($\zeta^{+}_{a,\Delta t}$, $\alpha_i \times \lambda_{\Delta t} \times E_b$, $\zeta^{-}_{hvac,\Delta t}$)

($a \in \mathcal{A}_i$) into account. Here, a is an AH appliance of i^{th} SR whose role as b or s is not yet decided. And, the factor *price sensitivity* tells us how end-user feels towards the cost deduction or addition.

Initially, all scheduled AH appliances in the community are included in the pool. And, the unscheduled appliances are added in real-time when started consuming the power. If HEMS realises that supplying energy to an unscheduled a by curtailing HVACR $\zeta^{-}_{hvac,\Delta t}(\psi_{i,\Delta t}, \mu_{a,\Delta t})$ violates the optimum comfort limit and retaining it $\zeta^{+}_{a,\Delta t}(\alpha_i, \lambda_{\Delta t})$ could be less expensive than the real-time cost ($\lambda_{\Delta t} \times E_a$), it enrols a in the pool as a buyer b. Then, the pool clears the b as per Algorithm-1. Here, $\lambda_{\Delta t}$, $\lambda^{bid}_{b,\Delta t}$ and $\lambda^{offer}_{s,\Delta t}$ are the real-time price offered by the grid, maximum price limit set by bidder and offer by the seller.

III. Findings and Conclusion

Preliminary results are encouraging and reveal the effectiveness in supplying the energy need of AH appliances without violating the pre-committed total demand.

References

[1] Y. Wu, M. Barati, and G. J. Lim, "A pool strategy of microgrid in power distribution electricity market," *IEEE Transactions on Power Systems*, vol. 35, no. 1, pp. 3–12, 2020.

[2] O. Erdinç, A. Taşcıkaraoğlu, N. G. Paterakis, Y. Eren, and J. P. S. Catalão, "End-user comfort oriented day-ahead planning for responsive residential hvac demand aggregation considering weather forecasts," *IEEE Transactions on Smart Grid*, vol. 8, no. 1, pp. 362–372, 2017.

[3] Y. Chen, S. Mei, F. Zhou, S. H. Low, W. Wei, and F. Liu, "An energy sharing game with generalized demand bidding: Model and properties," *IEEE Transactions on Smart Grid*, vol. 11, no. 3, pp. 2055–2066, 2020.

Targeted False Data Injection Attack against DC State Estimation without Line Parameters

Mingqiu Du, *Student Member, IEEE*, Georgia Pierrou, *Student Member, IEEE* , Xiaozhe Wang, *Senior Member, IEEE*

***Abstract*—A novel false data injection attack (FDIA) model against DC state estimation is proposed, which requires no network parameters and exploits only limited phasor measurement unit (PMU) data. The proposed FDIA model can target specific states and launch large deviation attacks using estimated line parameters. Sufficient conditions for the proposed method are also presented. Different attack vectors are studied in the IEEE 39-bus system, showing that the proposed FDIA method can successfully bypass the bad data detection (BDD) with high success rates of up to 95.3%.**

***Index Terms*—DC state estimation, false data injection attacks, stochastic process, phasor measurement unit**

I. Introduction

In this paper, we propose a novel FDIA model against DC state estimation that can target specific states without knowing any line parameters. Compared to network topology information critically protected and rarely transmitted, phasor measurement unit (PMU) measurements are easier to acquire through communication networks

In contrast to previous works that require measurements from remote terminal units (RTUs), the proposed attack model requires only PMU measurements for designing the FDIA and can target specific states without any pre-knowledge on line parameters.

II. FDIA Model

In order to launch a stealthy FDIA to bypass the BDD, the attack vector $\boldsymbol{a}$ needs to satisfy $\boldsymbol{a} = H\boldsymbol{c}$.

- substituting P_{tj} by the fake $\tilde{P}_{tj}$ for $\forall j \in \Omega_A, j \neq t$:

$$\tilde{P}_{tj} = B_{tj}(\tilde{\delta}_t - \delta_j) \tag{1}$$

- substituting P_t, P_j by the fake $\tilde{P}_t, \tilde{P}_j$:

$$\tilde{P}_t = \sum\nolimits_{j\in\Omega_A}^{j\neq t} \tilde{P}_{tj} \tag{2}$$

$$\tilde{P}_j = P_j + \tilde{P}_{jt} - P_{jt} \tag{3}$$

If the designed deviation $\boldsymbol{c} = [\tilde{\delta}_t - \delta_t]^T$, then the attack vector $\boldsymbol{a} = [\tilde{P}_{ti} - P_{ti}, \tilde{P}_i - P_i]^T, \forall j \in \Omega_A, j \neq t, \forall i \in \Omega_A$.

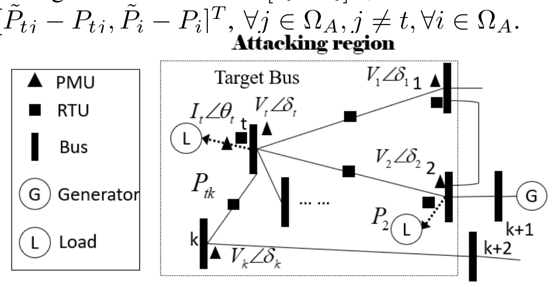

Fig. 1: The definition of attacking region

Inside an attacking region, the system can be represented by differential-algebraic equations:

$$\dot{\boldsymbol{x}} = f(\boldsymbol{x}, \boldsymbol{z}) \tag{4}$$

$$\boldsymbol{z} = H\boldsymbol{x} \tag{5}$$

$$\dot{\delta}_i = \frac{1}{\tau_{p_i}}(P_i^s(1+\sigma_i^p\xi_i^p) - P_i) \tag{6}$$

$$P_i = \sum_{j\in\Omega_i} B_{ij}(\delta_i - \delta_j) \tag{7}$$

$$\begin{bmatrix} \dot{\delta}_1 \\ \dots \\ \dot{\delta}_k \end{bmatrix} = \underbrace{\begin{bmatrix} \frac{-1}{\tau_{p_1}} & \dots & 0 \\ 0 & \dots & 0 \\ 0 & 0 & \frac{-1}{\tau_{p_k}} \end{bmatrix} \begin{bmatrix} \sum\limits_{j\in\Omega_i} B_{1j} & \dots & -B_{1k} \\ \dots & \dots & \dots \\ -B_{k1} & \dots & \sum\limits_{j\in\Omega_i} B_{kj} \end{bmatrix}}_{A} \begin{bmatrix} \delta_1 \\ \dots \\ \delta_k \end{bmatrix}$$
$$+ \underbrace{\begin{bmatrix} \frac{1}{\tau_{p_1}} & \dots & 0 \\ 0 & \dots & 0 \\ 0 & 0 & \frac{1}{\tau_{p_k}} \end{bmatrix} \begin{bmatrix} P_1^s & \dots & 0 \\ 0 & \dots & 0 \\ 0 & \dots & P_k^s \end{bmatrix} \begin{bmatrix} \sigma_1^p & \dots & 0 \\ 0 & \dots & 0 \\ 0 & \dots & \sigma_k^p \end{bmatrix}}_{S} \begin{bmatrix} \xi_1^p \\ \dots \\ \xi_k^p \end{bmatrix} \tag{8}$$

$$\dot{\boldsymbol{\delta}} = A\boldsymbol{\delta} + S\boldsymbol{\xi^p} \tag{9}$$

$$\frac{d}{d\tau}[C(\tau)] = AC(\tau) \tag{10}$$

$$C(\tau) = E[(\boldsymbol{\delta}_{t+\tau} - E[\boldsymbol{\delta}_t])(\boldsymbol{\delta}_t - E[\boldsymbol{\delta}_t])^T] \tag{11}$$

$$A = \frac{1}{\tau}\ln[C(\tau)C(0)^{-1}] \tag{12}$$

$$\hat{\boldsymbol{\mu}}_\delta = \frac{1}{N}\sum_{i=1}^{N}\boldsymbol{\delta}^{(i)} \tag{13}$$

$$\hat{C}(0) = \frac{1}{N-1}\sum_{i=1}^{N}[(\boldsymbol{\delta}^{(i)} - \hat{\boldsymbol{\mu}}_\delta)(\boldsymbol{\delta}^{(i)} - \hat{\boldsymbol{\mu}}_\delta)^T] \tag{14}$$

$$\hat{C}(\Delta t) = \frac{1}{N-M-1}\sum_{i=1+M}^{N}[(\boldsymbol{\delta}^{(i)} - \hat{\boldsymbol{\mu}}_\delta)(\boldsymbol{\delta}^{(i-M)} - \hat{\boldsymbol{\mu}}_\delta)^T] \tag{15}$$

Thus, the adversary can obtain the estimated matrix $\hat{A}$ and time constant as follows:

$$\hat{A} = \frac{1}{\Delta t}\ln[\hat{C}(\Delta t)\hat{C}(0)^{-1}] \tag{16}$$

$$\underbrace{\begin{bmatrix} \frac{1}{\Delta t}(\delta_t^{(2)} - \delta_t^{(1)}) \\ \dots \\ \frac{1}{\Delta t}(\delta_t^{(n)} - \delta_t^{(n-1)}) \end{bmatrix}}_{\boldsymbol{Y}} = \underbrace{\begin{bmatrix} \hat{\mu}_{P_t} - P_t^{(1)} \\ \dots \\ \hat{\mu}_{P_t} - P_t^{(n-1)} \end{bmatrix}}_{\boldsymbol{X}} \begin{bmatrix} \frac{1}{\tau_{p_t}} \end{bmatrix} \tag{17}$$

A Cooperative Game Theory-based Approach to Under-frequency Load Shedding Control

Mukesh Gautam, *Student Member, IEEE* and Mohammed Benidris *Member, IEEE*,
Department of Electrical & Biomedical Engineering,
University of Nevada, Reno, Reno, NV 89557
(emails: mukesh.gautam@nevada.unr.edu and mbenidris@unr.edu)

***Abstract*—This paper proposes a cooperative game theory-based under-frequency load shedding (UFLS) approach for frequency stability and control in power systems. UFLS is a crucial factor for frequency stability and control especially in power grids with high penetration of renewable energy sources and restructured power systems. Conventional UFLS methods, most of which are off-line, usually shed fixed amounts of predetermined loads based on a predetermined schedule which can lead to over or under curtailment of load. This paper presents a co-operative game theory-based two-stage strategy to effectively and precisely determine locations and amounts of loads to be shed for UFLS control. In the first stage, the total amount of loads to be shed, also referred to as deficit in generation or the disturbance power, is computed using the initial rate of change of frequency (ROCOF) referred to the equivalent inertial center. In the second stage, the Shapley value, one of the solution concepts of cooperative game theory, is used to determine load shedding amounts and locations. The proposed method is implemented on the reduced 9-bus 3-machine Western Electricity Coordinating Council (WECC) system and simulated on Real-time Digital Simulators (RTDS). The results show that the proposed UFLS approach can effectively return the system to normal state after disturbances.**

***Index Terms*—Adaptive load shedding, co-operative game theory, frequency control, Shapley Value.**

I. The Proposed UFLS Approach

The load shedding is the fastest and ultimate way of preventing power systems from blackouts and damages initiated due to frequency drops. Load shedding is done when spinning reserves are exhausted. In this work, the proposed two-stage under-frequency load-shedding scheme is implemented in the following steps.

1) Calculation of disturbance power, P_d, based on observed ROCOF; and
2) Determination of locations and amounts of load shedding using the Shapley values.

The flowchart of the proposed UFLS approach is shown in Fig. 1.

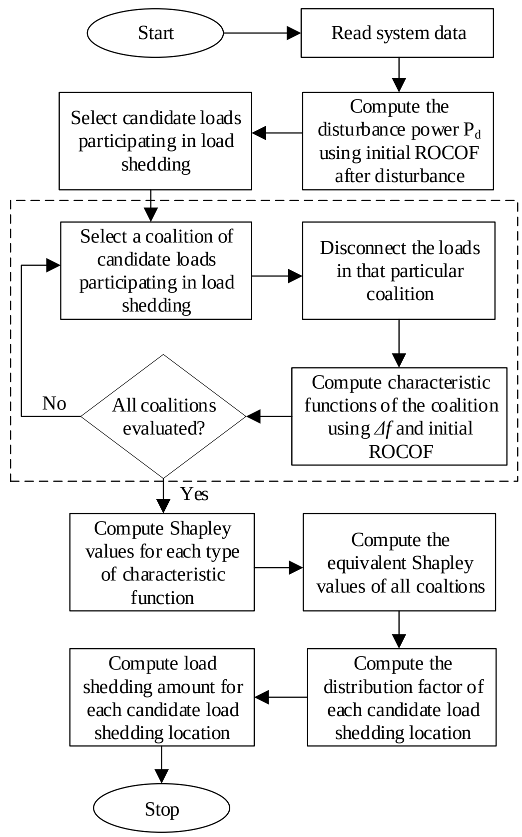

Fig. 1. Flow chart of proposed UFLS scheme

II. Case Study and Results

In order to study system dynamics with and without load-shedding, the WECC 9-bus system is simulated on RTDS considering the outage of machine-2 at second 5 and load-shedding after two seconds of the outage. The plot of system frequency (without and with load-shedding) of the reduced WECC 9-bus system, which are simulated on the RTDS, is shown in Fig. 2.

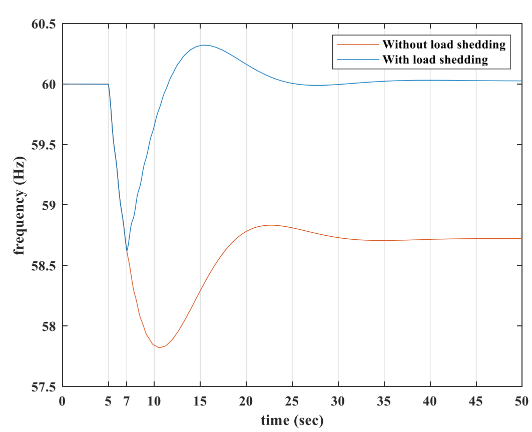

Fig. 2. Plot of system frequency

Home Energy Management System for Coordinated PV and HVAC Controls based on AI Forecasting

Huangjie Gong, *Student Member, IEEE*, Rosemary E. Alden, *Student Member, IEEE*, Dan M. Ionel, *Fellow, IEEE*

***Abstract*—Home Energy Management Systems (HEMs) are of growing importance and interest for the future smart grid. They facilitate energy savings and demand response (DR) at the individual home level and represent an opportunity for coordination among homes within a power system to reduce over all peak load and incorporate distributed energy resources. Artificial intelligence (AI) provides in academia satisfactory forecasting for both power usage and photovoltaic (PV) generation, and thus, a HEMs control schematic based on these forecasts is proposed in this work. Experimental data from a residential field demonstration managed by the Electric Power Research Institute (EPRI) is used to model the home by calculating the equivalent thermal resistance. An example case study for the control of the heating ventilation and air conditioning (HVAC) system shows that residences with HEMs could be used as dispatchable distributed energy generators and loads.**

***Index Terms*—Big data, demand response, variable loads, machine learning, residential, load shifting**

I. Home Energy Management Systems and Control

We propose for future smart residencies, such as the field demonstration by the Electric Power Research Institute (EPRI) as part of the SHINES project, a control scheme from data acquisition, processing, and load forecasting to a control scheme implementation in a HEMs. The EPRI SHINES homes, H1 and H2, are equipped with energy monitoring technology for total, HVAC, solar, and water heater. Three years of experimental data for theses smart houses are available to the public including power and weather.

In the proposed demand response (DR) control, the load and PV generation for the upcoming day could be forecast by an artificial intelligence (AI) model. The control algorithm could then plan ahead an optimal residential net power flow based on the predicted PV and load power. A visualization of the HEMs structure described is shown in Fig. 1. One application of this HEMs is to shift the peak power of the HVAC system to when renewable energy is available, reducing peak power and avoiding PV curtailment at the same time.

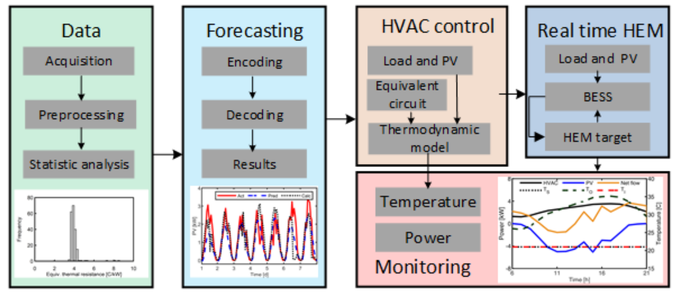

Figure 1. The proposed HEMs control schematic. Data is pre-processed before the ML procedure. The proposed HVAC control is based on the prediction for solar generation and outdoor temperature. A BESS is included in the HEMs and controlled by the difference between prediction and real-time data.

II. Experimental Case Study for HVAC System

An example case study into HVAC control for the SHINES H1 house, has been conducted using experimental data on July 11th, 2020 to represent a typical summer day. The data from June to September, 6am-9pm, 2018-2020 for the SHINES Homes was used to model the home's HVAC system through a calculation of the equivalent thermal resistance.

It was assumed that the HVAC was ON in cooling mode when the temperature difference between outdoor and indoor was larger or equal to 12°C. A constant temperature set point of 21°C was also assumed for the uncontrolled HVAC case, as shown in Fig. 2 (a). The HVAC system was controlled by changing the set point and calculating the new load based on the equivalent thermal resistance. The proposed HVAC control scheme results in a relatively constant net power flow for a longer duration as shown and explained in Fig. 2 (b.). Additionally, the HVAC energy usage was reduced by 5kWh as compared with the baseline case. It is important to note that the indoor temperature around 6pm, the expected occupant arrival time, was returned to 21°C and, thus, user comfort is unaffected.

Should a relatively small Battery Energy Storage System (BESS) be included, e.g., with a 5kWh capacity, the net power flow fluctuations would be eliminated, and power flow of the house would be equal to zero in the time during between 9am and 2pm. Additional control schemes will be conducted and presented based on AI electric load forecasting.

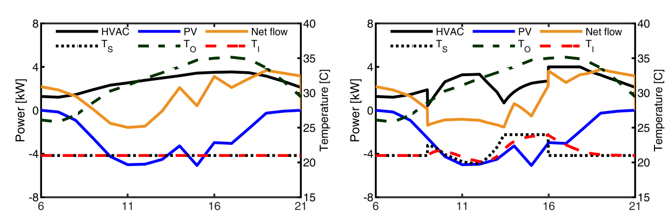

(a) (b)

Figure 2. The power and temperature on an example summer day of a) baseline case; b) controlled HVAC case. The house net power became near constant from 9am to 2pm, even though the HVAC system was the only controlled component. When battery is considered in the HEMs, the house can be a dispatchable distributed generator resource.

Data-driven Modeling of Power Electronic Converters with Grid Support Functions

Nischal Guruwacharya†, Ujjwol Tamrakar, Timothy M. Hansen, and Reinaldo Tonkoski
Department of Electrical Engineering and Computer Science
South Dakota State University
Brookings, South Dakota, USA 57007

***Abstract*—With the increase in inverter-based generation-integration in the modern grid and their different dynamics compared to traditional generation, power system dynamics need to be assessed using accurate models. This becomes of particular importance when they also provide voltage and frequency support to the grid. For instance, the IEEE 1547-2018 standard recommends distributed energy resources to provide grid support functions (GSFs). These GSFs are capable of providing a number of grid services such as volt-watt, volt-var, frequency-watt, voltage or frequency ride through, communication capabilities and ramp-rate control. This paper presents a development of statistical linear model for power electronic converters with GSFs. This linear model is used to explore the dynamics of converter under several GSFs. Results show that the developed linear model can be used for dynamic study of converter dominated power systems.**

I. Introduction

A significant amount of inverter-based generations, such as photovoltaic, wind, and energy storage systems are being integrated into the bulk electric power grid to fulfill the future electric demand. Such inverter-based distributed energy resources will be providing multiple grid support functions (GSFs) to support voltage and frequency control of the power system [1].

Power system dynamics changes depending on different GSFs. Due to which conventional linear modeling techniques, such as state-space averaging techniques and switching functions, become imprecise in capturing all the dynamics of interest. Non-linear modeling techniques can be complex and require detailed knowledge of the exact converter parameters, topology, and/or control strategy. Moreover, the non-linearity in modeling these converters across various operating point, results in complicated models that are computationally intractable for real-time control. So, this motivates data-driven system identification techniques to model power electronic converters (PECs) equipped with GSFs in different operating point. Based on different GSFs features, operating modes are divided into several multiple linear models. For example in volt-var mode, the droop curve is divided in to six region and six linear models are develop to represent these regions.

II. Key Figures

A schematic diagram of a grid-connected inverter system with both normal and GSFs features and operating in current control mode is shown in Figure 1.

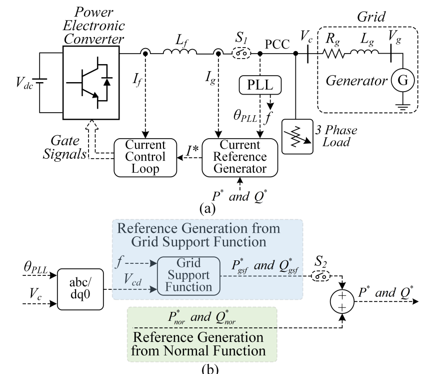

Fig. 1: Schematic diagram of the various components and control loops in a grid-connected inverter system with both normal and GSFs.

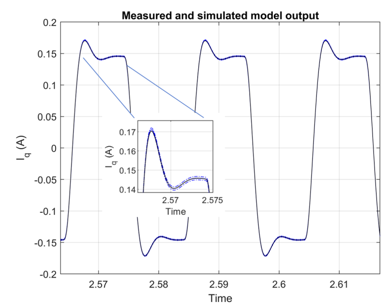

Fig. 2: Measured versus simulated output of the fitted transfer function along with the 95% confidence interval of the estimate.

III. Conclusions and Future Work

This paper presents a MATLAB/Simulink model for a PEC with the GSFs introduced in the IEEE 1547-2018 Standard. The model is intended for evaluation of power system dynamics with high penetration of DERs. Different linear models are developed based on different operating points. Result shows that the developed linear model can be used for voltage dynamic study of power systems. In future, data-driven model of the PEC with GSFs will be developed for frequency dynamics.

References

[1] N. Guruwacharya, N. Bhujel, T. M. Hansen, S. Suryanarayanan, R. Tonkoski, U. Tamrakar, and F. Wilches-Bernal, "Modeling inverters with grid support functions for power system dynamics studies," in *2021 IEEE Power Energy Society Innovative Smart Grid Technologies Conference (ISGT)*, 2021, pp. 1–5.

Detection of Small Changes in Power Systems with Hardware-in-Loop Testing

Sanjay Hosur and Dongliang Duan

***Abstract*—In this paper, the subspace based output only detection algorithm proposed in our previous work [1] is applied to detect small changes in power systems. In this work, the disturbances considered are the ones that cause the operating point of power systems to change gradually or subtly over time, which are difficult to be captured by most existing detection tools. The simulation is carried out using the Opal-RT Real Time Digital Simulator (RTDS). The IEEE 39-bus system is simulated with this hardware in the loop testing platform. The changes studied are slow load rampings in the system. Results show that these small changes can be well detected by our algorithm.**

I. Hardware-in-the-Loop Setup

The standard IEEE 39-bus power system is simulated on the Opal-RT Real Time Digital simulator (RTDS). The load is varied externally and given as an input to the simulated system. For simulation, the system model is built in simulink. Using the RT-Lab software, which is a proprietary software of Opal-RT, the modeled system is compiled and run on the RTDS.

The total simulation time is 5.5 hours. The load ramping starts at 1.5 hours and ramped up till 4.5 hours. The load connected to bus 20 of the simulated system is ramped up. The ramp has a slope of 5×10^{-6} as we want to see the behavior of algorithm for small changes. The data is collected at 100 samples/second and down sampled to 5 samples/second. The data from 30 mins to 1 hour is used for null space estimation. The algorithm is run from hour 1 to hour 5.5 of the simulation time with 10 min sliding window.

The Fig. 1(a) shows how the real power of the load connected to bus 20 is varied over time. The starting point of the load variation is taken directly from the solved power flow. The figure shows only the variation profile but not the absolute load values. It can be seen that the slope is very small and the increment in the load is not significantly large. The algorithm is able to detect the change in system's operating point even when it is this small.

II. Results

For the hardware-in-the-loop testing, the standard IEEE 39-bus system is used. This system will have 40 channels based on the order chosen. The channel responding first, i.e., the channel that first shows deviation from 0 will be shown here since this is the used for rising the alarm with the help of the OR rule. This is done to avoid the clutter created by drawing all the 40 curves. The results presented here are of only one test of the two tests being run in parallel based on which test responded earlier.

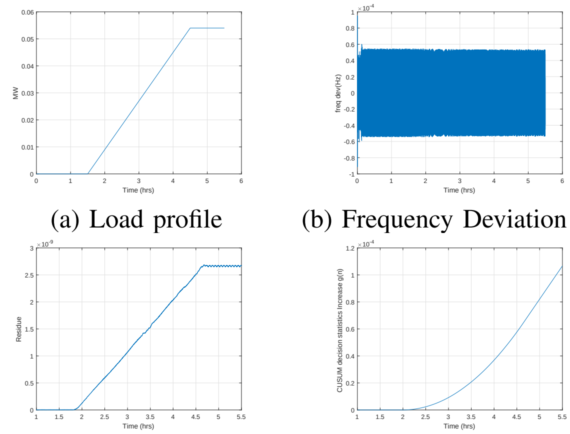

(a) Load profile (b) Frequency Deviation

(c)Residue (d) CUSUM Decision Statistics

Fig. 1: IEEE 39-bus system results

The Fig, 1(b) shows the frequency deviation exhibited by the system whose nominal operating frequency is 60 Hz which is also the nominal operating frequency of the North American grid. If the frequency deviation graph is observed it is impossible to conclude that any change is occurring in the system from 1.5 hrs to 4.5 hrs of the simulation.

Fig. 1(c) shows the residue corresponding to Eq. (5) in [2] from the channel which responded for the change. This figure starts at 1 hours as the algorithm is started after estimating the initial null space. The change is seen after about twenty minutes due the fact that the change in the system is very small and also the sliding window has about 10 minute memory.

Fig.1(d) shows the CUSUM decision statistics corresponding to Eq. (11d) in [2] indicating the test that responded first was the one checking for **increase** in mean. Here it can be seen that there is more delay before the change is seen. This is in agreement with results of our previous work in [1], where it was shown that for having lower false alarm rate and missed detection rate, the price is paid by having a slightly higher delay of detection.

References

[1] S. Hosur and D. Duan, "Sequential detection of forced oscillations in power systems using the cusum procedure," in *2019 IEEE Power & Energy Society General Meeting (PESGM)*. IEEE, 2019, pp. 1–5.

[2] ——, "Detection of small changes in power systems with hardware-in-loop testing," in *2021 IEEE Power & Energy Society General Meeting (PESGM)*. IEEE, 2021, pp. 1–5.

This work was in part supported by the Department of Energy under grant DE-SC0012671 and the National Science Foundation under awards ECCS-1828066 and OAC-1923983.Emails: shosur@uwyo.edu, dduan@uwyo.edu.

Impact of Phase-Lock-Loop Controller on the Small-signal Stability of Grid-connected Droop-controller Microgrid Connected to RL Load

Khalid Hurayb, and Dagmar Niebur
Electrical and Computer Engineering Department
Drexel University
Philadelphia, PA 19104
Emails: kmh465@drexel.edu; den22@drexel.edu

***Abstract*—Recent research efforts focused on microgrid (MG) models with the goal to improve power grid reliability and resilience. Most of the existing detailed grid-connected MG models, linear or nonlinear, assume perfect synchronization between the grid and MG leading to an inaccurate system representation. In this work, a Phase-lock-loop (PLL) controller has been implemented and the impact of its control parameters on small-signal stability of the MG has been investigated. The proportional and integral gains of the PLL controller have been varied and the corresponding small signal response characterized. It is shown that the system output response exhibits oscillations, amplitude overshoot/undershoot as a function of the controller gains.**

I. Main Contributions

Using the MG model proposed in [1] and building on the work published in [2] the following contributions were made:

- Construction of a linearized system model of the MG with PLL dynamics based on the model originally published in [1], and later modified in [2].
- Investigation of PLL converter dynamics on small-signal stability of grid-connected MG using PLL proportional and integral control.

II. System Description and PLL Modeling

The basic structure of the linearized state space model of the grid-connected MG with PLL controller and a RL load is shown in (1). Except for the PLL controller gains, all system parameters and corresponding state and input matrices are defined in [1]. Fig. 1 shows the implemented synchronous reference frame phase-lock loop controller (SRF-PLL) in the model. The inverter angle dynamics, which influences the resulting output voltage and current response, is given in (2).

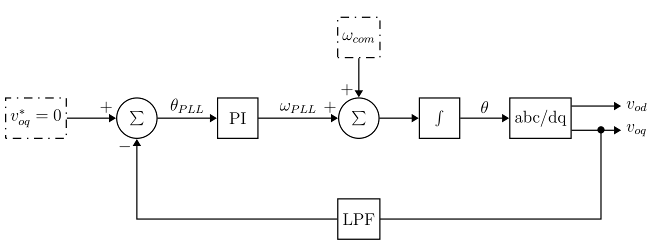

Fig. 1. Phase-lock loop controller

$$\triangle \dot{x} = A_{inv}[\triangle x] + B_{inv1}[\triangle v_{bDQ}] + B_{inv2}[\triangle \omega] \quad (1)$$

where the compact state variable x is

$$\triangle x^T = [\triangle\delta \, \triangle P \, \triangle Q \, \triangle\phi_d \, \triangle\phi_q \, \triangle\gamma_d \, \triangle\gamma_q \, \triangle i_{ld} \, \triangle i_{lq} \, \triangle v_{od} \, \triangle v_{oq} \, \triangle i_{od} \, \triangle i_{oq} \, \triangle i_{loadD} \, \triangle i_{loadQ} \, \triangle\theta_{PLL}].$$

$$\begin{aligned} \dot{\delta} &= \omega_n - \omega_{com} - K_{iPLL}\theta_{PLL} - Pm_p \\ &\quad + K_{pPLL}\omega_c\theta_{PLL} + K_{pPLL}\omega_c v_{oq} \end{aligned} \quad (2)$$

III. Results

The top plot in Fig. 2 displays the linearized system's eigenvalue pair associated with K_{pPLL} moving toward the unstable region, see arrows, as the gain is increased. The direct component of the output current i_{od} in response to a reactive power disturbance with different K_{pPLL} value is captured in the bottom plot. K_{iPLL} is fixed to 5×10^{-4}.

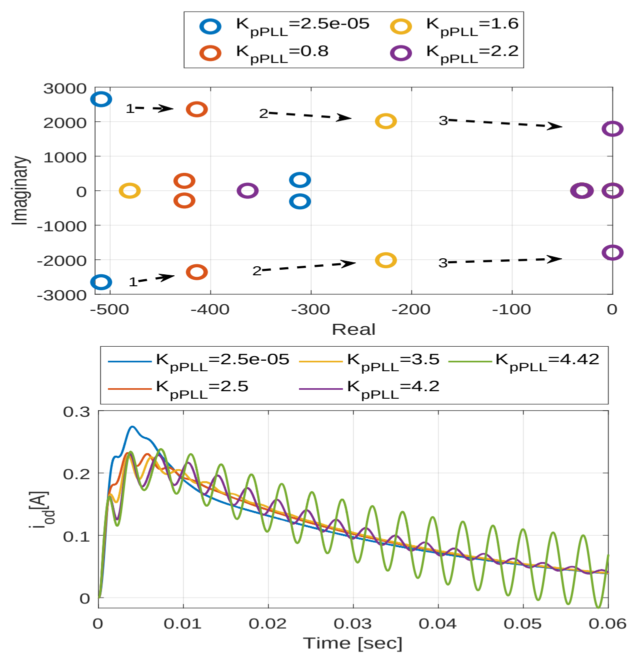

Fig. 2. The top and bottom graphs show the system eigenvalues and output current response i_{od} when only K_{pPLL} is varied.

References

[1] N. Pogaku, M. Prodanovic, and T. C. Green, "Modeling, analysis and testing of autonomous operation of an inverter-based microgrid," *IEEE Trans. Power Electronics*, vol. 22, no. 2, pp. 613–625, 2007.

[2] M. Kabalan, P. Singh, and D. Niebur, "Nonlinear lyapunov stability analysis of seven models of a dc/ac droop controlled inverter connected to an infinite bus," *IEEE Transactions on Smart Grid*, vol. 10, no. 1, pp. 772–781, 2019.

Estimating PV Plants Dynamic Model Parameters

Saima Ishaq, *Student Member, IEEE,* Timothy M. Hansen, *Senior Member, IEEE*

***Abstract*—Many efforts have been carried out in the past few years to develop dynamic models for simulation of photovoltaic (PV) as well as wind power plants that are open source, simple as well as generic. PVD1 was one such model developed with this objective. It was, however not adopted by all software platforms due to its limitations. Since the approval of the recent IEEE 1547 standard, and its added functionalities of voltage regulation as well as ride through capabilities of distributed energy resources (DERs), the DER_A model was proposed. This new generation of renewable energy source (RES) model had many advantages over the previous PVD1 model. However, it is limited in its representation of each inverters detailed dynamic modeling as well as assessing the total number of various inverters (legacy inverters as well as those following the most recent IEEE 2018 standards) behind the meter. This work will be highlighting the DER_A model's importance, utilization as well as limitation for DERs dynamic modelling. Detailed modeling of each inverter connected to the modern BPS may be complex due to data availability, computational time as well as usability. These factors will be compared and assessed in comparison with the DER_A model.**

I. Introduction

Due to the increasing perforation of DERs at the distribution level, the reliability of the BPS has been compromised. Therefore, interconnection standards like the IEEE 1547 and the California rule 21 have been introduced to regulate as well as monitor the effect of these DERs on the overall system. Hence, smart inverters were developed in an effort to provide controls and functionalities in accordance with these standards. Extracting inverters control parameters is imperative to study the systems dynamics as inverters participate in controlling voltage as well as frequency at different load conditions. PV Plant equipment suppliers do not provide all the information needed to study inverter dynamics due to confidentiality and IP concerns and even if this information is available, it is different from one manufacturer to another. Therefore, PV power plants model validation is a challenge in itself [1].

The current practice in the industry is to use RMS models of distributed energy resources (DER), such as DER_A [1]. The DER_A model (a newer form of the PVD1 model) is best suited to represent smaller scale solar PV plants that are connected at the distribution side or multiple solar PV plants that are aggregated at a high voltage bus, represented in power flow studies. However, these models use standard parameters to represent the inverter dynamics and control modes. There is a critical need for a method that properly extracts parameters and models PV plants as an aggregate to assess their dynamic response for power systems impact assessment studies. This motivates the design of data-driven non-linear system identification techniques to model power electronic converters equipped with advanced ancillary services (e.g., voltage and frequency support). Fig.1 shows the basic working principle of the system identification toolbox (SIT). Firstly, the unknown dynamic process is used to measure the input as well as the output signals. Once this dataset is gathered it is then fed into the system identification toolboxes algorithm [2]. This algorithm usually estimates the system model by minimizing a predefined cost function.

The relationship between the input as well as the outputs of the SIT, is defined in (1) where the number of poles and zeros of a system under consideration are represented by n and m respectively. Similarly, a_n and b_m are the parameters of the equivalent transfer function:

$$y(t)+a_1y(t-1)+...+a_ny(t-n) = b_1u(t-1)+...+b_mu(t-m) \tag{1}$$

The SIT uses the collected input and output data to fit a set of models with a varied number of poles and zeros. This model fit can be assessed using the normalized-root-mean-square-error (NRMSE) defined as:

$$NRMSE = 1 - \frac{\|y(t) - \hat{y}(t \mid \theta)\|}{\|y(t) - mean(\hat{y}(t \mid \theta))\|} \tag{2}$$

We present the development of these smart inverter models that will be aggregated together and connected to the main grid, to represent a PV plant, and will be used to study the changes on power system stability brought by these DERs. These inverter models can operate in both normal mode as well as in Grid Support Functions mode.

II. Key figure

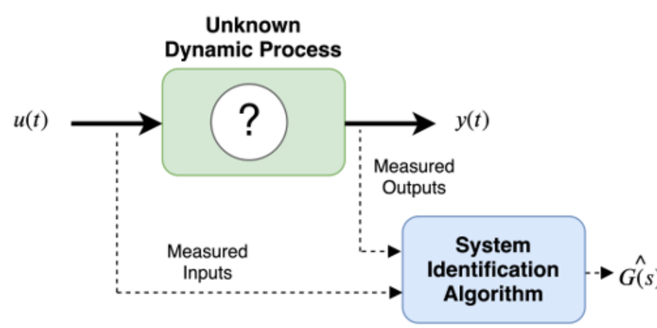

Fig. 1. System Identification Toolbox adapted from [1].

References

[1] N. Guruwacharya, N. Bhujel, U. Tamrakar, M. Rauniyar, S. Subedi, S. E. Berg, T. M. Hansen, and R. Tonkoski, "Data-driven power electronic converter modeling for low inertia power system dynamic studies," in *2020 IEEE Power Energy Society General Meeting (PESGM)*, 2020, pp. 1–5.

[2] System identification toolbox. [Online]. Available: https://www.mathworks.com/products/sysid.html

A Reinforcement Learning Method for Power Suppliers' Strategic Bidding with Insufficient Information

Qiangang Jia[1], *Student Member, IEEE*, Zhaoyu Hu[1], Yiyan Li[1,2], *Member, IEEE*, Zheng Yan[1] and Sijie Chen[1], *Member, IEEE*
1. School of Electronic Information and Electrical Engineering, Shanghai Jiao Tong University, Shanghai, 200240 China.
2. Department of Electrical and Computer Science, North Carolina State University, Raleigh, NC 27695 USA.
Email: jiaqiangang@sjtu.edu.cn, yli257@ncsu.edu

***Abstract*—The power market is a typical imperfectly competitive market. Power suppliers have enough incentives to exercise market power to gain higher profits. However, the issue of how to exercise market power becomes difficult when external information is extremely rare. To get a promising performance in an extremely incomplete information market environment, a novel model-free reinforcement learning algorithm based on the Learning Automata (LA) is proposed. Besides, the gaming process of the power suppliers is modeled as a repeated game rather than a stochastic game. Finally, numerical simulations show the effectiveness of the proposed algorithm.**

Keywords—reinforcement learning, learning automata, incomplete information, repeated game

I. Introduction

The contributions of this paper are outlined below:

-This paper constructs the gaming process of the power suppliers as a repeated Cournot game rather than a stochastic game to reflect the nature of the market-clearing process more accurately.

-This paper proposes a novel reinforcement learning algorithm that combines the advantages of the FALA and the CARLA to help power suppliers optimize bids in a repeated game with incomplete information. Rationality and convergence are tested in a Cournot model without and with transmission line constraints, respectively.

II. Proposed Algorithm for Supplier's Strategic Bidding

A. Proposed Algorithm

The action space in this bidding optimization problem in the repeated Cournot game is the lower and upper limits of the bidding quantities. We define the PDF at the t^{th} iteration as $N(\mu_t,\sigma_t)$. Each power supplier bids the random action x and the mean value μ of the action PDF to the environment alternately. Set b_x as the profit corresponding to the random action x, b_μ as the profit corresponding to the mean action μ. The update process only involves the adjustment of the two parameters, making the algorithm more computational trackable than the existing CARLA algorithm.

The detailed update rule of the proposed algorithm is demonstrated as follows.

$$\mu_{t+1} = \mu_t + k_\mu \cdot \delta_\mu \tag{1}$$

$$\sigma_{t+1} = \sigma_t + k_\sigma \cdot \delta_\sigma - c \tag{2}$$

The definitions of k_μ and k_σ are as follows.

$$k_\mu = \begin{cases} sign(x-\mu), & b_x > b_\mu \\ sign(\mu - x), & b_u > b_x \end{cases} \tag{3}$$

$$k_\sigma = \begin{cases} 1 & \begin{matrix} b_x > b_\mu \ \& \ x-\mu > \sigma \\ b_x < b_\mu \ \& \ x-\mu \le \sigma \end{matrix} \\ \text{-1} & \begin{matrix} b_x > b_\mu \ \& \ x-\mu < \sigma \\ b_x < b_\mu \ \& \ x-\mu \ge \sigma \end{matrix} \end{cases} \tag{4}$$

Besides, the update resolution of mean value μ and the standard deviation σ is fixed to a constant value, making the learning process more robust, guaranteeing better performance in convergence.

III. Case Study

A. Rationality of the algorithm

The rationality is judged from three criteria, e.g., the profit, the action, and the LMP. The percentage errors of the profits, the actions and LMPs are all within 1.9% regardless of whether there is congestion compared to the best response calculated by the analytical method (The rationality of this algorithm is proved if the percentage errors are between 0 to 2%).

B. Convergence of the algorithm.

To test the convergence of the proposed algorithm, the two suppliers are all strategic players using this algorithm. The percentage errors of the profits, the actions and LMPs are all within 4.4% compared to the Nash equilibrium calculated by the analytical method regardless of whether there is congestion (The convergence of this algorithm is proved if the percentage errors are between 0 to 5%).

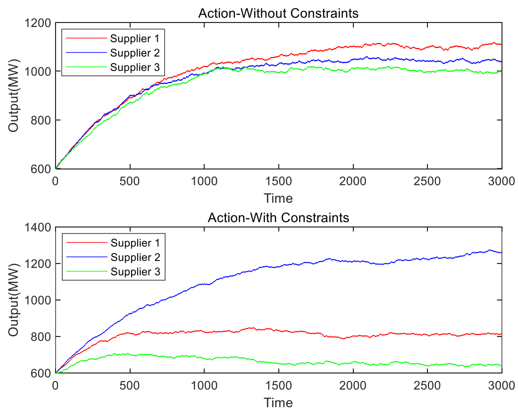

Fig. 1. Action of suppliers in the 3-bus system.

Co-simulation of Electric Power Distribution and Buildings with EnergyPlus and OpenDSS

Evan S. Jones, *Student Member, IEEE*, and Dan M. Ionel, *Fellow, IEEE*

***Abstract*—Co-simulation of tools for various power system components and subsystems modeling is a timely research topic as it offers enhanced testbed capabilities for distributed energy resources (DERs). A new co-simulation framework was developed to take full advantage of the capabilities offered by DER simulation software, such as EnergyPlus, by connecting them with OpenDSS as a platform for enhanced DER modeling, including solar photovoltaic (PV), heating ventilation and air-conditioning (HVAC), and water heater systems. Co-simulation of EnergyPlus with OpenDSS is enabled by three main components, including the Building Controls Virtual Test Bed (BCVTB), the Component Object Model (COM), and the Message Queuing Telemetry Transport (MQTT) protocol. Case studies to demonstrate the framework utilized three example digital twin building energy models based on the same floor plan, but with different building material characteristics and appliances. The houses were designed, built, and equipped to represent three distinct levels of energy efficiency, including conventional, retroactively improved, and near-net-zero. These digital twin building models provide representative energy profiles from which composite loads may be created and simulated in a distribution system simulator, OpenDSS. The case studies were observed on a modified IEEE 123 bus system, which includes solar PV generation from a PV simulator as well as multiple residential composite loads that are based on a number of digital twins.**

***Index Terms*—Co-simulation, smart building, digital twin, EnergyPlus, OpenDSS, building energy modeling, electric power distribution systems, smart grid**

I. Co-simulation Framework

The major software components of the co-simulation framework include EnergyPlus, OpenDSS, and a Message Queuing Telemetry Transport (MQTT) broker as illustrated in Fig. 1. EnergyPlus is a building energy simulator, which includes distributed energy resources (DERs) such as heating, ventilation, and air-conditioning (HVAC) and water heater appliance systems. Other stand-alone DER simulators may also be incorporated, such as the solar photovoltaic (PV) simulator that was developed and employed in the demonstration discussed in section II.

The framework was developed in Python by employing the Building Controls Virtual Test Bed (BCVTB) to interface with EnergyPlus and the Component Object Model (COM) with OpenDSS. Data and synchronization information is exchanged through an MQTT broker in a publish and subscribe manner.

II. Demonstration with the IEEE 123 Bus System

The co-simulation framework was demonstrated through case studies that utilized a modified IEEE 123 bus test system as well as three EnergyPlus building energy model digital twins that are based on the same floor plan, but with different building material characteristics and appliances. The original houses were designed, built, and equipped to represent three distinct levels of energy efficiency, including conventional, retroactively improved, and near-net-zero.

Equipped with the digital twins that are representative of three distinct building types, composite loads are created and implemented into the distribution system simulation as multiple OpenDSS load objects. A case study at bus 151, shown in Fig. 2, includes four PV systems simulated from a PV simulator and a composite load which incorporates one of each building type. Another case study was performed at multiple buses in the system where the corresponding composite loads include a mixture of multiple building types, each totaling 120 to 140 houses.

Evan S. Jones and Dan M. Ionel are with the SPARK Lab, Electrical and Computer Engineering Dept., University of Kentucky, Lexington, KY.

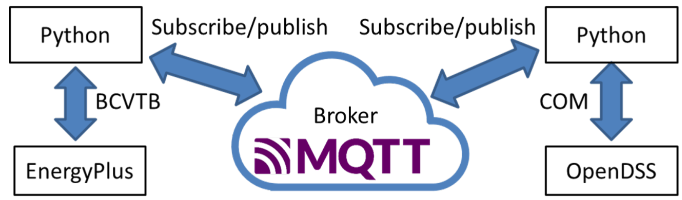

Figure 1. High level schematic for the co-simulation framework developed in Python. The Building Controls Virtual Test Bed (BCVTB) interfaces EnergyPlus with Python, the Component Object Model (COM) provides the interface for OpenDSS. Communication between the two interfaces, as well as with any additional DER simulators, is performed through a Message Queuing Telemetry Transport (MQTT) broker.

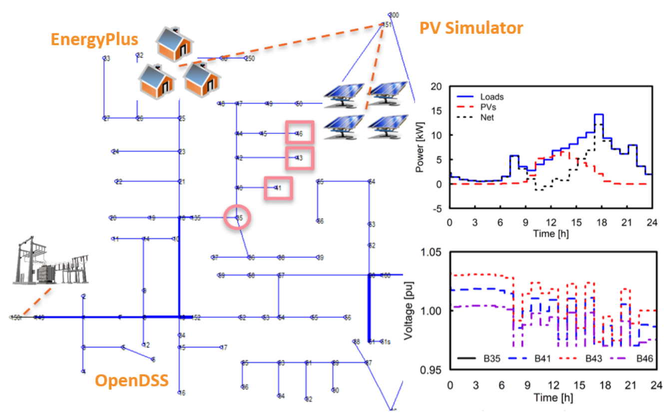

Figure 2. Schematic view of a modified IEEE 123 Bus system employed in the case studies that demonstrate the co-simulation framework. House-level power results are provided in the top-right figure for a case study in which a composite load of each building type and four PV systems were added at bus 151. The bottom-right figure illustrates system-level voltages at denoted buses 35, 41, 43, and 46. Buses 41, 43, and 46 each have a composite load of 120 to 140 total houses, which are based upon the three building types.

Low-order Dynamic Virtual Battery Model for a fleet of DERs under Packetized Energy Management

Adil Khurram, *Student Member, IEEE*, Luis A. Duffaut Espinosa, *Senior Member, IEEE*, and Mads Almassalkhi, *Senior Member, IEEE*

***Abstract*—This research work develops a low order virtual battery model for homogeneous as well as heterogeneous fleets of distributed energy resources (DERs) that are coordinated in a demand dispatch scheme called packetized energy management (PEM). A key feature of PEM based coordination is that it incorporates device-level energy constraints by allowing DERs to automatically and temporarily opt-out of PEM and revert to its native controller until the constraints are satisfied hence ensuring quality of service (QoS). The proposed virtual battery model captures the aggregate behavior of a fleet of thousands of DERs in the form of four key quantities that are representative of the energy content in the fleet including opt-out dynamics. Parametric heterogeneity is incorporated in the model as additive and multiplicative noise in a stochastic differential equation (SDE) framework that provides further information regarding the distribution of the state of charge (SoC) of the fleet. Simulation results are presented to validate the model.**

***Index Terms*—Distributed energy resources, packetized energy management, demand dispatch, distributed control, virtual power plant.**

I. INTRODUCTION

The availability of internet controllable and connected distributed energy resources (DERs) has made it technically and economically feasible to use DERs for providing dynamic grid services such as frequency regulation. Demand dispatch is the capability to aggregate and control DERs while ensuring the quality of service (QoS) to the end-user. Packetized energy management (PEM) is a device-driven demand dispatch scheme in which DERs probabilistically request the coordinator to consume or discharge power into the grid. DERs can charge or discharge only for a pre-specified time interval resulting in the notion of an *energy packet*. Fig. 1 shows the closed loop PEM system. Furthermore, a DER can opt-out of PEM if its local energy state is low and can opt-back into PEM after charging for a sufficient time interval so that QoS is satisfied.

II. VIRTUAL BATTERY MODEL FOR PEM

A virtual battery (VB) model for PEM enabled DERs without opt-out dynamics is developed in [1]. This work develops a model for the opt-out behavior. The proposed nonlinear virtual battery model is of the form,

$$x(k+1) = f(x[k], u[k]),$$

where, $x = (x_1, x_2, x_3, x_4)^\top$, x_1 is the SoC of the fleet, x_2, x_3 and x_4 are the total number of DERs that are in charging mode,

A. Khurram, L. Duffaut Espinosa and M. Almassalkhi are with the Department of Electrical and Biomedical Engineering, University of Vermont, Burlington, VT, 05405 USA e-mail: {akhurram,lduffaut,malmassa}@uvm.edu.

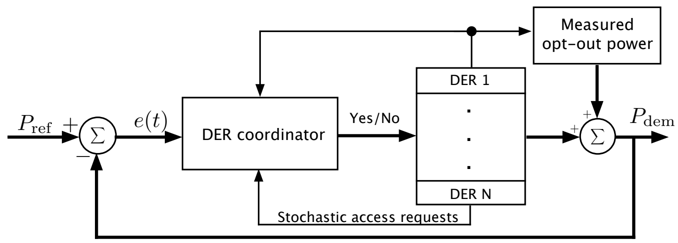

Fig. 1. Closed-loop feedback system for PEM with P_{ref} provided by the grid or market operator and the aggregate net-load P_{dem} measured by the coordinator.

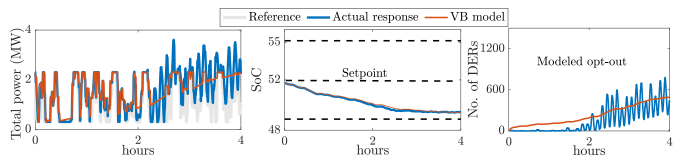

Fig. 2. VB model including the modeled opt-out dynamics is demonstrated for the case of $3,000$ EWHs.

discharging mode and opt-out mode respectively. Furthermore, $u = (\beta_{\mathrm{c}}, \beta_{\mathrm{d}}, \beta_{\mathrm{c}}^-, \beta_{\mathrm{d}}^-)^\top$ is the input to the VB model, β_{c} (β_{d}) is the proportion of charging (discharging) requests accepted, β_{c}^- (β_{d}^-) is the proportion of DERs turning OFF after consuming a charging (discharging) packet.

The total number of DERs opting out (x_4) of PEM decreases with an increase in the proportion of accepted charge requests (β_{c}). This is because increasing β_{c} allows more DERs to charge resulting in the SoC to increase. On the other hand, x_4 is directly proportional to the number of requests received by the PEM coordinator since DERs request more often when their energy state is low. The model for opt-outs can, therefore, be obtained as given below for a fleet of N electric water heaters (EWHs),

$$x_4[k+1] = x_4[k] + a_1((1-\beta_{\mathrm{c}}[k])P^{\mathrm{c}}_{\mathrm{req}}(x_1[k]))x_{\mathrm{off}}[k] - a_2 x_4[k],$$

where $x_{\mathrm{off}}[k] = N - x_2[k] - x_3[k] - x_4[k]$, $P^{\mathrm{c}}_{\mathrm{req}}(x_1[k])$ is the probability of making a charge request, a_1 and a_2 are normalization constants that can either be obtained from steady-state statistics of PEM or from data-driven approaches. The plot in Fig. 2 shows modeled opt-out behavior for the case of $3,000$ homogeneous EWHs. Furthermore, parametric heterogeneity can be incorporated as additive and multiplicative noise in a stochastic differential equation framework.

REFERENCES

[1] L. A. Duffaut Espinosa, A. Khurram, and M. Almassalkhi, “A virtual battery model for packetized energy management,” in *59th IEEE Conference on Decision and Control*, December 2020, pp. 42–48.

A New Model of Battery Degradation Cost for Reinforcement Learning-based Battery Control

Kyung-bin Kwon, *Student Member, IEEE*, and Hao Zhu, *Member, IEEE*

***Abstract*—Battery systems are playing a critical role in today's power system operations through uncertainty mitigation and ancillary service such as frequency regulation. As a result, finding optimal policy to minimize the battery operation cost becomes crucial. This paper aims to solve the battery control problem using the reinforcement learning (RL) with a novel model for cycle-based battery degradation cost based on the rainflow algorithm. Deep Q-Network (DQN) is adapted with the proposed model to find the optimal policy that minimize total cost. The numerical comparison with the linear degradation cost has demonstrated that the cycle-based battery degrdation model shows better total rewards.**

***Index Terms*—Battery degradation cost, rainflow algorithm, Markov decision process, deep reinforcement learning**

I. Battery Control Problem Formulation

The aging of battery cell mainly depends on material fatigue as a result of (dis)charging cycles of the SoC trajectory. Battery degradation is effectively modeled with rainflow algorithm [1] which identifies the (dis)charging cycle depths from the SoC trajectory.

Fig. 1 illustrates an example of battery SoC trajectory. The cycle depths, defined as the absolute SoC differences between the start and end switching points (SPs), are respectively d_0 and d_1 for these two cycles. The correpsonding battery degradation cost is computed as $\Phi_t = \alpha e^{\beta d}$ for cycle depth d. Notably, as d_1 is smaller than the difference between $A-B$ and the one between $C-D$, this trajectory is divided into one *full cycle* which from $K-B-C$ of depth d_1 and one continuous *half cycle* from $A-K(C)-D$ of depth d_0. This is termed as the rainflow condition which uses *four consecutive SPs* to determine the exact cycles and their depths.

As seen in Fig. 1, the cycle-based degradation cost involves the full SoC trajectory and does not follow the instantaneous function form. To overcome the issue, the novel approach to compute cycle-based battery degradation cost is adapted based on the rainflow algorithm to be improved from the approximation using linear degradation cost [2]. Three additional state variables, $c_t^{(0)}$, $c_t^{(1)}$, and $c_t^{(2)}$ are included to keep record of the last three switching points (SPs) from the oldest to latest in the SoC trajectory. The instantaneous battery degradation cost is given as the cost difference by the action in time t,

$$h_t^d = \alpha e^{\beta(c_t + b_t - c_t^{(2)})} - \alpha e^{\beta(c_t - c_t^{(2)})}. \tag{1}$$

The transition kernel of additional state variables $c_t^{(0)}, c_t^{(1)}, c_t^{(2)}$ is defined as in Table I to follow the rainflow algorithm. Deep Q-learning is adapted to the above model to optimize the total reward by defining the Q-function and regarding loss function.

This work has been supported by NSF Award ECCS-1952193.

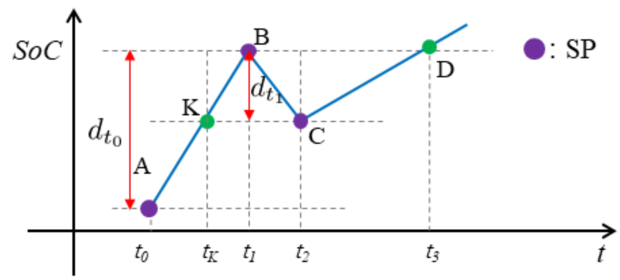

Fig. 1. An example of SoC trajectory

TABLE I
TRANSITION FUNCTION OF STATE VARIABLES

Next state	SP Second	SP Third	NR_a	NR_b	RA
$c_{t+1}^{(0)}$	$c_t^{(0)}$	$c_t^{(0)}$	$c_t^{(1)}$	$c_t^{(1)}$	$c_t^{(0)}$
$c_{t+1}^{(1)}$	c_t	$c_t^{(1)}$	$c_t^{(1)}$	$c_t^{(2)}$	$c_t^{(0)}$
$c_{t+1}^{(2)}$	c_t	c_t	$c_t^{(1)}$	c_t	$c_t^{(0)}$

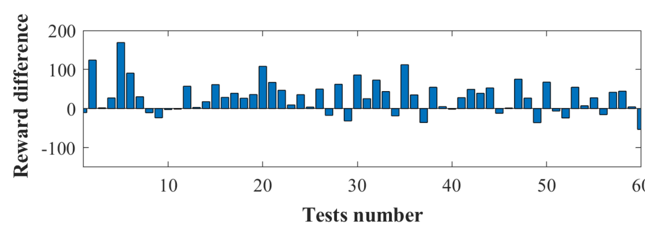

Fig. 2. Total reward difference between case CD and case LD

II. Case Study

Fig. 2 shows the difference in total rewards between the proposed *cycle-based* degradation cost model (case CD) and the linear degradation cost model (case LD). It shows that case CD has better performance in total reward for most tests, mainly because of the difference in battery degradation cost.

References

[1] B. Xu, A. Oudalov, A. Ulbig, G. Andersson and D. S. Kirschen, "Modeling of Lithium-Ion Battery Degradation for Cell Life Assessment," in *IEEE Transactions on Smart Grid*, vol. 9, no. 2, pp. 1131-1140, March, 2018.

[2] J. Cao, D. Harrold, Z. Fan, T. Morstyn, D. Healey and K. Li, "Deep Reinforcement Learning-Based Energy Storage Arbitrage With Accurate Lithium-Ion Battery Degradation Model," in *IEEE Transactions on Smart Grid*, vol. 11, no. 5, pp. 4513-4521, Sept, 2020.

Prescriptive Service Restoration for Improved Distribution System Outage Management

Tumininu Lawanson, Valentina Cecchi
Department of Electrical and Computer Engineering
Energy Production and Infrastructure Center
Charlotte, USA
Email: {tlawanso, vcecchi}@uncc.edu

***Abstract*—This study proposes a prescriptive service restoration framework for improving outage management in distribution systems. The proposed framework integrates outage prediction with service restoration in the distribution system to provide a holistic and proactive approach to outage management.**

***Index Terms*—mixed-integer linear programming, outage management, outage prediction, service restoration**

I. Introduction

Electric power outages disrupt businesses and societies. In the U.S., nearly 90% of outages in the power grid occur at the distribution system level [1], [2]. In the past, limited situational awareness in the distribution system forced system operators to heavily rely on customers to report outages before dispatching repair crews to outage locations.

Since the introduction of smart meters, the data flow in the distribution system has increased, improving visibility into the system. Through smart meter notifications, utilities can identify outages before customers report them, allowing utilities to locate outages and determine their causes more efficiently. This method of managing outages, however, remains predominantly reactive, as an outage may occur before the utility responds, and restorative actions are taken. This often leads to longer duration outages affecting several customers, depending on the cause and location of the outage. Leveraging distribution system data provides opportunities for a more proactive approach to outage management.

To date, a considerable amount of literature has been published on outage prediction. Many of these studies have focused on analyzing and identifying outage causes using various machine learning techniques. A number of studies have also been published on service restoration in distribution systems. These studies are largely restricted to just outage prediction or just service restoration, failing to make the synergistic connection between outage prediction and service restoration, both of which are key important components of a robust outage management approach.

Hence, this study proposes a novel holistic approach to outage management that integrates outage prediction with prescriptive service restoration. The objective is to combine predictive and prescriptive analytics so that outage management becomes more proactive. While predictive analytics deals with the outage prediction, the focus of prescriptive analytics is on service restoration. Specifically, this study examines the following questions:

- Given a set of predicted possible outage scenarios, can we prescribe and implement proactive actions in the distribution network that would prevent predicted outages from even occurring?
- If predicted outages cannot be prevented, can actions be taken in the distribution system (in real-time) to minimize the outage duration or number of affected customers?

To address these questions, this study presents a prescriptive service restoration framework that leverages outputs from outage prediction. Fig. 1 below shows the three components of the framework: an outage prediction model, an impact evaluation stage, and a multi-objective service restoration (MOSR) stage.

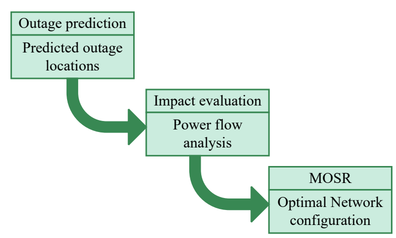

Fig. 1. Prescriptive service restoration framework

In the third stage of the proposed framework, the multi-objective service restoration problem is formulated as a mixed-integer linear programming (MILP) model, which is solved using *Pyomo* [3], an open-source package used to formulate optimization problems in Python. The framework is evaluated using the modified IEEE 123-node test feeder.

References

[1] H. Farhangi, “The path of the smart grid,” *IEEE Power and Energy Magazine*, vol. 8, no. 1, pp. 18–28, Jan 2010. [Online]. Available: http://ieeexplore.ieee.org/document/5357331/

[2] V. C. Gungor, D. Sahin, T. Kocak, S. Ergut, C. Buccella, C. Cecati, and G. P. Hancke, “A Survey on Smart Grid Potential Applications and Communication Requirements,” *IEEE Transactions on Industrial Informatics*, vol. 9, no. 1, pp. 28–42, Feb 2013. [Online]. Available: http://ieeexplore.ieee.org/document/6298960/

[3] W. E. Hart, C. D. Laird, J.-P. Watson, D. L. Woodruff, G. A. Hackebeil, B. L. Nicholson, and J. D. Siirola, *Pyomo – Optimization Modeling in Python*, 2nd ed., ser. Springer Optimization and Its Applications. Cham, Switzerland: Springer, 2017, vol. 67.

[4] B. Chen, Z. Ye, C. Chen, and J. Wang, “Toward a MILP Modeling Framework for Distribution System Restoration,” *IEEE Transactions on Power Systems*, vol. 34, no. 3, pp. 1749–1760, May 2019.

Market-Based Volt-Var Optimization and Its Applications on Bottom-Up Load Modeling Method

Ang LI, *Student Member, IEEE*
Department of Electrical and Electronic Engineering, The University of Hong Kong,
Email: angli@eee.hku.hk

I. Introduction

Volt-Var optimization is used to determine optimal sets of voltage regulation devices and reactive power compensation devices for different objectives. Scientific research results and industrial practical experiences show that energy-saving achieved by VVO projects ranges from 5% to 8%. To further improve the effects, the following issues are significant to be tackled: 1) the commonly used load-to-voltage (LTV) parameters in load models cannot accurately describe the long-term characteristics of loads equipped with droop-control devices; 2) the classical energy-related VVO models aim at reducing customers' energy consumption, which leads to a decrease in profits of distribution companies (DisCos). Therefore, more robust and accurate load models are needed to improve the optimality of energy-saving VVO schemes; VVO models should consider DisCos' energy purchasing strategies in electricity markets to improve their motivations.

II. Tri-Level Bottom-Up Load Model

Based on the emerging statistical end-use data sets, we propose a component-based load model with a tri-level bottom-up structure to calculate energy-to-voltage (ETV) parameters that represent long-term energy consumption changes with voltages, as well as the LTV parameters in classical load models, as is shown in Fig. 1.

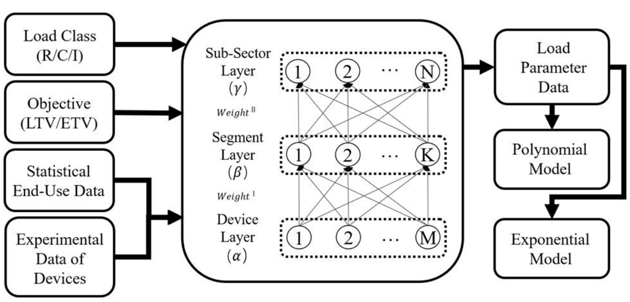

Fig. 1. Structure of the proposed load model

III. Market-Based Volt-Var Optimization Model

The proposed mVVO model aims at minimizing overall energy costs considering different energy values from wholesale markets and retail markets under different loading conditions. The optimization problem is decomposed into an NLP problem and a MIQCP problem, which are solved separately and efficiently.

Objective:

$$\begin{aligned} Min\,F &= Cost(P_{EX\,i} + P_{EG\,i}) \\ &= \sum_{i=1}^{N} a_i P_{EG\,i}^{\;2} + b_i P_{EG\,i} + c_i P_{EX\,i} + d_i \quad \forall i \in N_{Node} \end{aligned} \tag{1}$$

IV. Case Study and Key Results

The ETV and LTV parameters of civil loads in Hong Kong are calculated using the proposed load model; based on the ETV parameters, cost-saving and energy-saving results of the mVVO model are calculated in a modified IEEE 33-bus test system.

A. ETV and LTV Parameters of Load Model

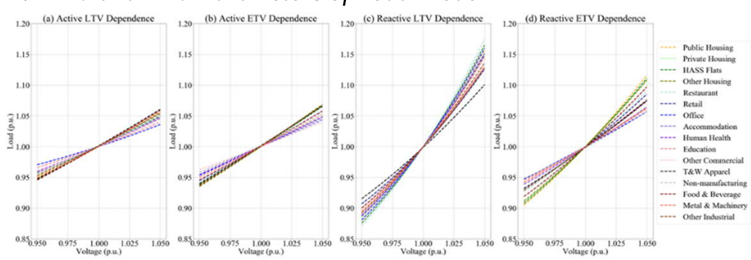

Fig. 2. LTV and ETV dependence for sub-sectors in Hong Kong

B. Results for Energy Saving and Cost Saving

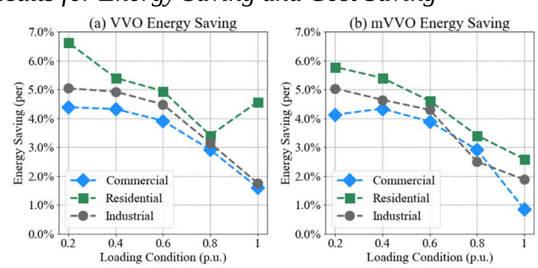

Fig. 3. Energy-saving results

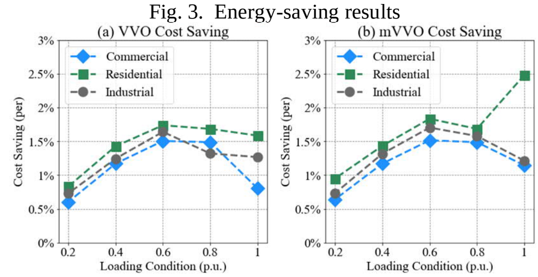

Fig. 4. Cost-saving results

V. Conclusions

In this paper, a tri-level bottom-up load model and a market-based volt-var optimization (mVVO) model are proposed. The energy-to-voltage (ETV) parameter proposed in the load model can reflect long-term load characteristics accurately. The mVVO model decides the optimal voltage regulation strategies and electricity purchase strategies from wholesale and retail markets for maximum cost saving. The case studies based on real load data of Hong Kong show that utilities can reach a higher level of cost-saving, in addition to energy saving using the proposed models.

A Feasible Region Analysis Method for Continuous Commutation Failure in HVDC

Yuan Zeng[1], Yang Li[1], Waiying Guo[2], Wei Wei[1], Hongmei Wang[3]
[1]Key Laboratory of Smart Grid of Ministry of Education, Tianjin University, Tianjin 300072, China
[2]Substation Production Department, State Grid Nanchang Electric Power Supply Company, Nanchang 330000, China
[3]Boyce Thompson Institute, Cornell University, Ithaca, NY, USA

***Abstract*—In order to mitigate continuous commutation failure that often occurs in High Voltage Direct Current (HVDC) systems, the concept of the feasible region of continuous commutation is proposed combined with the principle of commutation failure and the feasible region theory, which can be used as a criterion for continuous commutation failure. Through the analysis of the fault transient process and DC control system, the continuous commutation failure is predicted. Based on this, the feasible region of continuous commutation in the pre-fault operating parameter space of HVDC system is established. According to the positional relationship between the current operating point and the feasible region of continuous commutation, control strategy can be formed to provide help for operators in operation parameter selection and mitigation of continuous commutation failure.**

***Index Terms*—continuous commutation failure, feasible region of continuous commutation, HVDC, prediction criterion.**

I. Introduction

With the deepening of AC/DC hybrid connection, continuous commutation failure has become a common fault in power grid operation. It may result in ac line overload and trigger cascading trips. In extreme cases, it will even lead to major blackouts. This poster focuses on the study of the second commutation failure when continuous commutation failure occurs. Based on the research of HVDC system commutation process and feasible region theory, a feasible region analysis method for continuous commutation failure prediction is proposed. By predicting the continuous commutation failure, the feasible region of continuous commutation in pre-fault parameter space can be constructed which can provide help for operators in operation parameter selection and mitigation of continuous commutation failure. Based on this, a method of constructing boundary line of the feasible region by local linearization is proposed.

II. Feasible Region of Continuous Commutation

Continuous commutation failure is not determined by a single parameter but by a combination of multiple parameters. If an operating state corresponds to a set of parameter values, then all operating states that satisfy the formula will form a hyperspace region in the multidimensional parameter space. This area Ω_a can be expressed as follows.

$$\Omega_{\mathrm{a}} = \left\{ A \middle| f(A) - \gamma_{min} \geq 0 \right\} \tag{1}$$

Where, A denotes an operating state or the value of (E, X_c, I_d, β). The function f denotes the relationship that these parameters are expected to satisfy to commutate successfully. There are some requirements that the actual turn-off angle of two consecutive commutation after fault is not less than γ_{min} and each variable is within the value range. The operating points that meet these requirements will form a closed space body region, so that all operating points within the region will not fail in continuous commutation. Such a space region is defined as the Feasible Region of Continuous Commutation (FRCC) in this poster. FRCC can be built on the two-dimensional section composed of I_d and γ due to the steady-state control mode of regular HVDC system.

It is necessary to establish the FRCC in the pre-fault parameter space in order to achieve preventive control. By establishing the mapping relationship between the pre-fault parameter space and the post-fault parameter space, an analytical method for establishing FRCC in the pre-fault parameter space is proposed. In other words, the focus of the FRCC construction is to predict continuous commutation failure. In this way, when the fault occurs, control strategy can be formed to provide help in the mitigation of continuous commutation failure according to the positional relationship between the current operating point and the FRCC.

III. Description of the Studies and Results

In order to verify the accuracy of the proposed method in the prediction of continuous commutation failure, the FRCC constructed by analytical method is compared with the simulation judgment result to obtain the judgment result distribution, as shown in Fig. 1.

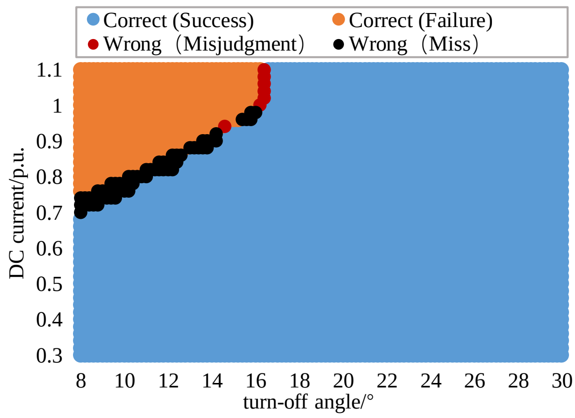

Fig. 1. The judgment result of FRCC constructed by analytical method

The blue part in the figure is the successful operation point of commutation, which constitutes the FRCC. It can be seen that the judgment result of most points is correct, and the judgment result is wrong only when the operation point is near the boundary of the feasible region. Therefore, a more conservative FRCC can be obtained by changing the sensitivity of the criteria. Although this will increase the number of misjudgments, it can achieve zero missed judgments, which is of greater significance to actual projects.

Grid-Edge Spatio-temporal Learning for Behind-the-Meter Solar Disaggregation

Shanny Lin, *Student Member, IEEE*, and Hao Zhu, *Senior Member, IEEE*

***Abstract*—Behind-the-meter (BTM) solar disaggregation is highly beneficial for the protection system design and the feeder operational tasks of distribution grids. This poster puts forth a solar disaggregation framework by leveraging the solution from a spatio-temporal load recovery problem and the sparse change characteristic of non-solar loads. The proposed approach first utilizes the load recovery problem to infer the solar irradiance profile. The recovered solar profile is then used to estimate the total BTM solar output from feeder-level aggregated power measurements. To address the non-solar loading in the aggregated measurements, we exploit the sparse change characteristic of non-solar loads such as household appliances and electric vehicles due to their infrequent activities. Numerical tests using real-world data demonstrate the effectiveness of the proposed approach in estimating the total BTM solar generation at the grid-edge.**

***Index Terms*—machine learning, behind-the-meter solar, load disaggregation**

I. Proposed Methodology

The generation output of solar photovoltaics (PVs) typically depend on localized factors such as solar irradiance and weather conditions [1]. Hence, the active power generation of co-located solar PVs will exhibit a similar temporal pattern which can be leveraged to infer the total BTM PV output from aggregated power measurements. We can recover the solar irradiance profile from the solution of a spatio-temporal load recovery problem given by

$$\begin{aligned}\min_{\mathbf{L},\mathbf{D} \text{ or } \mathbf{v},\mathbf{D}} \quad & \{\|\mathbf{L}\|_* + \lambda\|\mathbf{D}\|_G\} \text{ or } \{\frac{1}{2}\|\mathbf{v}\|_2^2 + \lambda\|\mathbf{D}\|_G\} \\ \text{s.to} \quad & (\mathbf{L}+\mathbf{DU}) \text{ or } (\mathbf{u}\mathbf{v}^\mathsf{T}+\mathbf{DU}) \\ & \text{satisfies measurement error bounds;}\end{aligned} \tag{1}$$

see [2] for comprehensive details. The $N \times T$ matrix $\mathbf{L}$ is of low-rank with strongly correlated rows, where N and T denote the number of load nodes and time slots, respectively. Thus, $\mathbf{L}$ captures the temporal pattern of co-located solar PV generation. A special case is to assume a rank-one $\mathbf{L} = \mathbf{u}\mathbf{v}^\mathsf{T}$, where $\mathbf{u}$ denotes the solar capacity per node which can be obtained from customer reporting or historical data analysis. The solar irradiance profile $\hat{\mathbf{v}}$ of the total BTM PV output can be inferred from the solution of (1) by using the first right singular vector of $\mathbf{L}$ or $\mathbf{v}$ itself. Using $\hat{\mathbf{v}}$, the solar disaggregation from any aggregated power measurement $\mathbf{z}$ is given by

$$\min_{\alpha,\beta,\mathbf{d}} \quad \|\mathbf{z} - (\alpha\mathbf{1} + \beta\hat{\mathbf{v}}) - \mathbf{U}^\mathsf{T}\mathbf{d}\|_2^2 + \lambda\|\mathbf{d}\|_1 \tag{2}$$

where α denotes the offset, β the total PV capacity, and $\mathbf{U}^\mathsf{T}\mathbf{d}$ the non-solar component of $\mathbf{z}$. Note that the L1-norm regularization encourages sparse changes in the non-solar loading [2]. In addition, one can add constraints to (2) such as zero solar generation during non-daytime periods to better improve the total BTM PV output estimation.

II. Key Results

The proposed solar disaggregation algorithm was tested on a 111-node feeder system with 100 residential houses, half with solar PVs installed, using real-world data obtained from Pecan Street Dataport [3]. Fig. 1 illustrates the effectiveness of estimating the total BTM PV output from the aggregated power data using (2) and the recovered solar irradiance profile from (1).

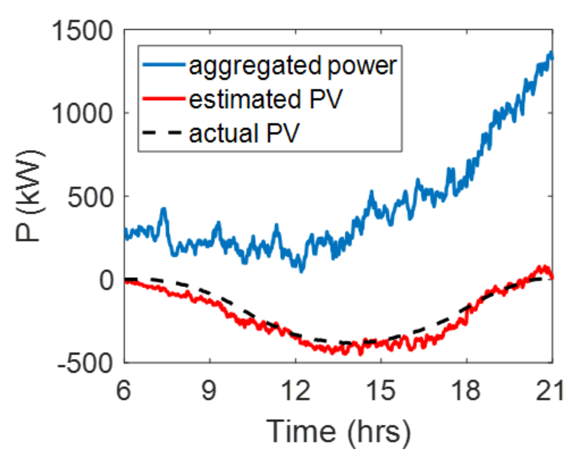

Fig. 1. PV output estimation using aggregated data.

References

[1] N. Sharma, P. Sharma, D. Irwin, and P. Shenoy, "Predicting solar generation from weather forecasts using machine learning," in *2011 IEEE International Conference on Smart Grid Communications (SmartGridComm)*, 2011, pp. 528–533.

[2] S. Lin and H. Zhu, "Enhancing the spatio-temporal observability of grid-edge resources in distribution grids," *arXiv preprint arXiv:2102.07801*, 2021.

[3] "Pecan Street Dataport," Pecan Street Inc. [Online]. Available: https://www.dataport.pecanstreet.org/

This work has been supported by NSF Grants 1802319, 1807097, and 1952193.

The authors are with the Department of Electrical & Computer Engineering, The University of Texas at Austin, Austin, TX, 78712, USA; Emails: {shannylin,haozhu}@utexas.edu.

Bus battery equalization with nonlinear energy efficiency and time efficiency

Jiquan Zhao
School of Automation
Chongqing University
Chongqing, China
1724430585@qq.com

Rui Ling, Member, IEEE
School of Automation
Chongqing University
Chongqing, China
rui.ling@cqu.edu.cn

Shu Liu
School of Automation
Chongqing University
Chongqing, China
15723174594@163.com

Dongcue Li
Vicor Corporation
Andover, MA, America
DLi@vicr.com

***Abstract*—The imbalanced parameter among cells of a battery pack inevitably results in the imbalance of state of charge, which seriously decrease actual capacity and life cycle of the battery. Active battery equalization techniques can greatly reduce the imbalance of cells. Including the energy efficiency and speed of equalization, a nonlinear optimization model is proposed, which considers that the energy efficiency is a nonlinear function of input current and voltage of the equalizer and is more consistent with the actual energy efficiency model of equalizer. The model predictive control is used to achieve dynamic equalization. The method proposed in this paper can significantly improve the energy and time efficiency of battery equalization.**

Keywords—Energy equalization, nonlinear energy efficiency, time efficiency, model predictive control.

I. INTRODUCTION

The state imbalance will cause performance degradation, early termination of charge and discharge, and shorten the service life of the battery pack. Therefore, to achieve the balance of the SOC of cells in the battery pack is one of the focuses in battery equalization research.

As an online control method, model predictive control (MPC) can adjust the references in real time according to the SOC of each cell. Considering both energy efficiency and time efficiency can improve the equalization speed and reduce energy loss at the same time. A nonlinear energy efficiency model is used in this paper, which is more consistent with the actual energy efficiency model of equalizer.

II. MODEL OF BUS BATTERY EQUALIZATION SYSTEM

The structure of the equalization system is shown as fig. 1.

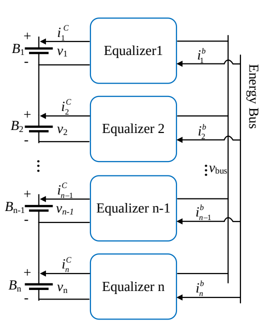

Fig. 1. Bus battery equalization system

Considering the self discharge of cells, the energy of the cell can be obtained by ampere hour method, which is independent of the voltage of cells.

$$\dot{x}_j = -\tau x_j + i_j^c \tag{1}$$

Where x_j represents the residual energy of the jth cell. τ is the self-loss rate of cells.

For the jth equalizer, its energy efficiency can be expressed by formula (2).

$$\begin{cases} -\eta_j^c i_j^c v_j = -i_j^b v_{bus} (i_j^c \le 0) \\ i_j^c v_j = \eta_j^p i_j^b v_{bus} (i_j^b \ge 0) \end{cases} \tag{2}$$

Where η_j^c and η_j^p are nonlinear functions of input current and voltage of the jth equalizer. Formula (1) can be transformed as

$$\dot{x} = -\tau x_j + \frac{h_{\eta_p}(u_{j,1}) v_{bus} u_{j,1}}{v_j} - u_{j,2} \tag{3}$$

In order to improve the equalization rate, the equalization time is added to the optimization objective function. The goal is to reduce energy loss and equalization time at the same time. MPC is used in the control of equalizers.

III. SIMULATION VERIFICATION

The result shows that the method proposed in this paper is feasible. The shorter the working cycle t_0, the smaller the equalization time. In addition, when the time efficiency weight coefficient β is too small, the equalization time is long, which indicates that the part of time efficiency in optimization objective function doesn't work. When β is too large, the cells are over equalized in the early stage. Compare the linear model with the nonlinear model, when the maximum current of equalizers i^m increases, the energy loss of the nonlinear model increases, but the energy loss of the linear model is basically unchanged. The equalization time of the nonlinear model is slightly longer than that of the linear model, but the energy loss of the nonlinear model is far less than that of the linear model.

IV. CONCLUSION

Considering the energy efficiency model as a nonlinear model is more consistent with the actual energy efficiency model of equalizer. To improve the speed of equalization, the equalization time is added to as a part of the objective function. Simulation is carried out to verify the effectiveness of nonlinear multi-objective algorithm of the function of energy efficiency. The result shows that the proposed method not only ensures the fast equalization speed, but also reduces the energy loss compared with linear mode.

This work was supported in part by the National Natural Science Foundation of China (61973048) and the Basic Research and Frontier Exploration Project (cstc2018jcyjAX0297).

Data Generation for Transient Stability Assessment to Address Lack of Training Data

Rui Ma, *Student Member, IEEE,* Sara Eftekharnejad, *Senior Member, IEEE,*
Department of Electrical Engineering and Computer Science
Syracuse University
Syracuse, New York, USA
Emails: rma102@syr.edu and seftekha@syr.edu

***Abstract*—Real-time Transient Stability Assessment (TSA) is essential for prompt decision making on control actions that lead to a stable power system. With the wide deployment of Phasor Measurement Units (PMUs) in power grids, data-driven TSA approaches, particularly machine learning approaches, have become increasingly relevant in recent years. Within cycles, the well-trained machine learning classifiers accurately assess the postfault transient stability of a power system. Considering that unstable events are rare, not much real data exists from these events. As a result, the machine learning-based classifiers face the problem of an imbalanced training dataset. An imbalanced dataset, where the number of unstable samples is significantly lower than the number of stable samples, will result in an inaccurate and biased classifier. To address the problem of imbalanced data, in this study, a Generative Adversarial Network (GAN) is proposed to generate synthetic unstable datasets from the unstable transient data, with a goal to balance the distribution of the stable and unstable datasets. To learn the spatial and temporal correlations of the PMU data, a Recurrent Neural Network is developed to construct the GAN model. The developed GAN model addresses the problem of an imbalanced training dataset, and results in more accurate machine learning-based algorithms for TSA.**

***Index Terms*—Imbalanced data, Generative Adversarial Networks, Transient Stability Assessment**

I. Introduction

The process of predicting the transient stability of a power system after clearance of a fault [1], is referred to as Transient Stability Assessment (TSA). The objective of TSA is to provide accurate assessment of the system stability in a short time. Various TSA models have been developed that can be grouped into model-based and machine learning-based methods. A model-based TSA mathematically solves the system's nonlinear differential algebraic equations, while the high computational complexity limits its applicability. To circumvent this limitation, machine learning-based TSA utilizes the obtained PMU data to train a classifier that in turn can be utilized to predict the transient stability in real-time. To ensure a high prediction accuracy of a classifier, the training data of both stable and unstable transients need to be sufficient. However, since power systems are designed to be robust to contingencies, unstable transient data are rare. This will result in a severe imbalanced distribution between the two classes, i.e., stable and unstable transient data. As machine learning-based algorithms are designed with the assumption of an equal distribution for each class, the imbalanced dataset will lead to a biased, and an inaccurate classifier, especially for recognizing the minority class, i.e., the unstable transients.

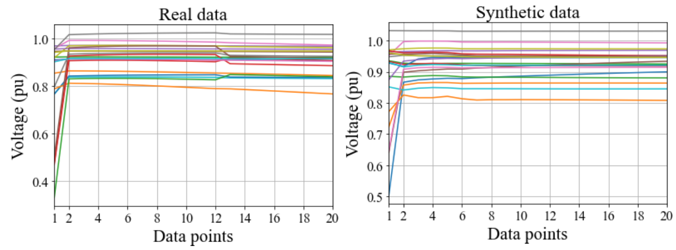

Fig. 1. Illustration of the real and synthetic unstable post-contingency transient data for 20 PMUs. The length of each PMU time series is 20 data points, which corresponds to 10 cycles after a fault clearance. The sampling frequency of PMUs is 120 messages per second.

II. Developed Methodology

In this study, a Generative Adversarial Network (GAN) model is developed to learn the dynamic behavior of the real unstable transient data, and generate synthetic unstable data to balance the number of instances in each class. Specifically, the GAN model has two networks: generative and discriminative networks. Given a random Gaussian Noise, the generative model generates synthetic PMU data, while the discriminative network evaluates the input PMU data as either real or synthetic. The objective of the discriminative network is to maximize the difference between the real and synthetic PMU datasets, while the objective of the generative model is to minimize this difference. These two networks are trained together, and the final result indicates a Nash equilibrium.

Since the transient data are time-series data, the Recurrent Neural Network (RNN) is used to construct the two networks in GAN. To evaluate the proposed GAN model, three-phase faults on different buses and lines in the IEEE 118-bus system are simulated. In total, 600 unstable transient datasets are used to train the GAN model. Examples of the generated synthetic and real datasets are given in Fig. 1. It can be observed that the proposed GAN model accurately learns the dynamic behavior of the real transient data and generates synthetic data that are similar to the real datasets.

References

[1] J. James, D. J. Hill, A. Y. Lam, J. Gu, and V. O. Li, "Intelligent time-adaptive transient stability assessment system," *IEEE Transactions on Power Systems*, vol. 33, no. 1, pp. 1049–1058, 2017.

Optimal Sizing and Techno-Economic Analysis of a Grid-Connected Solar Photovoltaic System

Taniya Manzoor
Department of Electrical Engineering
Guru Nanak Dev Engineering College
Ludhiana, India
manzoortaniya096@gmail.com

Preetinder Singh
Department of Electrical Engineering
Guru Nanak Dev Engineering College
Ludiana, India
preetindersidhu15@gmail.com

***Abstract*—The benefits of integrating renewable energy sources into the grid include the increase in energy efficiency and local reliability, reduction in transmission energy losses and the need for grid expansion. This poster investigates the optimal sizing and various techno-economic factors like net present cost (NPC), cost of energy (COE) and payback period of a grid connected solar photovoltaic system located in Ladakh, India. The system is designed and modelled using the Hybrid Optimization of Multiple Energy Resources (HOMER) software. The results can be used to predict the size of the components and the associated economics at a preliminary design phase. Finally, the environmental benefits in terms of reduced greenhouse gas emissions are also studied.**

***Index Terms*—Optimization, renewable energy, solar energy, distributed energy resources, greenhouse gases**

I. Introduction

Due to the increasing price of fossil fuel-based products and deteriorating environmental conditions, there seems to be increased prospects for distributed energy resources to address electricity generation. However, the economic aspect acts as a significant variable in the promotion of renewable energy. Hence, to configure and design a grid connected renewable energy system, system planning in terms of component design and sizing is very important.

II. Model development

The discount rate, inflation rate and the project lifetime considered in the study are 8%, 2% and 25 years respectively. The component costs are relevant to the market value.

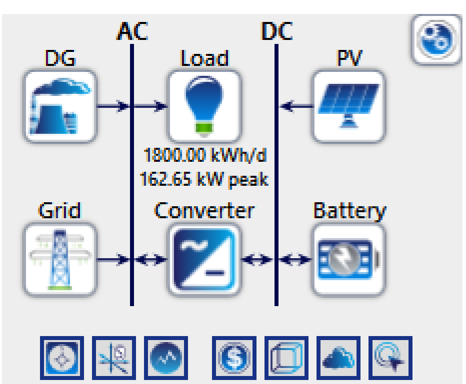

Fig. 1. Schematic model in HOMER Pro.

III. Key Results

TABLE I
Details of the system architecture of the most feasible configurations

	PV (kW)	*DG (kW)*	*Battery*	*Grid (kW)*	*Converter (kW)*
Case 1	200	100	400	200	122
Case 2	200	150	0	200	107
Case 3	0	150	0	200	0
Case 4	0	150	200	200	10

TABLE II
Simulation results based on NPC, COE and Renewable fraction

	NPC ($)	*COE ($)*	*Ren Frac %*
Case 1	455,911	0.0537	35.6
Case 2	570,859	0.0672	30
Case 3	664,197	0.0782	0
Case 4	705,676	0.0831	0

TABLE III
Comparison of the emission levels

Quantity	*Case 1* Value (kg/yr)	*Case 3* Value (kg/yr)
Carbon Dioxide	269,250	427,952
Carbon Monoxide	43.3	396
Unburned Hydrocarbons	1.75	16
Particulate Matter	0.173	1.58
Sulfur Dioxide	1155	1746
Nitrogen Oxides	561	816

The payback period of the most optimal system configuration (Case 1) is calculated to be 4.9 years, which is reasonable.

IV. Conclusion

The results show that as the renewable energy fraction increases from 0% to 35.6% the cost of energy decreases from $0.0831 to $0.0537. Also, the emission levels of the greenhouse gases significantly reduce by integrating renewable energy sources into the grid.

Fast Frequency Response Using Packet-based Coordination and Control

Hani Mavalizadeh, Student Member, IEEE, Luis A. Duffaut Espinosa, Senior Member, IEEE, and Mads Almassalkhi, Senior Member, IEEE

***Abstract*—Fast frequency response is an essential service for power systems. In this work, the capacity of distributed energy sources (DERs) is harnessed to provide fast response to frequency events. To do so, a local controller is designed that makes devices responsive to frequency deviations and increases the damping and inertia of the system. This work's primary goal is to calculate the minimum damping provided by a given fleet of DERs for an arbitrary AGC signal using a probabilistic approach. To do so, the AGC signal is decomposed in the frequency domain using fast Fourier transform. Using the decomposition, a formulation is presented to calculate the statistics of the fleet aggregate power . The proposed formulation will be tested on a two-area test system as well as IEEE 39 bus system to verify its performance.**

***Index Terms*—Fast frequency response, Distributed energy sources, Synthetic damping, Fast Fourier transform, Decentralized control**

I. Introduction

With the increased penetration of renewable energy sources (RES) in power systems, balancing generation and consumption has become more challenging. This is mainly caused by the intrinsic uncertainty in RES, making it difficult for the power system operator to maintain the nominal frequency at 60 Hz. DERs can be used as a source for ancillary services in power systems if coordinated efficiently. To use DERs for fast frequency control, devices should respond to deviations in frequency. This will lead to a decrease in the aggregate consumption of the fleet as a function of frequency. Therefore, the fleet can be considered as a source of synthetic damping. The authors have presented a method to calculate the synthetic damping for special cases of reference signals in [1]. This work is attempted to generalize the results presented in [1].

A fully decentralized local control law is designed in this paper to coordinate DERs and use their capacity for frequency control in power systems, enabling DERs to instantly react to frequency deviations without the need for online communication with a coordinator. This makes the method more practical compared to previously published papers in the field. The main goal is to provide fast and automatic responses to frequency events based on the designed local controller. The effect of the proposed controller of frequency response is shown for a fleet of 400,000 DERs in Fig. 1. As seen in Fig. 1, the controller interruptts packets immediately after deviation occurs. Both nadir and final frequency are improved.

Besides, a novel mathematical method is presented to estimate the fleet's equivalent behavior, using the off-line data available to the coordinator. The number of ON devices at each time determines the fleet's capacity to react to a frequency deviation. The number of On devices is a function of the reference signal, which means that the capacity to provide synthetic damping depends on the reference signal and, therefore, is time-dependent. To generalize the results for any arbitrary AGC signal, a probabilistic lower bound on the synthetic damping is calculated as the actual value depends on the reference signal and can not be calculated beforehand. The calculated minimum lower bound provides the amount of synthetic damping that can be provided with a given population of the fleet at any time. The main goals of this work are summarized below:

- Finding generalized lower bounds for the amount of damping provided by a given fleet of DERs at any time.
- Designing a fully decentralized local controller to increase the damping and inertia of the power system for an arbitrary AGC signal.
- Determining the trade-off between frequency regulation and fast frequency response capability of a fleet of DERs.

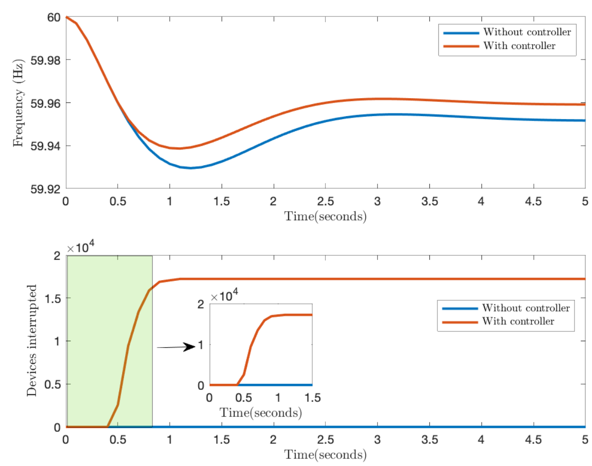

Fig. 1. The frequency response can be improved using the proposed controller

The authors are with the Department of Electrical and Biomedical Engineering, University of Vermont, Burlington, VT 05405 USA.

References

[1] H. Mavalizadeh, L. A. Duffaut Espinosa, and M. R. Almassalkhi, "Decentralized frequency control using packet-based energy coordination*," in *2020 IEEE International Conference on Communications, Control, and Computing Technologies for Smart Grids (SmartGridComm)*, 2020, pp. 1–7.

Joint Offering Strategy of Strategic GenCo in FTR Auction and Day-Ahead Market Considering Virtual Bidding

Hossein Mehdipourpicha, *Student Member, IEEE*, Rui Bo, *Senior Member, IEEE*
Missouri University of Science and Technology, Rolla, USA

***Abstract*— In electricity markets, market participant's (MP's) revenue in financial transmission right (FTR) auction is dependent on the day-ahead (DA) market prices, and it is possible for price-maker MPs to manipulate the FTR value through its strategic behavior in DA markets. Furthermore, virtual transactions designed to converge the price difference between the DA and real-time (RT) markets, may create more opportunities for the MP to improve its strategy by wisely offering the amount of virtual bids and manipulating the DA LMPs, thus increasing the FTR value. For instance, the presence of virtual demand at the "sink" bus may increase the DA LMP at this node and consequently increase the value of FTR. However, uncontrolled amount of virtual demand at this bus may cause the reverse divergence of DA and RT market prices, which leads to a negative virtual profit. Therefore, this paper proposes a joint offering strategy in FTR auction and DA markets from the perspective of a generating company (GenCo) with virtual bidding capability, to maximize its total profit. First, the possibility of FTR value manipulation by placing virtual bids in the DA market is demonstrated using the 5-bus system. Then, the proposed offering strategy model for the GenCo with virtual bidding capability is developed step by step. Next, four different cases are designed to illustrate the effectiveness and applicability of the proposed model. Finally, applying the proposed approach for the strategic MP in 5-bus and 24-bus test systems showed that this MP may arbitrarily lose a small amount of money in the DA market to increase the FTR value by using virtual bids and its physical generation that thereby, maximize its total profit. Furthermore, comparing the results of different case studies demonstrated that the strategic MP could obtain more total profit than the combined profits in FTR auction and DA market using individually developed strategies.**

***Index Terms*—Bidding, Day-Ahead market, FTR auction, manipulation, offering strategy, virtual bidding.**

I. Manipulation of FTR Value by Virtual Bidding

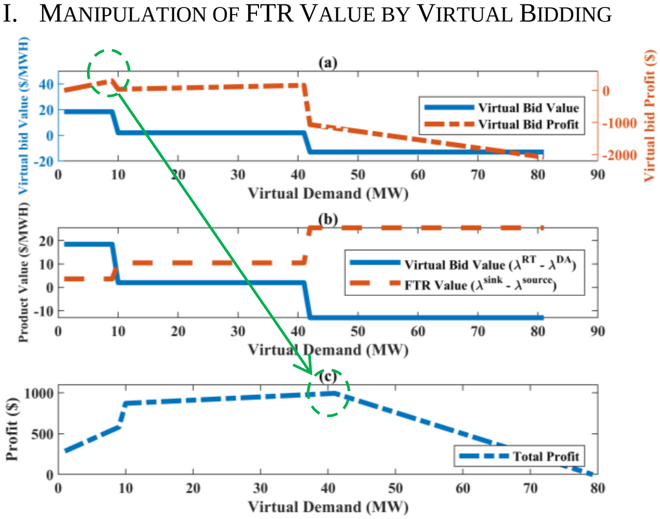

Fig. 1. Test results on 5-bus test system (a) Virtual demand value and virtual profit of MP, (b) Virtual demand value and FTR value profiles by placing DECs at "sink" bus, and (c) Total profit of MP after placing DECs at "sink" bus

II. Proposed Joint Offering Strategy Model

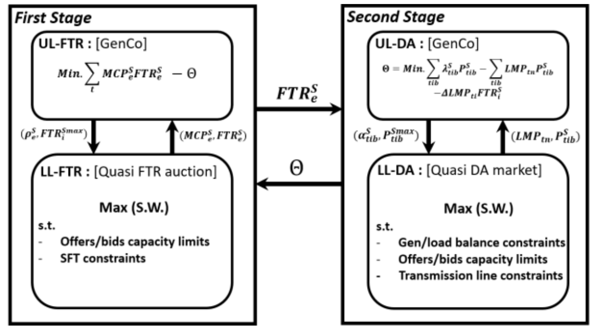

Fig. 2. Proposed two-stage bi-level optimization model

III. Case Study

Following cases are considered for the case study results:

- **Case 1**: the strategic MP bids separately in FTR auction and DA market with accurate prediction of DA LMP difference between sink and source buses (DLMP).
- **Case 2**: this case is similar to Case 1, except that the accurate DLMP forecast is not available.
- **Case 3**: bidding decisions in FTR auction are included in the MP's decision-making process in DA market.
- **Case 4**: applies the proposed joint bidding strategy decision making model that simultaneously optimize the decisions of the MP in FTR auction and DA market.

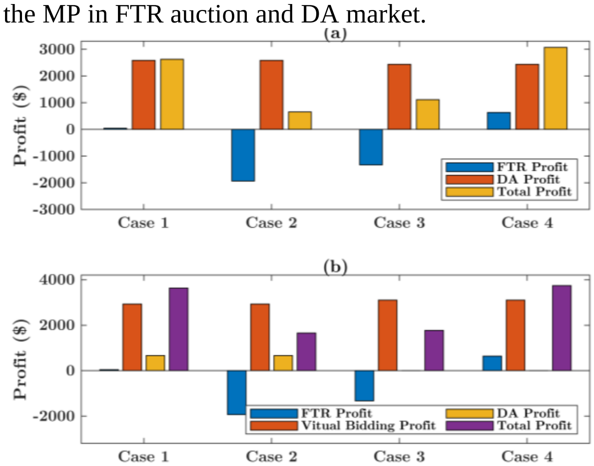

Fig. 3. MP's profit from different markets in different cases, (a) without considering virtual bids, (b) with considering virtual bids

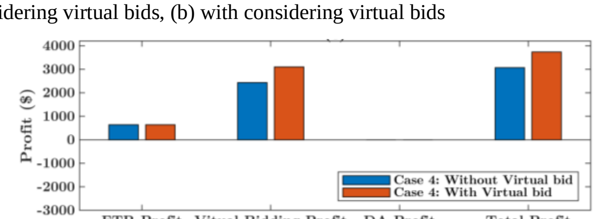

Fig. 4. MP's profit from FTR, virtual bidding, physical generation, and Total profit in Case 4 with and without employing virtual bids

Voltage Unbalance Mitigation in Distribution Networks Using Single-Phase BESS Inverters

Ioannis Mexis
College of Engineering
Swansea University
Swansea, UK
943364@swansea.ac.uk

Grazia Todeschini
College of Engineering
Swansea University
Swansea, UK
grazia.todeschini@swansea.ac.uk

***Abstract*—This work introduces a novel control algorithm for single-phase battery energy storage inverters to reduce voltage unbalance in distribution networks. The unbalance in the modelled distribution system arises from the background unbalance of the upstream grid, as well as from the single-phase connected residential loads and low-carbon technologies (LCTs), i.e. photovoltaics (PVs) and electric vehicles (EVs). The load and LCT profiles are retrieved from an online repository and represent typical winter and summer operating conditions in the UK. Simulations in MATLAB/Simulink are carried out to assess the effectiveness of the control algorithm on mitigating voltage unbalance at various PV and EV penetration levels. The results show that the inverters can effectively reduce voltage unbalance by adjusting the active and reactive power exchange with the power grid. The reference signals for the inverters are obtained from downstream current measurements.**

***Index Terms*—Voltage unbalance, distribution network, battery energy storage systems, single–phase loads, symmetrical components**

I. INTRODUCTION

The increasing penetration of single–phase loads and generating units in the power system may lead to an increase in voltage unbalance levels due to the cumulative large power rating and the variable output of devices such as photovoltaic (PV) panels and electric vehicles (EVs). Among the main concerns for the distribution system operators are neutral conductor overloading, transformer overheating due to zero–sequence fundamental currents and voltage band management across the three phases. In addition, the flow of unbalanced currents may increase the network losses and reduce the effective utilization of the distribution line capacity.

One common solution for voltage unbalance mitigation is to maintain load symmetry on the three phases; this approach may not be possible in systems with large penetration of single-phase equipment. Alternatively, active compensation equipment (i.e. power electronics–based devices) can be installed in the distribution system. The development of control algorithms to provide unbalance compensation by regulating single–phase Battery Energy Storage Systems (BESSs) is a relatively unexplored research area. This research provides a novel control strategy to compensate voltage unbalance by coordinating three single–phase BESS inverters to inject both active and reactive power into the distribution system.

The authors acknowledge the funding from the UK Engineering and Physical Sciences Research Council.

II. PROPOSED METHOD AND RESULTS

Voltage unbalance is quantified by the negative–sequence voltage unbalance factor (k_{v2}), which is defined as the ratio of the negative–sequence to the positive-sequence voltage fundamental component according to IEC 61000-2-2.

Fig. 1 shows the BESS units connected at the secondary side of the distribution transformer to mitigate the unbalance caused by single-phase loads and low-carbon technologies (LCTs). The inverters are controlled to reduce the unbalance at bus i below the regulatory limit of 2% by injecting negative– and zero–sequence fundamental current components to be equal in magnitude and 180^o out of phase compared to the current sequence components measured at the bus. Fig. 2 presents the 10-min aggregated values (based on IEC 61000-4-30) of k_{v2} for 20% PV penetration, with and without the BESS.

The results demonstrate that single-phase BESS units can effectively mitigate voltage unbalance in residential distribution networks under the presence of LCTs. The next step of this research will consist in validating the proposed method experimentally using an OPAL–RT simulator.

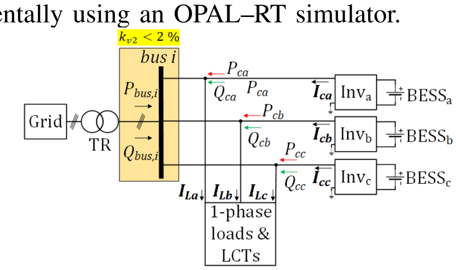

Fig. 1. Single-line diagram showing the BESS inverters used for unbalance compensation, the load, and the equivalent grid.

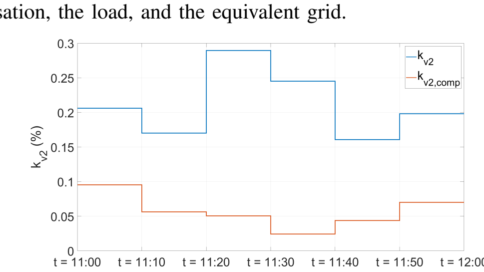

Fig. 2. Voltage unbalance factor at the secondary side of the transformer, withouth (blue) and with (orange) compensation.

A Resilience Quantification Framework and Enhancement Scheme for Active Distribution Networks

[1]Dillip K Mishra, [1]Li Li, [2]Jiangfeng Zhang, [1]Md. J. Hossain
[1]School of Electrical and Data Engineering, University of Technology Sydney, Australia
[2]CLEMSON University, SC, USA

Abstract— **Power outages across the globe are drawing attention to the impact of a deleterious event on distribution system resilience. Although the event's probability is low, it significantly impacts critical services such as medical, business, water, and other important sectors. Thus, to address the impact of the deleterious event, a proper resilience quantification framework and its accociated enhancement technique are needed. In this study, a resilience performance curve is proposed, where four major attributes such as withstand, recover, adapt, and prevent phases are discussed. Further, the different combinations of resources such as distributed energy resources including mobile energy storage devices are utilized to enhance each phase of the curve and thus the newtwork resilience. The mathematical model of each phase of the curve is developed and quantified through the IEEE 33-bus test system. The proposed approach clearly highlights resilience quantification and its improvement through appropriate enhancement strategies.**
Keywords-**Active distribution network, Resilience framework**

I. Key Contributions

This study demonstrates the resilience quantification framework for active distribution networks (ADN) through four different factors: withstand, recover, adapt, and prevent (WRAP) in terms of coping capacity after the event, rapid recovery through available resources, measured stability during and after the event, and preventive measurement, respectively. In order to enhance the ADN resilience, different combination of resources are used, such as microgrids (MG), tie-lines (TL), and mobile storage units (MSU).

II. Proposed Methodology

To define the resilience quantification framework as WRAP, a performance curve is developed, shown in Fig. 1, according to the event period, such as pre-, during-, and post-event. The pre-event is the normal operation, i.e., before t_{ds}; from t_{ds} to t_{de} is the during-event; from t_{de} to t_{re} is the post-event. Each phase of the framework is discussed as follows.

Withstand refers to the system that can cope with the event; for instance, if the grid fails, the system can supply power through the MG connection, presented as 1 and 2 (in the blue circle). Thereafter, the recovery process begins according to the fault location. Different resources can be used, such as MG with TL and then MSU, presented as A and B. Moreover, the recovery is divided into three phases, namely, c, d, and e. As far as adaptability is concerned, sufficient resources, including distributed generations, storage, and alternative paths, such as TLs, can increase the system's flexibility. This finding implies that the system can quickly switch from one point to another towards the system stability (voltage stability index (VSI)), which could follow better resilient characteristics, presented as I. Finally, the preventive phase indicates the impact of the event according to the failure rate and outage duration.

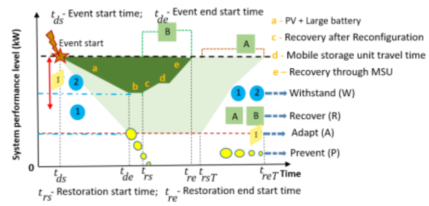

Fig.1. System performance curve with four major attributes to resilience

Eqs. (1-4) represents the withstand, recover, adapt, and prevent index, where P_{CL} is the critical load restored, P_{CL}^{R} is the critical power availavle, i and j are the steps for load recovery, S_{sc}^{t} is the short circuit capacity, N is the number of event type, P_{lost} is the power lost due to an event, and t_{f_i} is the failure time.

$$\mathbb{R}_{Wi} = \left(P_{CL,i} - P_{CL0}\right) \times \left(t_{de} - t_{ds}\right) \tag{1}$$

$$\mathbb{R}_{Rj} = \left(P_{CL,j}^{R} - P_{CL,0}\right) \times \left(t_{rs,j+1} - t_{rsj}\right) \tag{2}$$

$$\mathbb{R}_{A,t} = VSI_t = \frac{1}{N_{bus}^{t}} \sum_{j=1}^{N_{bus}^{t}} \left(\frac{S_{sc,min,j}^{t}}{S_{sc,j}^{t}}\right) \tag{3}$$

$$\mathbb{R}_{P} = \sum_{i=1}^{N} \left(t_{f_i} \times P_{lost_i}\right) \tag{4}$$

III. Key Results and Discussion

This study considers PV unit, battery energy storage in addition with MSU in MGs. In the event of multiple faults, resilience characteristics are evaluated through the WRAP framework using IEEE 33-bus test system, presented in Fig. 2. Further, three scenarios are created; in scenario-I, event time is 2.00 and PV power is zero with battery SOC 0.9; in scenario-II, event time is 14.00 and PV power is available with battery SOC 0.2; in scenario-III, event time is 14.00 and PV power is available with battery SOC 0.9. Fig. 3 indicates the resilience enhancement using different resources.

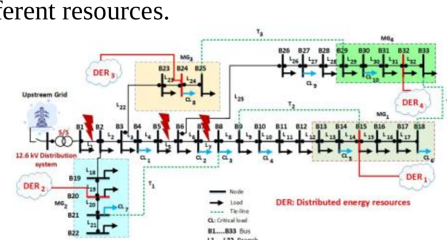

Fig. 2. IEEE 33-bus test system

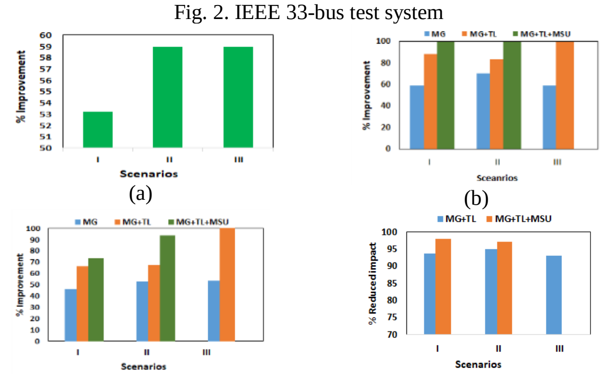

(a) (b) (c) (d)

Fig. 3. (a) Withstand, (b) Recovery, (c) Adapt, (d) Prevent

The Impact of Different Control Strategies on Residential Battery Degradation

Ahmed A.Raouf Mohamed, Robert J. Best, Xueqin Liu, D. John Morrow
EPIC Research Cluster, School of Electronics, Electrical Engineering and Computer Science
Queen's University Belfast
Belfast, UK

***Abstract*— Residential batteries are attracting prosumers due to their ability in reducing the electricity bill by maximizing the solar PV self-consumption as well as optimizing the time of use tariff (ToUT). Furthermore, the deployment of residential batteries is increasing due to their potential in supporting the network from the operator's point of view. The control of residential batteries can be categorized into real-time and look-ahead. The real-time control usually aims to achieve self-consumption maximization (SCM) by charging the battery using the excess PV generation. The SCM can be adjusted to optimize the ToUT by charging during low ToUT periods when the PV generation is insufficient. The look-ahead control utilizes the forecasting to schedule the battery using an optimization solver. This work investigates the impact of these three different control strategies on battery degradation for different capacities. Other comparisons for the electricity bill reduction and network losses are also considered.**

***Index Terms*—Degradation, residential battery control, photovoltaic.**

I. Methodology

In this work, three residential control methods are used: 1) conventional SCM control, 2) SCM control in addition to ToUT optimization, and 3) day-ahead scheduling with perfect foresight to minimize the electricity bill using WORHP optimizer [1]. The battery model, SCM control method, and the day-ahead optimization are adopted from [2], the second strategy is modified to consider the ToUT optimization by charging the battery during low ToUT periods with a fixed percentage per season that represents the average drop in PV production in each season w.r.t the summer. One-year half-hourly measurements were used for a typical household in London with an average daily consumption of 11 kWh/day equipped with a 3.3 kWp PV, and electric vehicle charging profile for the 3 kW standard charger. For each control method, simulation is conducted for one-year and the battery state of charge (SoC) results are fed into a rainflow counting algorithm (RCA). Afterwards, the results obtained from the RCA are fed into Li-ion semi-empirical cycling degradation model [3] to quantify the battery state of health (SoH) at the end of a one-year operation for different control strategies. Five Li-ion batteries with capacities range from 2.4 kWh to 15 kWh and power ratings range 1.2 to 5 kW are considered for actual batteries in the market. Depth of discharge (DoD) of 80% and round-trip efficiency of 90% are considered for all batteries based on the market data.

II. Results and Discussion

The results show that there is a significant relationship between battery capacity and degradation. Small batteries tend to degrade faster due to the undergoing complete cycles that small batteries undertake w.r.t to large capacities as shown in Fig. 1. According to Fig. 1, the SCM control method has a lower impact on battery degradation. Combining the ToUT optimization with SCM has shown to accelerate the degradation. While the day-ahead scheduling has the worst impact on degradation. This because day-ahead scheduling utilizes the battery completely to reduce the electricity bill, especially with a robust forecast. Most of the residential batteries have a lifetime of 10 years, however, the actual battery lifetime can be affected by the control method. For instance, the battery reaches its end of a lifetime when its SoH reaches 60% - 80% [3], with the day-ahead scheduling, smaller batteries may have to be replaced before the end of 10 years as the SoH after 10 years for the 2.4 kWh is 49.6% and 56.7% for the 4.8 kWh battery. Yet, the day-ahead scheduling has a better impact on the electricity bill and loss reductions (11.5% and 57% increase on average in electricity bill and loss reductions respectively compared to the other two methods). Optimizing the ToUT with SCM has been shown to have a moderate impact on the degradation where the SoH after 10 years operation of the 2.4 kWh and 4.8 kWh batteries are 58.7% and 68.6% respectively. On average, the electricity bill can be reduced further by 10%, and the loss reduction can be improved by 10.2% compared to the SCM only.

References

[1] C. Büskens and D. Wassel, 'The esa nlp solver worhp', in *Modeling and optimization in space engineering*, Springer, 2012, pp. 85–110.

[2] A. A. R. Mohamed, R. J. Best, X. Liu, and D. J. Morrow, 'Domestic Battery Power Management Strategies to Maximize the Profitability and Support the Network', IEEE PES General Meeting, 2021, pp. 1–5, to be published.

[3] B. Xu, A. Oudalov, A. Ulbig, G. Andersson, and D. S. Kirschen, 'Modeling of lithium-ion battery degradation for cell life assessment', *IEEE Transactions on Smart Grid*, vol. 9, no. 2, pp. 1131–1140, 2016.

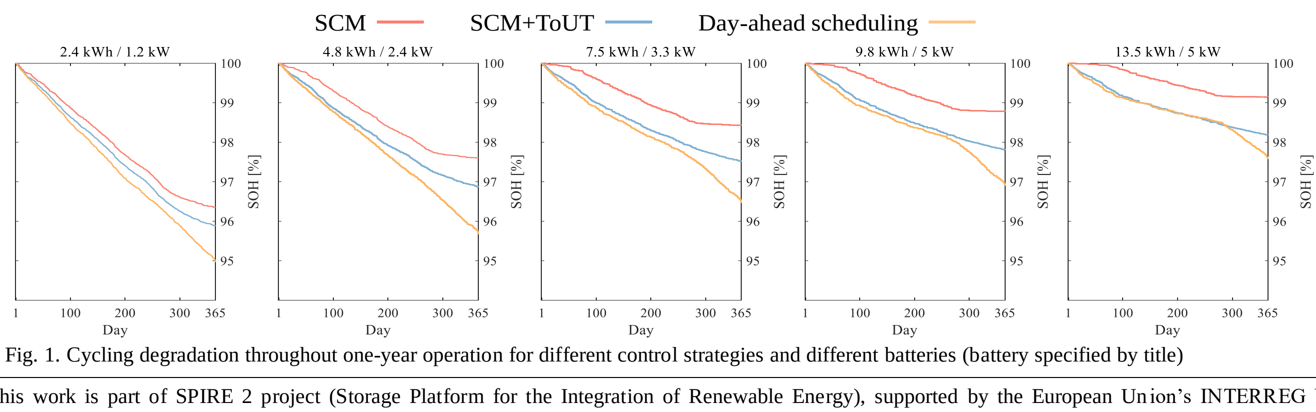

Fig. 1. Cycling degradation throughout one-year operation for different control strategies and different batteries (battery specified by title)

This work is part of SPIRE 2 project (Storage Platform for the Integration of Renewable Energy), supported by the European Union's INTERREG VA Programme, managed by the Special EU Programmes Body (SEUPB). The views and opinions expressed in this paper do not necessarily reflect those of the European Commission or the SEUPB.

Guaranteeing a physically realizable battery dispatch without charge-discharge complementarity constraints

Nawaf Nazir*, *Student Member, IEEE* and Mads Almassalkhi*, *Senior Member, IEEE*

Abstract— **The non-convex complementarity constraints present a fundamental computational challenge in energy constrained optimization problems. In this work, we present a new, linear, and robust battery optimization formulation that sidesteps the need for battery complementarity constraints and integers and prove analytically that the formulation guarantees that all energy constraints are satisfied which ensures that the optimized battery dispatch is physically realizable. Simulation results further illustrate the effectiveness of this approach.**

I. Standard, relaxed and simplified battery models

Consider a battery with SoC at (discrete) time-step k, $E[k] \in [0, E_{\text{max}}]$, where each time-step represents a duration $\Delta t > 0$. The battery also has charging and discharging inputs that can be applied over time-step k defined as $P_{\text{c}}[k], P_{\text{d}}[k] \in [0, P_{\text{max}}]$, respectively, and charging and discharging efficiencies $\eta_{\text{c}}, \eta_{\text{d}} \in (0,1]$, respectively. Then, starting with a given initial SoC E_0 and a sequence of inputs over period $\mathcal{T} = \{0, 1, ..., T-1\}$, the battery SoC dynamics evolve along a admissible trajectory described by the following equation:

$$\mathbf{E}(\mathbf{P}_{\text{c}}, \mathbf{P}_{\text{d}}) = \mathbf{1}_T E_0 + \eta_{\text{c}} \mathbf{A} \mathbf{P}_{\text{c}} - \frac{1}{\eta_{\text{d}}} \mathbf{A} \mathbf{P}_{\text{d}}, \tag{1}$$

where $\mathbf{E} = \text{col}\{E[k+1]\}_{k \in \mathcal{T}}$, $\mathbf{P}_{\text{c}} = \text{col}\{P_{\text{c}}[k]\}_{k \in \mathcal{T}}$, and $\mathbf{P}_{\text{d}} = \text{col}\{P_{\text{d}}[k]\}_{k \in \mathcal{T}}$ and $\mathbf{A}$ is a lower triangular matrix that relates the input at time k to $\Delta t E[l]$ at time $l \geq k$, and $\mathbf{P}_{\text{c}} \cdot \mathbf{P}_{\text{d}} = \mathbf{0}$.

The relaxed model's SoC trajectory is defined by

$$\mathbf{E}^r(\mathbf{P}^r_{\text{c}}, \mathbf{P}^r_{\text{d}}) = \mathbf{1}_T E_0 + \eta_{\text{c}} \mathbf{A} \mathbf{P}^r_{\text{c}} - \frac{1}{\eta_{\text{d}}} \mathbf{A} \mathbf{P}^r_{\text{d}}. \tag{2}$$

where $\mathbf{P}_{\text{c}} - \mathbf{P}_{\text{d}} = \mathbf{P}^r_{\text{c}} - \mathbf{P}^r_{\text{d}}$ and $\mathbf{P}^{\text{r}}_{\text{c}} \cdot \mathbf{P}^{\text{r}}_{\text{d}} \geq \mathbf{0}$ The simplified model's SoC trajectory is given by

$$\mathbf{E}^s(\mathbf{P}_{\text{b}}) = \mathbf{1}_T E_0 + \eta \mathbf{A} \mathbf{P}_{\text{b}}. \tag{3}$$

where $\eta \in [\eta_{\text{c}}, \frac{1}{\eta_{\text{d}}}]$ and $\mathbf{P}_{\text{b}} = \mathbf{P}_{\text{c}} - \mathbf{P}_{\text{d}}$

Lemma I.1. *If inputs $\mathbf{P}_b = \mathbf{P}_c - \mathbf{P}_d = \mathbf{P}^r_c - \mathbf{P}^r_d$ satisfy $\mathbf{P}_c \cdot \mathbf{P}_d = \mathbf{0}$ and $\mathbf{P}^r_c \cdot \mathbf{P}^r_d \geq \mathbf{0}$, then $\mathbf{E}^r(\mathbf{P}^r_c, \mathbf{P}^r_d) \leq \mathbf{E}(\mathbf{P}_c, \mathbf{P}_d) \leq \mathbf{E}^s(\mathbf{P}_b)$.*

II. Optimal battery dispatch formulation

Based on the analysis in Lemma I.1, the two battery models bound the actual SoC. The linear robust battery dispatch (RBD) problem can then be formulated as follows:

$$\textbf{(RBD)} \qquad \min_{\mathbf{P}_{\text{c}} - \mathbf{P}_{\text{d}}} \quad f(\mathbf{P}_{\text{c}} - \mathbf{P}_{\text{d}}) \tag{4a}$$

$$\text{s.t} \quad \mathbf{0} \leq \mathbf{1}_T E_0 + \eta_{\text{c}} \mathbf{A} \mathbf{P}_{\text{c}} - \frac{1}{\eta_{\text{d}}} \mathbf{A} \mathbf{P}_{\text{d}} \tag{4b}$$

$$\mathbf{E}_{\text{max}} \geq \mathbf{1}_T E_0 + \eta \mathbf{A}(\mathbf{P}_{\text{c}} - \mathbf{P}_{\text{d}}) \tag{4c}$$

$$0 \leq \mathbf{P}_c \leq \mathbf{1}_T P_{\text{max}} \tag{4d}$$

$$0 \leq \mathbf{P}_d \leq \mathbf{1}_T P_{\text{max}} \tag{4e}$$

$$\mathbf{P}_{\text{c}} + \mathbf{P}_{\text{d}} \leq \mathbf{1}_T P_{\text{max}} \tag{4f}$$

*The authors are affiliated with the Department of Electrical and Biomedical Engineering, The University of Vermont, Burlington, VT 05405, USA.

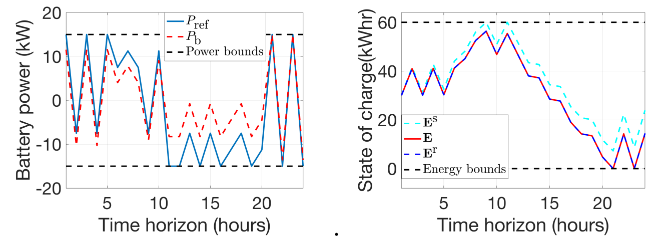

(a) (b)

Fig. 1. (a) Tracking a battery reference power signal P_{ref} with the net battery output $P_{\text{b}} \in [-P_{\text{max}}, P_{\text{max}}]$. (b) Comparison between predicted SoC ($\mathbf{E}^s$, $\mathbf{E}^r$) and actual SoC $\mathbf{E}$ resulting from optimized dispatch with the energy limits [0,60]. Clearly, the actual SoC trajectory $\mathbf{E}$ satisfies energy limits.

III. Simulation Results

Consider a battery with $P_{\text{max}} = 15$kW and $E_{\text{max}} = 60$kWh. Let $\eta_c = 0.95 = \eta_d$ and choose $\eta = (\eta_n + \eta_d)/2 = 1.0013$. The time-step Δt is 1 hour and the control and prediction horizon length T is 24 hours. The objective in (4a) is chosen as $\sum_k (P_{\text{ref}}[k] - (P_{\text{c}}[k] - P_{\text{d}}[k]))^2$. In Fig. 1a, the results shows one battery tracking a reference power signal while Fig. 1b compares the predicted (upper and lower bounds) SoC resulting from (4) to the actual battery SoC obtained from (1). Fig. 1b illustrates that trajectory $\mathbf{E}$ is within its energy limits, which means the optimized power dispatch $\mathbf{P}_{\text{b}}$ is guaranteed to be realizable.

Furthermore, to highlight computational efficiency, Table I compares the RBD in (4) to exact mixed-integer (MIP) and non-linear (NLP) formulations as the number of batteries N increases and we track NP_{ref}. The table shows that the RBD method is 10-200 times faster than MIP for $N \leq 200$ batteries. For $N \geq 500$, MIP does not find a solution with MIP-gap $< 10\%$ within 3600s. The RBD approach is also 5-50 times faster than the NLP, which only achieves local optimum. Note also that the RBD outperforms the NLP with respect to open-loop tracking performance (RMSE) and is still within 10% of the globally optimal, exact MIP. The RBD's fast solve time enables a receding-horizon implementation that should greatly reduce RMSE. Thus, with (4), we sidestep the challenges with non-convex or integer-based complementarity constraints and provide a linear formulation that guarantees a realizable dispatch.

TABLE I
Solve time (sec) and power tracking RMSE (kW) comparison with increasing batteries for RBD vs MIP vs NLP

	RBD		MIP		NLP	
Batteries	Time	RMSE	Time	RMSE	Time	RMSE
10	1.7	47.8	16.3	43.7	5.1	54
100	3.1	478.7	271.8	437.8	50.5	478.7
200	6.3	957.4	1114	866	133.2	1190.2
500	11.5	2327.4	–	–	351.6	2415.2
1000	22.6	4787.1	–	–	1115	4787.1

Analysis of Diverse and Dynamic Effects of DERs in Residential Microgrid Using RAPSim Software

Travis Newbolt, *Student Member, IEEE* and Paras Mandal, *Senior Member, IEEE*
Department of Electrical and Computer Engineering,
The University of Texas at El Paso
El Paso, TX-79968, U.S.A
tmnewbolt@miners.utep.edu and pmandal@utep.edu

EXTENDED ABSTRACT

In recent years, there has been an increasing introduction of distributed energy sources (DERs) into residential microgrid applications. Although this process has been able to provide end users the capability to offset their load demands, there still remains an uncertainty regarding the effects of an increase in DERs from residential microgrids toward the power grid. The challenges of knowing the full-scale ramifications of these DERs, such as solar photovoltaic (PV) systems and wind turbines, are difficult to determine. These resources have an intermittent behavior due to their reliance on weather conditions to produce electrical power. Specifically, PV systems rely heavily on solar radiation and cloud factors that can limit their power productions. Similarly, wind turbines have a dependency on wind speed to produce their power productions. This behavior causes these systems to have a variability in power output that can potentially lead to disruptions within power networks. This can typically be mitigated by system operators through the use of real-time data that monitors sudden occurrences. However, this may not be possible if there is a sudden unpredicted change to the state of a power grid. As DERs (or these variable energy sources) within residential neighbourhoods increase, so could the occurrences of undervoltages or overvoltages, which could have negative effects on capacity limits of lines and transformers at the distribution and transmission levels.

In this paper, a simulation software called "Renewable Alternative Power Simulator (RAPSim)" is used to analyze the effects that residential DERs may have within the power grid as their penetration levels increase. A 9-bus topology, as shown in Fig. 1, is used as the base case topology. There will be four separate simulations that will utilize different penetration levels of around 30%, 50%, 75%, and 100%. An annual average load curve will be utilized for all load profiles to ensure that the only variations occurring are a direct effect of the different penetration levels. All DERs (PV and wind) will be designed based upon default settings within RAPSim software that will fluctuate the power outputs based upon windspeeds for wind turbines and cloud factors for PV systems. The capacity limits of these systems will all first be set in equilibrium to maintain an accurate measurement in order to investigate if the penetration levels play a role in the causation of negative effects. After, each capacity limit will be changed retrospectively for each percentage of penetration level to further simulate an imbalanced power production. This will provide further insight into the diverse and dynamic effects of residential variable energy sources within power grids.

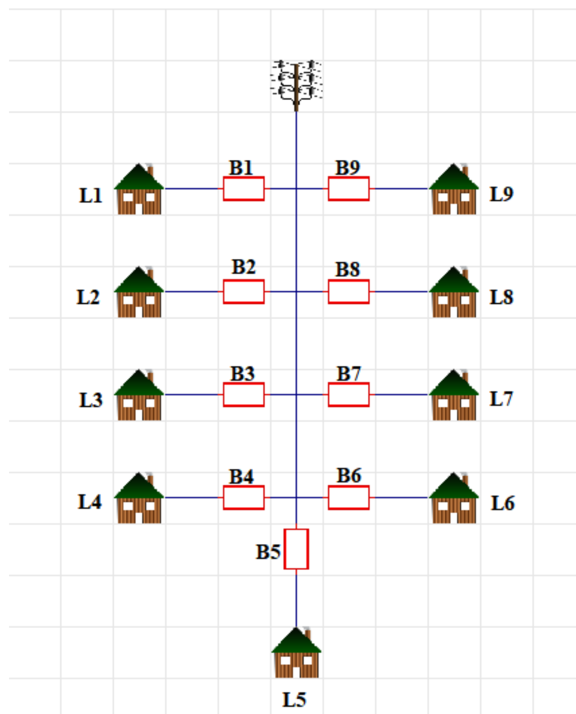

Fig. 1. Base topology.

REFERENCES

[1] S. Impram, S. V. Nese, and B. Oral, "Challenges of renewable energy penetration on power system flexibility: A survey," Energy Strategy Reviews, 13-Aug-2020. [Online]. Available: https://www.sciencedirect.com/science/article/pii/S2211467X20300924. [Accessed: 14-May-2021].

[2] M. Penz, M. Meisel, and T. Sauter, "Implementation of New Consumer Model in RAPSim to Allow Home Management System Integration," *in Proc.* IECON 2018 - 44th Annual Conference of the IEEE Industrial Electronics Society, pp. 200-205, 2018.

[3] M. Pöchacker and W. Elmenreich, "Model implementation for the extendable open source power system simulator RAPSim," *in Proc.* 2015 12th International Workshop on Intelligent Solutions in Embedded Systems (WISES), pp. 103-108, 2015.

[4] C. Long, J. Wu, C. Zhang, L. Thomas, M. Cheng, and N. Jenkins, "Peer-to-peer energy trading in a community microgrid," *in Proc.* 2017 IEEE Power & Energy Society General Meeting, pp. 1-5, 2017.

The authors would like to acknowledge the National Science Foundation (Award #1941524) and Kenneth R. Heitz/El Paso Electric Company Endowed Scholarship for supporting this project partially.

XXX-X-XXXX-XXXX-X/XX/$XX.00 ©20XX IEEE

Optimal Power Flow Analysis Using Power World Simulator: Enhancing Power Engineering Education at Undergraduate Level

Travis Newbolt, *Student Member, IEEE* and Paras Mandal, *Senior Member, IEEE*
Department of Electrical and Computer Engineering,
The University of Texas at El Paso
El Paso, TX-79968, U.S.A
tmnewbolt@miners.utep.edu and pmandal@utep.edu

EXTENDED ABSTRACT

The power industry within recent decades has been moving towards a more decentralized infrastructure to transmit its electrical power to end users. This movement requires methodologies that enable power system operators the capability to manage power productions and constrain marginal costs throughout the system. Power flow analysis provides techniques that allow us to determine how the system will operate when power productions and load demands fluctuate. This process can provide additional confidence to operators because it allows them to determine if transmission line capacities are within safe operating limits while meeting supply and demand. This type of analysis could prevent inadvertently causing negative effects that could lead to system blackouts. Another important methodology that system operators can use is economic load dispatching to manage marginal costs throughout the system. This method could be considered a combination of unit commitment and load dispatching procedures that focus on the fuel costs of power production facilities and load demands. This technique can allow for a minimization of operating costs while still maintaining a balance between supply and demand.

The two techniques of economic load dispatching and power flow analysis can be combined to create an optimal power flow methodology. Optimal power flow allows system operators to mitigate cost of production while also considering transmission line capacities. This ensures that the system operates efficiently and reliably, while also making it more sustainable.

A. *Proposed Methodology*

In this paper, a method of using the simulation software Power World Simulator will be used to explore the advantages of implementing an optimal power flow approach on an IEEE 9-Bus topology. Several simulations will be conducted to ensure that we can observe the behavior that load demand, transmission line capacity constraints, and transmission line losses have within power systems. The first case will simulate a power flow analysis to determine the initial behavior of the system before an optimal power flow technique is utilized. The second will explore an optimal power flow approach while not considering transmission line capacities as well as transmission line losses due to penalty factors at each generation facility. We will then simulate two scenarios; one will solely consider transmission line capacities and the second will add penalty factors to the former. We will then change load demands within these last two scenarios to see how this might affect the optimal power flow analysis.

B. *Expected Outcomes*

This paper explores the behavior of an IEEE 9-bus topology when implementing an optimal power flow. Test results demonstrate that this type of approach has a capability of reducing the total cost of electrical power productions by approximately 2%. Additionally, the system appeared to be most affected by dramatic shifts in load demands that caused several bus locations to reach suboptimal capacity limits. This result can be expected since the behavior between supply and demand should be directly proportional to ensure that the system will operate reliably. It was also evident that transmission line losses, or penalty factors, also have impacts on the cost of generation. The highest marginal cost of 45 $/MWh was found during the simulation that included these factors. To remedy this, it would be advantageous to have power plants relatively close to where load demands are located. Otherwise, the penalty factors will increase due to the extended length of transmission lines, which would also cause power generation costs to increase. Therefore, what we can infer from this research is that the implementation of an optimal power flow methodology can reduce the cost of generation while also making are power systems more reliable, efficient, and more sustainable.

REFERENCES

[1] S. Tan, S. Lin, L. Yang, A. Zhang, W. Shi and H. Feng, "Multi-objective optimal power flow model for power system operation dispatching," *in proc.* 2013 IEEE PES Asia-Pacific Power and Energy Engineering Conference (APPEEC), Hong Kong, China, 2013, pp. 1-6, doi: 10.1109/APPEEC.2013.6837208.

[2] B. Hanna and A. El-Shahat, "Optimal power flow for micro-grids," *in Proc.* 2017 IEEE Global Humanitarian Technology Conference (GHTC), 2017, pp. 1-3, doi: 10.1109/GHTC.2017.8239313.

[3] J. Liu, H. Zhang, W. Qiao and L. Qu, "DC (Optimal) Power Flow-Based Models for Simulation and Mitigation of Overload Cascading Failures," *in Proc.* 2019 North American Power Symposium (NAPS), 2019, pp. 1-5, doi: 10.1109/NAPS46351.2019.9000269.

The authors would like to acknowledge the National Science Foundation (Award #1941524) and Kenneth R. Heitz/El Paso Electric Company Endowed Scholarship for supporting this project partially.

IoT-based Building Energy Management System for Advanced Grid Services

Farinaz Nezampasandarbabi and Masoud H. Nazari, IEEE Senior Memebr

***Abstract*—This paper introduces a design of Internet of Things (IoT)-based Building Energy Management System (BEMS) with high energy efficiency objectives and demand response capability for a real-world building. We develop IoT-based model predictive control (MPC) to minimize the building's energy costs and synchronize the buildings' controllable components with power grid operation. The pilot test is the Engineering and Computer Science (ECS) building at California State University, Long Beach (CSULB). The simulation results show that due to the fast response and flexibility of distributed energy resources, short-term scheduling is effective to achieve maximum energy efficiency. However, the optimization results are sensitive to the demand response penalty factor and the efficiency of battery energy storage system. The results of this paper can provide a road map for the co-optimization of IoT-based smart buildings.**

I. Introduction

A building microgrid, which can represent a commercial, residential, and/or an industrial building, is a small prosumer (producer-consumer) with local controllers, local consumers, flexible loads, and/or distributed energy resources (DERs). The advent of prosumer-based building microgrids has opened quality possibilities for retail electricity market. For instance, building microgrids can provide increased-reliability as-a-service to end users [1], [2]. Moreover, the self-reliance brought on from the utilization of DERs makes these technologies attractive for environments where satisfying power demand is critical, such as hospitals, police stations, and emergency operating centers.

The main contributions of this paper are: 1) Designing building's IoT-based BEMS to synchronize building's energy consumption with environmental conditions and occupant behavior; 2) Developing the building microgrid model; 3) Proposing a new IoT-based MPC method for building energy management system; and, 4) Evaluating the performance of IoT-based MPC for short-term (one day prediction horizon, 15-minutes interval) and long-term (one-week prediction horizon, 15-minutes interval) scheduling. 5) Analyzing the sensitivity of energy management with respect to the time horizon of the optimization as well as critical system parameters.

II. Approaches

IoT-based MPC method developed in this paper is based on Karush-Kuhn-Tucker (KKT) constraint optimization with near real-time prediction horizon to provide demand response and reduce energy consumption and operating costs. Also, a perturbation-based sensitivity analysis method is used to identify and evaluate the significance of parametric uncertainties in the energy scheduling. IoT-based controllable loads, which participates in demand response and energy scheduling, include lighting and plug-in loads.

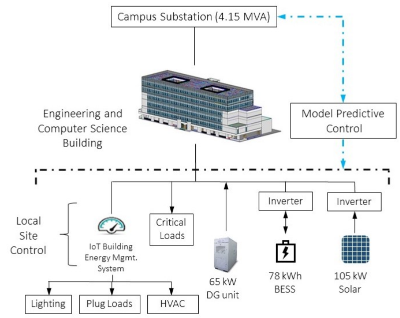

Fig. 1. CSULB-ECS Building Microgrid

III. Simulation Results and Conclusions

The ECS building microgrid (Fig. 1) is simulated based on one month operational data of May 2019. The IoT-based MPC allows achieving 77% savings in terms of total monthly operating costs. Also, the results (Fig. 2) show that short-term energy scheduling can achieve maximum efficiency and minimum operational costs for building microgrids, due to the negligible On/Off costs of DERs . Next, we analysis the sensitivity of system parameters with respect to uncertainties. The results show that the battery efficiency $E^{ch/dis}$ and demand response penalty factor ρ are the most sensitive (critical) parameters. Thus, for reliable operation and control of building microgrids, it is essential to accurately model the battery energy storage as well as the demand response parameters.

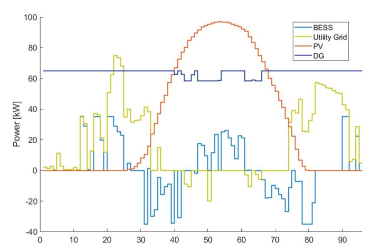

Fig. 2. Short-term Energy Scheduling

References

[1] E. Sanchez, and M. H. Nazari, "Model predictive energy scheduling for building microgrid," 2017 North American Power Symposium (NAPS), 2017.

[2] D. H. Tran, E. Sanchez, and M. H. Nazari, "Model Predictive Energy Management for Building Microgrids with IoT-based Controllable Loads," IEEE, North American Power Symposium (NAPS), 2019.

The authors are with Wayne State University, Detroit, MI 48202, USA, farinaz.ne@wayne.edu, masoud.nazari@wayne.edu

Critical Risk Analysis and Price Effects of Texas Power Outage

Olukunle O. Owolabi[1] *Student member IEEE*, Chukwuemeka O. Oguike[1], Deborah A. Sunter[1,2]
[1] Department of Mechanical Engineering, Tufts University, [2] Department of Civil and Environmental Engineering Tufts University,
Email: olukunle.owolabi@tufts.edu; chukwuemeka.oguike@tufts.edu, deborah.sunter@tufts.edu

***Abstract*—In this study we analyze the cause and effects of the Texas power crisis of February 2021 which occurred as a result of extreme weather conditions from winter storms that resulted in shortage in generation. First, we use data on generation and long-term load forecast for the period of the outage to illustrate the dynamic and temporal relationship between the power system health and a critical risk indicator of load imbalance in the system relative to year-ahead predicted demand. We then compare residential customer savings from variable-rate wholesale and fixed retail price subscriptions. Our analysis reveals that despite wholesale price spikes due to the power crisis resulting in catastrophic post-outage electric bills, wholesale subscription gives a significant net profit margin over fixed rate subscription in the long term.**

Keywords—critical risk, outage, crisis, price, Texas

I. Introduction

In February 2021, the state of Texas experienced one of the worst winter conditions in history resulting in loss of electric power, heating, and water supply for approximately 4.5 million households – the effect of three severe winter storms on February 10-11; 13-17 and 15-20 [1]. Figure 1A shows the pattern of Generation to Forecast Load ratio – a critical risk indicator (CRI) calculated as a ratio of total system generation to the year-ahead long-term predicted demand. Figure 1A shows an increase in this CRI greater than 1 (above the baseline) in the pre-storm period leading to the near system collapse of February 15 which coincides with the beginning of widespread outages reported by the Electricity Reliability Council of Texas (ERCOT) that lasted until February 20-21. Also notable is the role of natural gas in the crisis whose generation contributed to the lost power during the crisis (as shown in Figure 1B).

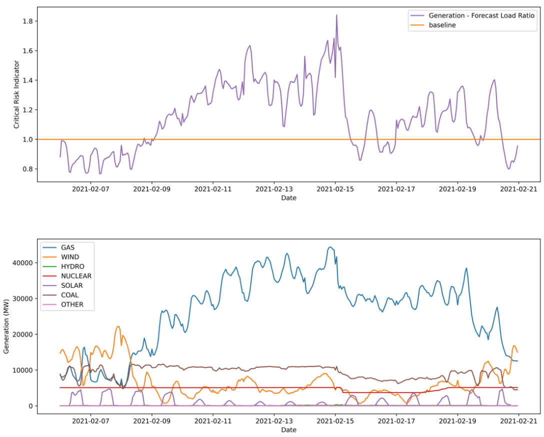

Figure 1: (A) Critical Risk Indicator indicating temporal patterns of generation to load forecast ratio. (B) Generation resource contribution during the Texas power outage. Based on obtained from [2]

II. Results and Discussion

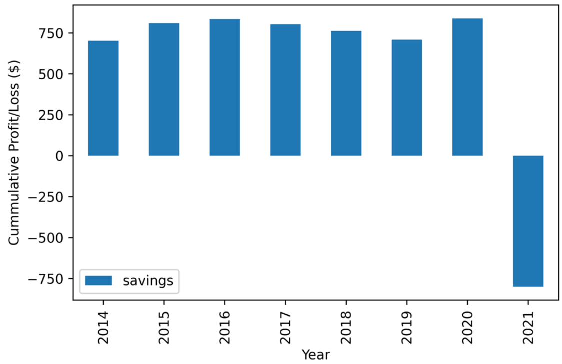

Figure 2: Cumulative annual savings from variable-rate wholesale price relative to fixed retail price. Based on data obtained from [2]

A fixed-consumption pattern was assumed in order to compare the price effects these outages had on residential customers. Wholesale analysis is based on high-resolution hourly ERCOT hub-averaged settlement point price. Figure 2 gives the cumulative annual profit/loss margin for variable rate customers relative to fixed rate retail price (based on a fixed average rate of ¢11.67/kwh [3]). The results show that wholesale residential subscribers have a positive margin annual savings over fixed rate customers of $700 - $840 in the years from 2014 to 2020. However, the cumulative effect of wholesale subscription in the first quarter of 2021 gives a net loss of $800 for wholesale price subscription as a result of price spikes during the outage.

III. Conclusion

Price surges as a result of the February 2021 power outages in Texas raised concerns on the vulnerability of residential customers (specifically wholesale-price subscribers) to price volatility effects as a result of unexpected weather events. In this study, we did a comparative analysis in terms of profit/loss for wholesale price subscription relative to fixed price subscription. Our analysis shows that despite short-term price surge as a result of weather events, wholesale price subscription gives a net profit margin and substantial electric bill savings over fixed-rate retail subscription in the long term. The net savings of wholesale price subscribers was $4662.49 dollars over the 8-year study period when compared to fixed price subscribers.

References

[1] Homeland Security Digital Library. (2021). 2021 Texas Power Crisis. Retrieved May 16, 2021, from https://www.hsdl.org/c/tl/2021-texas-power-crisis/

[2] ERCOT. (2021). Market Information. Retrieved May 16, 2021, from http://www.ercot.com/mktinfo

[3] Compare Power. (2021). Texas Electricity Rates . Retrieved May 16, 2021, from https://comparepower.com/electricity-rates/texas/

i-Autonomous: Standardization and integration of modular and autonomous components in intelligent local substations

Rajkumar Palaniappan, Sebastian Raczka, Björn Bauernschmitt, Dominik Hilbrich, Christian Rehtanz
Institute for Energy Systems, Energy Efficiency and Energy Economics, TU Dortmund University
Dortmund, Germany
{rajkumar.palaniappan, sebastian.raczka, bjoern.bauernschmitt, dominik.hilbrich, christian.rehtanz}@tu-dortmund.de

***Abstract*— Driven by the electrical energy turnaround in Germany and Europe, there is also an increasing need for automation in medium and low-voltage networks. This automation is intended to increase the electrical grids' capacity to absorb decentralized energy generation systems and delay the grid expansion required for this purpose. While some automation functions already exist in the higher voltage levels, the requirements for these functions to be deployed in the distribution grids vary significantly. A large number of protection and automation functions in the distribution grids require the combination of all functions on a standardized system. In addition, the individual functions must be able to operate semi-autonomously, be fail-safe and robust, and without having to run every piece of hardware redundantly. This project focuses on the separation of software and hardware and the implementation of an engineering concept for the overall system.**

Keywords—Smart Grid Automation, IEC 61850, Distributed measurements, Containerization

I. INTRODUCTION

The integration of significant amounts of distributed energy generation is prompting a change within the electrical distribution networks. It can be assumed that in the future the distribution grids will be automated, at least in part, down to the low voltage level. However, the integration of innovative solutions in smart grids still faces many hurdles in terms of the associated costs and effort. To date, there are no standardized, cross-grid installation concepts that manufacturers can use as a guide. As a result, existing solutions are usually specialized solutions adapted to the respective field conditions. In the predecessor project i-Automate, a flexible system architecture was designed that separates hardware from software and maps protection and smart grid automation functions on standardized hardware and was experimentally verified.

For transferring the research results to real network operation, a complete standardization of both hardware and processes is required. However, given the large number of components and the various challenges that arise during network operation, such standardization is not easy to implement. So far, such standardization does not exist and it is not currently defined how such standardization should or can look like - especially for components with adaptive runtime functionality. Therefore, such a standardization must be developed in close exchange with distribution network operators, taking into account all aspects such as hardware, software, communication, functionality and security. In the project i-Autonomous, a concept to standardize the integration process of smart grid automation functions will be researched and tested, reducing the effort for system integration in the future.

This paper is based upon work in the project i-Autonomous (No. 03EI6001A), within the future-proof power grids initiative supported by the German Federal Ministry for Economic Affairs and Energy (BMWi)

II. PROJECT GOALS

The results from the predecessor project will be used and further researched in this project. Based on these results, a standardized protection and automation system for use in medium and low-voltage electrical networks, including a project planning, installation and maintenance concept covering the entire lifecycle, is to be designed and applied as an example in the i-Autonomous project. For this purpose, the requirements, particularly for automated local substations, will first be developed within this project in close cooperation with network operators. From this, specifications for the system and a concept will be derived and documented in an integration guide. The required protection and automation functions, interface adaptations, a suitable engineering process and automated test procedures are implemented in hardware and software. The aim is to check whether the functions can run on previously specified hardware in their own containers and communicate with each other, as shown in Fig. 1. Subsequently, the prototype protection and automation system will be deployed and validated in a selected network area using the specified processes.

Thus, the aim is to create a template for an industry standard for the in-field deployment of smart grid automation systems at the medium grid level. It is also to minimize the effort and costs involved and reduce the risk for manufacturers in developing automation systems and the hurdles for distribution grid operators in setting up smart grids. The focus is on the standardization of the system and the processes. Finally, the project results will be presented to the relevant standardization bodies in the form of a draft and thus find their way into future industry standards.

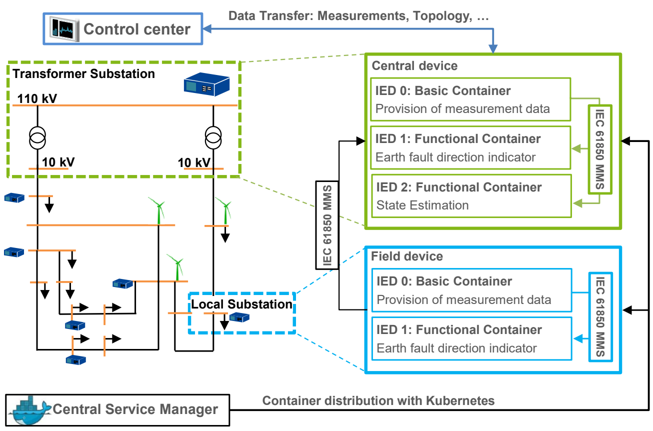

Figure 1: Overall Integration Process

Impact of the Inertia Constant of Synchronous Condenser to Nadir Frequency in HVDC Interconnected Jeju Power System

1st Jeonghoo Park
School of Electrical Engineering
Korea University
Seoul, Republic of Korea
pjhoo2397@korea.ac.kr

2nd Jaeyeop Jung
School of Electrical Engineering
Korea University
Seoul, Republic of Korea
babyyg@korea.ac.kr

3rd Byongjun Lee*
School of Electrical Engineering
Korea University
Seoul, Republic of Korea
leeb@korea.ac.kr

***Abstract*—The Jeju power system is interconnected to the Korean mainland power system via 2 routes of HVDC. Due to the fast dynamics of HVDC, the synchronous inertial response of the generator and fast frequency response effects the system frequency. However, increasing amount of renewable energy sources leads to decrease in inertia which could cause the frequency instability. This could be prevented by additional inertia provided by synchronous condensers. This paper studies the impact of synchronous condenser with different inertia constant. Also, to restore system frequency, we determine the required inertia constant of the synchronous condenser that compensates the loss of inertia. With compensated inertia, renewable energy sources could be connected to the system without violating the frequency stability standard.**

Keywords—Renewable Energy sources, Inertia constant, Synchronous Condenser, Nadir Frequency, HVDC(High Voltage Direct Current)

I. Jeju Island Power System

Jeju Island power system is connected to the Korean mainland power system by 2 routes of HVDC. The renewable energy generation as of 2020 July is 697 MW. Due to fast response of the HVDC, the synchronous inertial response and fast frequency response effects the nadir frequency of the Jeju power system. However, the continuous increase of renewable energy sources could lead to decrease in inertia and frequency instability in Jeju power system. To prevent this, we study the impact of synchronous condenser with different inertia constant. Also, we determine the required inertia constant of the synchronous condenser to compensate the loss of inertia. Renewable energy sources could be connected to the system without violating the frequency stability standard.

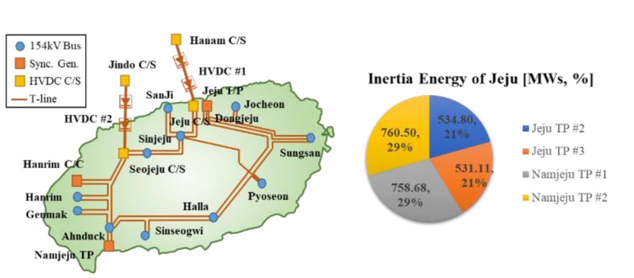

	Structure	Available Contingency	Installed Capacity	Control Mode	Operating Modes
#1 HVDC	Bipole	1, 2 Pole Simultaneous	300MW (150MW * 2Pole)	Frequency Control Slope 0%	• Mainland to Island (Power/Freq. Control) • Island to Mainland (Power Control)
#2 HVDC	Double-Monopole	1 Pole Only	400MW (200MW * 2Pole)	Frequency Control Slope 1%	• Mainland to Island (Power/Freq. Control) • Island to Mainland (Power Control) • Circulation (Power/Freq. Control)

Fig. 1. Configuration and characteristics of Jeju power system with the description of HVDC

II. Simulation Method and Result

The simulation was performed with the basecase assuming the load level as 491MW and the number of must-run generators according to the load level is 4. To consider maximum HVDC transfer amount, the generation of the renewable energy sources are adjusted. HVDC #1 transfers 60MW while HVDC #2 transfers 140MW from mainland to Jeju, and generation by renewable energy sources is 136MW. To simulate the increase in renewable energy sources, we created another case with one of the must-run generator turned off according to the merit order, and generation by renewable energy sources is increased to 166MW. While the basecase doesn't have the synchronous condenser, it is connected to the Hanrim bus at the another case. GENROU model was used for the synchronous condenser, while user defined models were used for HVDC(LCCBP) and ESS(UKEPCOESS).

For both cases, a busfault was conducted at 2.0 sec, which is removed at 2.1 sec with tripping the Jeju TP #2. The simulations were terminated at 7.0 sec. These were perform with different inertia constant of the synchronous condensers.

The simulation results are given in Fig. 2. Fig. 3 depicts the frequency with FFR resources deviation when the inertia constant is 14.06s.

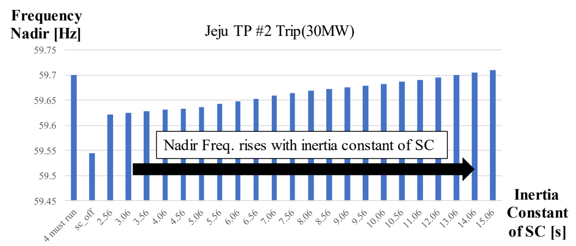

Fig. 2. Impact of inertia constant of SC to the nadir frequency

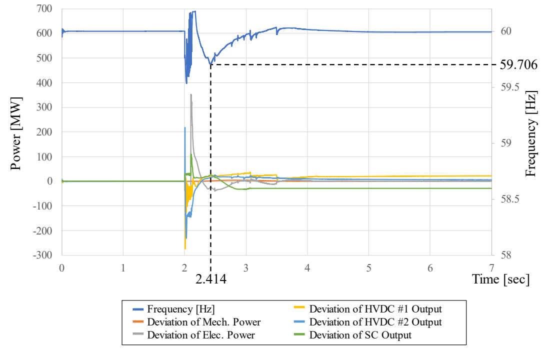

Fig. 3. Frequency and freqency response resources deviation when inertia constant of SC is 14.06s

Machine Learning Applications for Photovoltaic Power Forecasting

Arturo Perez, *Student Member, IEEE* and Paras Mandal, *Senior Member, IEEE*
Department of Electrical and Computer Engineering,
The University of Texas at El Paso
El Paso, TX-79968, U.S.A
aperez88@miners.utep.edu and pmandal@utep.edu

EXTENDED ABSTRACT

Some of the major challenges associated with the integration of solar photovoltaic (PV) power generation into the power grid are that the PV power output is variable, data is non-stationary, and the PV power output depends on weather, primarily on solar radiation and other factors such as rainfall and how cloudy the weather might be on a specific day. Forecasting can be an efficient tool to integrate the output power generated by PV power systems in to the grid. This study focuses on the development of machine learning models to forecast short-term solar PV power. The proposed approach consists of the use of two types of neural networks. The first neural network utilized is the Feed-forward Backprop (FFNN) which takes variable inputs such as historical data of solar PV power, global solar radiation, and temperature, then derives a single prediction for the power output. Fig. 1 shows the general architecture of FFNN.

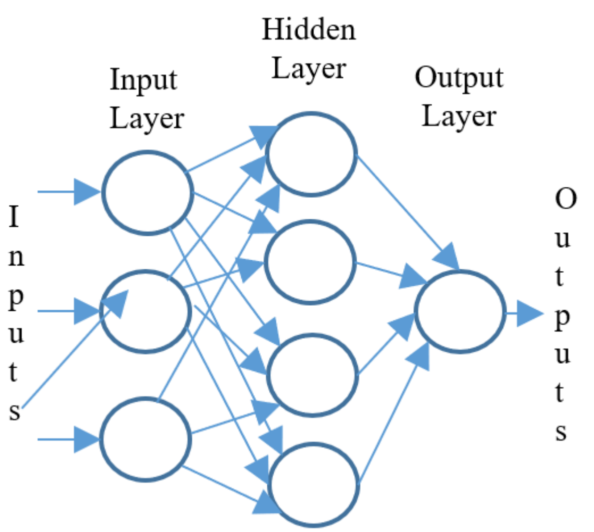

Figure 1: Diagram for a feed-forward backprop neural network

The second neural network utilized is the Elman Backprop (EBNN) whose algorithm accepts input variables (i.e., PV power) and propagates those inputs with data that it had learned previously to derive a single output for the PV power output. Fig. 2 shows the general architecture of EBNN.

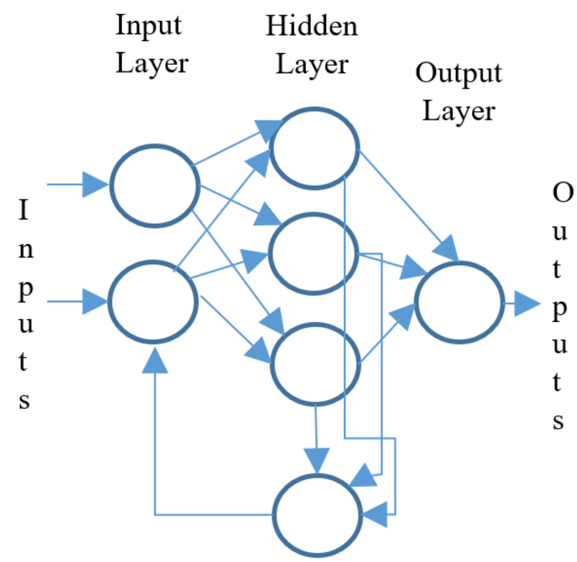

Figure 2: Diagram for a Elman backprop neural network

This study utilizes the real solar PV farm data. The data set consists of global solar radiation, temperature, and PV power generated in intervals of 1-hour for the whole year. The proposed machine learning approach for forecasting PV power will utilized to perform day-ahead and three-day-ahead solar PV power generation forecasts. Since the goal is to get multi-season forecasting, we will test different cases year-round, i.e., performing forecasting in spring, summer, fall, and winter. For the day-ahead case studies, two days for each of the four seasons will be selected. For the three-day-ahead case studies, we will select three consecutive days for each of the four seasons. The effectiveness of both forecast models (FFNN and EBNN) will be evaluated and compared by using three accuracy measures: (i) mean absolute percentage error (MAPE), (ii) normalized root mean squared error (NRMSE), and (iii) normalized mean absolute error (NMAE).

The author would like to acknowledge the National Science Foundation (Award #2021470) for supporting this project.

Synergistic Frequency Regulation Control Mechanism for DFIG Wind Turbines with Optimal Pitch Dynamics

Rashmi Prasad, *Student Member, IEEE* and Narayana Prasad Padhy, *Senior Member, IEEE*

***Abstract*—Conjoint participation of wind generation with conventional power plant, necessitate wind-farms to participate in automatic generation control (AGC) for frequency regulation. This implicates wind farms operator to monitor commands, received from the transmission system operator (TSO). Consequently, advanced control techniques are deployed, which assuredly helps in power tracking, but increases pitch angle controller dynamics. This has resulted in mechanical stress on equipment involved. In order to improve wind-farms response, a synergistic frequency regulation control mechanism (SFRCM) is proposed by the authors. The scheme considers the response time and reserve availability depending on forecasted wind data and also examine load curve pattern to obtain the reference signal for the wind-farm controllers. The work provides a distinct solution to address the following: 1) Optimal pitch dynamics regulated operating point tracking with revised-pitch angle control (R-PAC), 2) Maximization of rotational kinetic energy viz attuned-rotor speed control (A-RSC), to increase stored kinetic energy in the rotor. Case studies at constant and variable wind speed are presented to show the effectiveness of proposed algorithm. To test robustness of the technique, transient operation is conducted as well as forecasted data prediction error is also invoked in the study. The simulations, performed in the real time environment, depict the fulfillment of the above objective in an efficient manner compared with other conventional approaches.**

***Index Terms*—Automatic generation control(AGC), doubly fed induction generator (DFIG), frequency regulation, pitch controller dynamics, rotor speed control.**

I. Introduction

Nowadays renewable generation is considered as semi or quasi dispatchable, to address the concern of frequency regulation. In case of DFIG wind generator, the coordinated control mechanism of rotor speed control (RSC) and pitch angle control (PAC) has been widely discussed for frequency support, as shown in Fig.1, but this has also exploited the pitch dynamics. Frequent variation in pitch angle causes mechanical stress on the blades of the wind turbine. A synergistic control strategy is proposed that will minimize the rate of variation of pitch angle and hence lessen the stress on the equipment involved, besides contributing in improvement of system secondary frequency response. Stability constrained rotor limit is considered, by introducing a novel coefficient of variation term to obtain the set power reference for the WTG coordinated controller. This technique utilizes the pre-existing forecasted wind and the load curve data which help in smoothly tracking the set point reference. The scheme provide a legitimate solution to maximize the rotor speed that will increase inertial power in the WTG while keeping into consideration stress on the mechanical parts. Also the prediction error in the forecasted data is invoked, to obtain a realistic solution. The proposed control mechanism not only respond accurately to the power command sent by the TSO but also provide an improved transient state response.Transient response revamp in terms of added inertial power reserve availability as shown in Fig. 2.

This work is supported by DST India smart grid research initiatives under the research grants: UI-ASSIST: IUS-1132-EED, ZED-I: DST-1161-APD, D-SIDES:DST-1237 EED and (ID-EDGe: DST-1390-EED

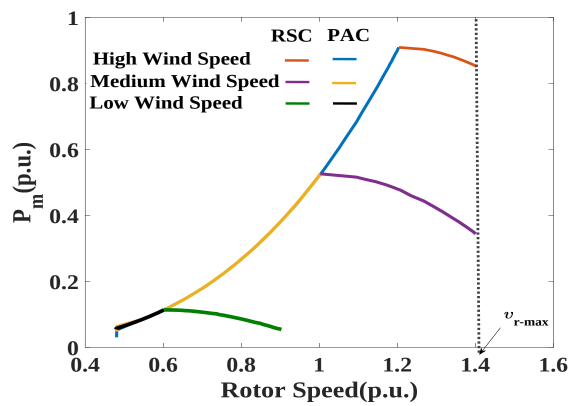

Figure 1. Mechanical Power variation at different wind speed emphasizing turbine reserve capacity

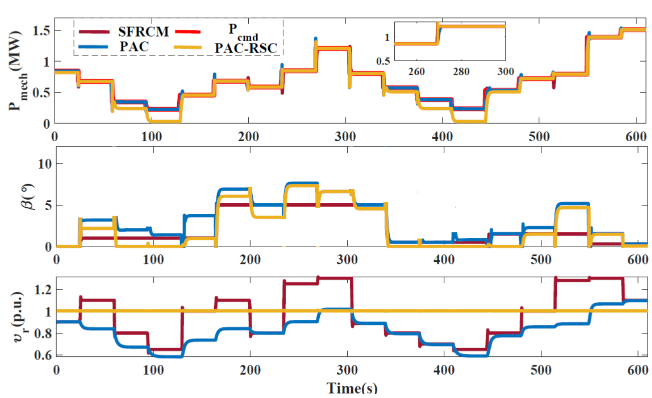

Figure 2. Simulation result: Variation of mechanical power, pitch angle and rotor speed with time

Electric Vehicles for Residential Emergency Response During Power Outages

Orlando Quezada Simental, *Member, IEEE*
Dept. of Electrical and Computer Engineering
University of Texas at El Paso
El Paso,TX 79968. USA
oquezadasi@miners.utep.edu

Paras Mandal, *Senior Member, IEEE*
Dept. of Electrical and Computer Engineering
University of Texas at El Paso
El Paso, TX 79968. USA
pmandal@utep.edu

Eric Galvan, *Member, IEEE*
Economic Research Department
El Paso Electric
El Paso, TX 79901. USA
eric.galvan@epelectric.com

EXTENTED ABSTRACT

The transition to electric vehicles (EVs) is underway globally and EVs are expected to become more widely adopted in the coming years. One of the main characteristics of EVs is that they are not only seen as mean for transportation but also potentially as a flexible energy storage resource in vehicle-to-grid (V2G) applications. This paper proposes an analysis on the feasibility to use EVs for power restoration and supply of residential households experiencing a power outage due to grid contingencies.

Electric vehicles (EVs) are becoming popular, and their use has increased over the past years and is expected to continue to grow in the years to come. EVs are attractive to users not only due to their esthetics and technological features, but also due to the benefits they offer, i.e., their environmentally friendly, have low maintenance costs, and are highly efficient. Furthermore, technological advancements coupled with increased battery capacity make EVs a viable option as a flexible energy storage resource.

EV vehicle-to-grid (V2G) operation has been extensively analyzed in the literature for a variety of applications such as, frequency regulation [1], economic operation of the power grid [2], mitigate renewable energy resource effects, charging demand fluctuation reduction. However, available literature on vehicle-to-home (V2H) applications is limited, especially for resiliency improvement applications where EVs are used as an emergency backup during power outages [3]. While blackouts are considered low-probability events, they can have very serious costs and impacts when they occur. In the past decades alone, there have been hundreds of major blackouts in the U.S. with over 90% occurring at the power distribution level and causing over one trillion dollars in total damages [4].

Therefore, given the impacts these events have on the distribution side of the power grid, the proposed analysis aims to look into the potential of using EVs as a backup power supply for a home during a blackout to improve the resiliency of residential households to grid outages.

In order to demonstrate the effectiveness of EVs as backup power supply, this paper presents a case study where a power outage occurs affecting a residential area and the residential households operate in island mode during the outage. EV operation in V2H mode to supply the residential demand during the outage is tested under three demand scenarios, i.e., low, medium, and high. It is assumed the power outage occurs during a storm on a summer day. Results indicate that EVs could provide basic electricity needs for residential households experiencing an outage.

Fig. 1. V2H system in Islanded Mode.

The authors would like to acknowledge the National Science Foundation (Award #1941524) for supporting this project.

REFERENCES

[1] K. Janfeshan and M. A. S. Masoum, "Hierarchical Supervisory Control System for PEVs Participating in Frequency Regulation of Smart Grids," IEEE Power and Energy Technology Systems Journal, vol. 4, no. 4, pp. 84-93, Dec. 2017.

[2] H. U. R. Habib, U. Subramaniam, A. Waqar, B. S. Farhan, K. M. Kotb and S. Wang, "Energy Cost Optimization of Hybrid Renewables Based V2G Microgrid Considering Multi Objective Function by Using Artificial Bee Colony Optimization," IEEE Access, vol. 8, pp. 62076-62093, 2020.

[3] H. Shin and R. Baldick, "Plug-In Electric Vehicle to Home (V2H) Operation Under a Grid Outage," IEEE Transactions on Smart Grid, vol. 8, no. 4, pp. 2032-2041, July 2017.

[4] E. Galvan, P. Mandal, and Y. Sang, "Networked Microgrids With Roof-Top Solar PV and Battery Energy Storage to Improve Distribution Grids Resilience to Natural Disasters," International Journal of Electrical Power and Energy Systems, Vol. 123, Dec. 2020.

A Deep Learning Approach to Model Pseudo-Measurements in Active Distribution Power Networks

Sepideh Radhoush
ECE Department
Montana State University
Bozeman, MT, U.S.A
sepideh.radhoush@student.montana.edu

Maryam Bahramipanah
ECE Department
Montana State University
Bozeman, MT, U.S.A
maryam.bahramipanah@montana.edu

Hashem Nehrir
ECE Department
Montana State University
Bozeman, MT, U.S.A
hnehrir@montana.edu

***Abstract*— High integration of distributed generations, and limited number of smart measuring devices in active distribution networks pose new challenges. In this study, we address the poor observability of active distribution networks due to the lack of real measurements by generating pseudo-measurements via a novel deep learning approach. For this purpose, dropout approach is used as a regularization technique in the hidden layers of the proposed neural network to improve the accuracy of the training model. The results illustrate that the training model is robust against disturbances in comparison with the conventional artificial neural network approaches. The effectiveness of the proposed method is validated by comparing the errors between the proposed and the conventional methods using the modified IEEE 13-bus standard distribution system.**

Keywords—active distribution network, deep neural network, dropout technique, pseudo measurements

I. INTRODUCTION

Due to the intermittent power injections by stochastic Distributed Generations (DGs), lack of direct control over them, and limited number of smart measuring devices, Active Distribution Networks (ADNs) face new challenges in terms of control and monitoring. Generating pseudo-measurements are presented in order to address the poor observability of the ADNs due to the lack of sufficient real measurements. In the conventional methods, pseudo-measurements are modeled as nonlinear functions using historical data. These nonlinear functions are well treated in small-sized power networks while are not very powerful in large-sized networks. So, in recent years, Artificial Neural Network (ANN) approaches are introduced to obtain pseudo-measurements from available data and address the computational complexity. However, these approaches are not able to address the overfitting problem of the pseudo-measurement modeling. Moreover, they are not robust against load changes. In this work, a new Deep Neural Network (DNN) method along with dropout technique is proposed to model pseudo-measurements (i.e., nodal active/reactive power injections/absorptions). In this approach, the rate of dropout is tuned in the hidden layers based on the error between the target injection values and the output of the training model.

II. PROPOSED METHOD

Although regularization techniques used in the training model (e.g., L1 and L2 weights penalties) are introduced to reduce the overfitting issues, they could not completely correct the problem of overfitting. In this respect, we propose a novel application of the dropout regularization, and deep neural network methods to generate pseudo-measurements. Fig. 1 shows the general concept of the dropout technique. As it can be seen, the dropout technique does not use all the neurons in the hidden layer of the deep neural network. In each training iteration, the neurons with the probability p in each layer are selected ($0.2 \leq p \leq 0.8$). The problem of overfitting is therefore corrected by this method.

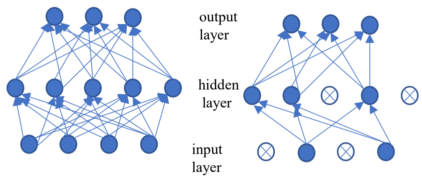

Fig. 1. Performance of Dropout Technique

In this work, first a DNN is trained using historical data. Then, the output of the training model is compared with the actual load profile to regulate the probability p. The p is tuned based on a validation set. The block diagram of the proposed method is shown in Fig. 2. In the offline part the best rate of p is chosen in the hidden layers to have an accurate training model for the new measurements in the online part.

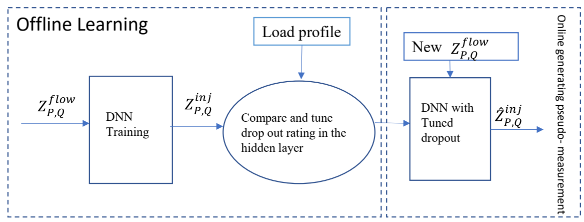

Fig. 2. Block digram of method

III. RESULTS AND FUTURE WORK

The effectiveness of the proposed method is tested in a modified IEEE 13-bus distribution network suitably adapted to include residential loads and a stochastic DG. A set of experimental data (available for a time period of one year) obtained from Open Energy Information (OpenEI) is utilized and 1-hour time-step is selected. The experimental data for the first and second half of the year is used for training purposes and evaluating the proposed training model, respectively. The proposed DNN has one input layer, three hidden layers and one output layer. The Rectified Linear Units and linear activation functions are used in the hidden layers and output layer, respectively. The rate of the dropout is tuned in the hidden layers. Comparing our proposed approach with the two layers feed-forward ANN, we found that the mean absolute and square errors are reduced from 13.82% to 9.8% and 18.01% to 10.7% respectively using the proposed technique.

A Moving Horizon Parameter Estimation and Model Validation of Diesel Generators

Manisha Rauniyar†, Niranjan Bhujel, Timothy M. Hansen, Robert Fourney, and Reinaldo Tonkoski
South Dakota State University
Brookings, South Dakota, USA
Email: †manisha.rauniyar@jacks.sdstate.edu

Phylicia Cicilio and Mariko Shirazi
University of Alaska Fairbanks
Fairbanks, Alaska, USA

Ujjwol Tamrakar
Sandia National Laboratories
Albuquerque, New Mexico, USA

***Abstract*—Diesel hybrid microgrids including inverter-based generation have faster and more stochastic dynamics than traditional systems (e.g. remote microgrids). It is necessary to develop accurate models of the system components to ensure stability of these systems and proper controller design. This work presents a moving horizon estimation (MHE) based approach to obtain the parameters in time-varying hybrid microgrid systems and the estimated parameters are further used to validate the frequency dynamics of the simplified model.**

I. Introduction

Remote islanded microgrids are primarily powered by diesel generators, with increasing contributions from inverter-based wind generators. This has resulted in reduction of the highest energy costs incurred on fossils fuels. Diesel hybrid power systems including inverter-based generation introduce faster and more stochastic dynamics compared to the traditional power system model. Thus, it becomes crucial to understand the dynamic response of diesel-backed microgrids for the accurate modeling of power system components to implement an online estimation technique. The estimation of time-varying parameters in the inverter-interfaced microgrids ensures proper controller design and the system stability.

II. Proposed Model

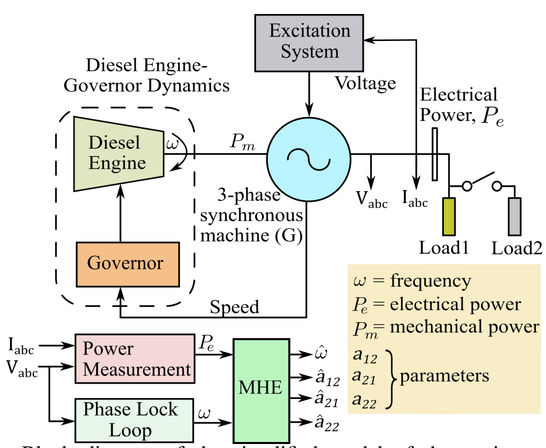

Fig. 1. Block diagram of the simplified model of the engine-governor-generator frequency dynamics.

III. Key Equations

$$\min_{\hat{x}_k,\hat{u}_k,\mathcal{P}} J_H = \sum_{k=q-L+1}^{q} ||y_k - C_d\hat{x}_k||_V^2 + \sum_{k=q-L+1}^{q-1} ||u_k - \hat{u}_k||_W^2$$

$$\text{subject to : } \hat{x}_{k+1} = A_d\hat{x}_k + B_d\hat{u}_k \quad \forall\ k \in \mathcal{H} - \{q\}$$
$$\mathcal{P}_{min} \leq \mathcal{P} \leq \mathcal{P}_{max}$$

where x_k is state, y_k are measurements, and u_k represents input to system at discrete instant k, $\mathcal{H}$ is discrete instant $\{q-L+1, q-L+2, ..., q\}$, L is backward horizon length,$\mathcal{P} = [a_{12}, a_{21}, a_{22}]^\top$ are parameters to be estimated,$||a||_A^2$ is norm of vector a, $\mathcal{P}_{min}$ and $\mathcal{P}_{max}$ are minimum and maximum value of parameters,J_H is cost function, y is difference between measured and estimated values, V and W are weights, matrices A_d and B_d contains parameters as decision variables.

IV. Key Results

A. Parameter Estimates

The unknown parameters estimated using MHE presented in Fig. 2.

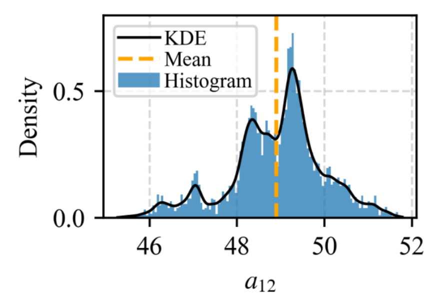

Fig. 2. Histogram showing the distribution of estimated parameter

B. Model Validation Results

The estimated parameters are validated by using them to represent the frequency dynamics shown in Fig. 3.

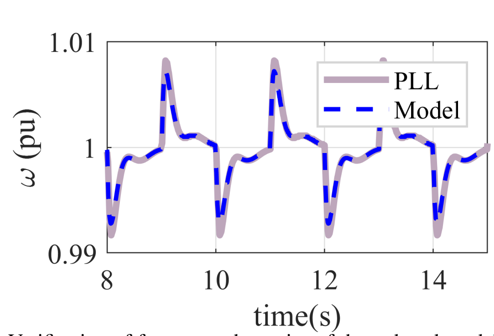

Fig. 3. Verification of frequency dynamics of the reduced model with actual diesel genset model based on MHE estimates.

Sizing Energy Storage System for Energy Arbitrage in Extreme Fast Charging Station

Waqas ur Rehman, *Student Member, IEEE*, Rui Bo, *Senior Member, IEEE*
Missouri University of Science and Technology, Rolla, USA

Abstract*—Integration of energy storage system (ESS) with extreme fast charging station (XFCS) for electric vehicles (EVs) can serve multiple purposes: it can help mitigate the voltage transients and power swings caused by the extreme fast charging of EVs in the host power distribution network (PDN), thus acting as 'power buffer'. It can also act as 'energy buffer' and be used to decrease the operational cost of charging stations by exploiting the energy arbitrage. Optimal sizing and energy management of an ESS integrated XFCS is an important step to ensure cost minimization of its operation and ESS investment, while satisfying its performance requirements and ESS degradation considerations. In this regard, a non-linear programming (NLP) model is proposed that can determine the optimal power and energy ratings of the ESS as well as the optimal energy management of the XFCS, whereas in most literature ESS power rating is not optimized. This work considers ESS degradation in the proposed NLP formulations and ensures that ESS will not be replaced during the project lifetime; thus, not incurring extra cost. In contrast to ESS sizing and degradation models in the literature, this work adopts a more accurate approach by using the polynomial curve fitting to approximate the correlation between allowed ESS cycles and its depth of discharge. Different from reported work related to ESS sizing, this work uses a pragmatic approach to accurately count the ESS cycles using cumulative discharging/charging energy. Moreover, this work considers reduction in monthly and annual demand charges, associated with the XFCS peak power import from the PDN, which have not been considered in literature. Finally, a thorough sensitivity analysis is performed to offer insights into how investment cost of ESS, allowed ESS charge/discharge cycles, and wholesale electricity market prices influence sizing of the ESS and savings from the energy arbitrage.

***Keywords*— energy storage system, degradation modeling, energy sizing, energy arbitrage, power sizing, sensitivity analysis.**

I. Case Study

TABLE I. Simulation Parameters

Parameter	Value	Parameter	Value
ESS technology	Li-ion	SF^D, SF^M	365, 12
ESS power rating cost [$/kW]	300	$\eta_{AC-DC}, \eta_{DC-DC}$	0.95
ESS annual O&M cost [$/kW]	-	LT [years]	10
ESS energy rating cost [$/kWh]	695	z [%]	4
ESS installation cost [$/kWh]	3.6	π [kWh/min]	20
ESS γ^{min}, γ^{max}	1,8	ξ [min]	15
ESS η_{ch}, η_{disch}	0.98	$\lambda_{ADC}, \lambda_{MDC}$ [$/kW]	18, 10

A. Case Description

A case study has been performed to obtain the optimal ESS power and energy sizing and optimal energy management of the XFCS. In XFCS, each charging port is rated > 200 kW. The simulation time step (Δt) is taken as 1/60 h and scheduling horizon (T) of one-year is considered. The input parameters to run simulations are presented in Table I.

B. Case Study Results

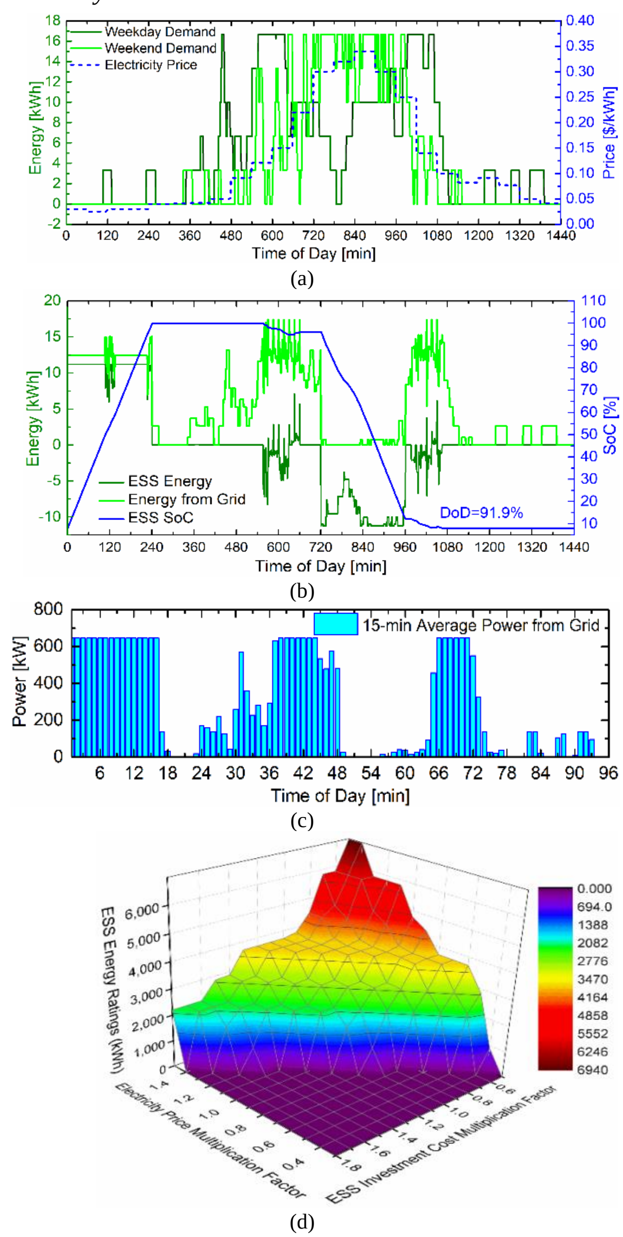

Fig. 1. Input data and results: (a) Charging station energy demand and electricity market price (b) optimal energy management: energy from the PDN, ESS charging/ discharging energy, and corresponding SoC variations of the ESS (c) average power imported from the PDN (d) combined impact of changing the EPMF and EIMF on ESS sizing

A Novel Assessment Method of Resilient Power System Using Stochastic Geometry

Chenhao Ren
Department of Electrical and Electronic Engineering
The University of Hong Kong
Hong Kong, China
chren@eee.hku.hk

Yunhe Hou
Department of Electrical and Electronic Engineering
The University of Hong Kong
Hong Kong, China
yhhou@eee.hku.hk

***Abstract*—Resilience has been well identified as an essential task for power systems to cope with extreme weather events. Resilience assessment of power systems is the precondition for resilience-oriented planning, operation, and establishing restoration strategies. However, no standardized and well-accepted metrics are available yet. In this paper, an assessment method of a resilient power system based on stochastic geometry is proposed. First, an index measuring the distance features for restoration is established. A Poisson point process is then utilized to model all possible spatial patterns for power systems after extreme weather events. The stochastic distributions of distances to restore disconnected components of the survived systems are analyzed. Finally, a coverage probability index that quantifies the overall performance (i.e. restorability) of power systems is derived. Simulation results conducted on the IEEE 14-bus and 118-bus system show the feasibility of the proposed method.**

***Index Terms*—Resilience assessment; Stochastic geometry; Extreme weather events; Structural resilience**

I. Introduction

Power system resilience has gained wide attention in recent years. Many inspiring works have been conducted to construct operational resilience strategies and assessment techniques.

Network science, especially complex network theory, provides another pathway to assess power system resilience. The topology structure affects the functionalities of power systems significantly. The impacts of extreme weather on power systems are mainly reflected on system components' reliability attributes, e.g., failure rate. Although system-level simulations can provide valuable information for the analysis and design of power systems, the need for complementary analytical methods has long been urgent for the sake of comparison. Theoretical analysis can demonstrate key correlation and dependency in the system and reference trends and features that require closer inspection. Stochastic geometry provides a powerful tool that helps us to capture the spatial characteristics of random networks. In stochastic geometry-based methods, spatial locations of the nodes are modeled by stochastic point processes. Some critical metrics, e.g., connectivity, capacity, outage probability, and other fundamental metrics can be analytically derived.

In this paper, a novel assessment method of a resilient power system based on stochastic geometry is proposed. The main contributions of this paper are two folds: 1) An index measuring the distance features for restoration is established to capture the characteristics of components' connections under different extreme weather scenarios. A suitable point process is utilized to model possible spatial patterns for post-event systems. 2) A restorability index is introduced to describe the restorability of components. We derive the formulation of coverage probability to quantify the overall performance of power networks under extreme weather events.

II. Main Results

Restorability reveals an overall ability that power systems can be restored after extreme weather events. The restorability index of load i is defined as follows:

$$RI_i = \frac{\left(P_{Load,i} / P_{G,nearest}\right) r^{-1}_{i\to G_{nearest}}}{\sum_{j\in\Phi/B_O}\left(P_{Load,i} / P_{G_j,farther}\right) R^{-1}_{i\to j}}$$

where $r_{i\to G,nearest}$ and $R_{i\to j}$ denote the electrical distance from load i to its nearest generator and other farther generator G_j;

The coverage probability is derived analytically to quantify the resilience of power systems under different events.

$$P_R = E_r\left[p\left(RI > p_f \middle| r\right)\right]$$

where p_f denotes the failed probability of components.

Simulation results conducted on the IEEE 14-bus and 118-bus system show certain intrinsic structural features of the power system to manage resiliency.

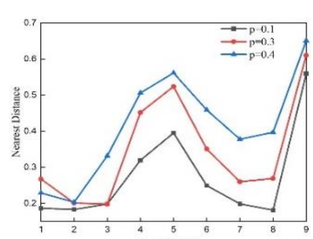

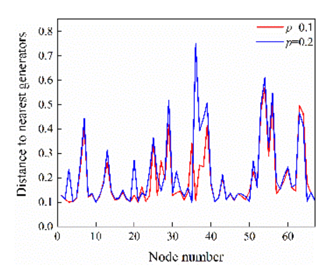

Unsupervised Hybrid Deep Generative Models for Photovoltaic Synthetic Data Generation

Dan A. Rosa De Jesús
Department of Electrical and Computer Engineering
University of Texas at El Paso
El Paso, USA
danrosa@miners.utep.edu

Paras Mandal
Department of Electrical and Computer Engineering
University of Texas at El Paso
El Paso, USA
pmandal@utep.edu

Tomonobu Senjyu
Department of Electrical and Electronics Engineering
University of the Ryukyus
line 4: Nishihara, Japan
b985542@tec.u-ryukyu.ac.jp

Sukumar Kamalasadan
Department of Electrical and Computer Engineering
University of North Carolina at Charlotte
Charlotte, USA
skamalas@uncc.edu

I. Extended Abstract

Modeling electric power generation from solar photovoltaic (PV) panels is essential due to its significant impact on realizing smart and intelligent power grids. However, as energy prosumers comprise heterogeneous renewable energy sources, modeling the PV system components becomes extremely complex. Additionally, the spreading of advanced metering infrastructures in the distribution network has led to enormous amounts of energy generation data. While transmission datasets are relatively easier to get a hand on, the accessibility and availability of distribution level datasets are particularly challenging due to security and privacy considerations. Moreover, PV power output primarily depends on solar radiation, which is highly intermittent due to the presence and movement of clouds at a particular location. This calls for novel techniques for the generation of high-quality synthetic PV datasets. Synthetic data generation is considered to be the way of alleviating the aforementioned issues.

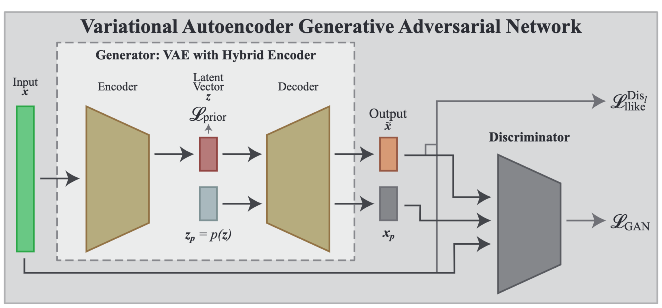

Fig. 1. Hybrid deep generative model illustrating VAEGAN's high-level architecture incorporating the HDNN in the encoder. Data samples forward pass through the encoder, which gives the distribution parameters to sample latent representations. The regularization term is computed using the Kullback-Leibler divergence. The decoder maps latent representations back to data space, and the reconstruction error is computed. A latent representation is sampled from prior and its associated reconstruction is passed to the discriminator along with the ones of the true and generated samples.

Existing literature includes several methods for generating PV synthetic data. For instance, a Markov model was applied in for simulating solar radiance time-series, which were converted to PV power time-series. PV synthetic data is generated through a three-step method that builds relationships between high and low frequency data for different locations obtained from hourly satellite irradiance and sub-minute ground measured solar irradiance, respectively. A Bayesian method for residential demand and PV generation. An alternative to these methods to alleviate these issues is the development and application of novel Deep Generative Models (DGM). DGMs learn the underlying ground-truth data probability distributions through unsupervised learning. In recent years, DGMs have gained popularity due to their superiority to perform a wider number of tasks, including but not limited to, feature extraction for dimensionality and noise reduction. Notably, two of the most commonly used and efficient DGMs are Variational Autoencoders (VAE) and Generative Adversarial Networks (GAN). VAEs aim at maximizing the lower bound of the data log-likelihood, whereas GANs achieve an equilibrium between two networks, the generator, and discriminator. In the literature, VAEs and GANs have been used for data compression and denoising as well as for anomaly detection applications. Furthermore, the combination of the VAE and GAN into the VAEGAN has improved the generation of synthetic data in terms of its quality and diversity. However, to the best of our knowledge, the application of DGMs has not been thoroughly studied in the context of power system time-series data applications, in particular, solar PV power synthetic data generation.

The work described in this work contributes to developing DGMs to obtain PV synthetic data and leverage from previously developed performance measures for other applications to measure the performance of the generated PV data samples. This paper presents a novel hybrid DGM which is a combination of VAE and GAN models, i.e., VAEGAN (See Fig. 1) incorporating convolutional and long short-term memory networks layers at the encoding level. The major advantages of the hybrid DGMs over the existing techniques are: (1) lower degree of risk of overfitting, (2) avoiding the need for extensive feature engineering or hyperparameter tuning, and (3) better generalization and reconstruction diversity through a more robust loss that learns the joint distribution over the real data and their corresponding latent representations. The simulations on actual data acquired from a real PV system demonstrate the effectiveness of the DGMs to produce high-quality samples for multiple seasons of the year.

Machine Learning Based Utility Measure for Expected Value of Sensed Information in the Context of Renewable Energy Prediction

Dan A. Rosa De Jesús
Department of Electrical and Computer Engineering
University of Texas at El Paso
El Paso, USA
danrosa@miners.utep.edu

Paras Mandal
Department of Electrical and Computer Engineering
University of Texas at El Paso
El Paso, USA
pmandal@utep.edu

I. Extended Abstract

The utilization of Renewable Energy Sources (RES) in power system applications has increased substantially in the last decade due to lower maintenance requirements, reduced energy generation and consumption costs, decreased carbon emissions, and higher life expectancy. However, the integration of some of the most popular RES, such as solar and wind energy, into the grid is challenging mainly because of their dependence on weather conditions such as cloud cover and wind speed, respectively. Recently, several approaches have been developed for short-term energy generation forecasting to alleviate the issues related to the operation of renewables under highly uncertain conditions. Machine Learning (ML) has become the dominant solution showing a higher degree of accuracy than other conventional algorithms such as moving average and linear regression. Nevertheless, ML requires massive amounts of sensed information to extract features and learn sequential patterns to produce accurate predictions. This brings the question as to *"what is the best sensor tasking within a time horizon considering the grid operator foundational knowledge and previously acquired sensed information from the system?."*

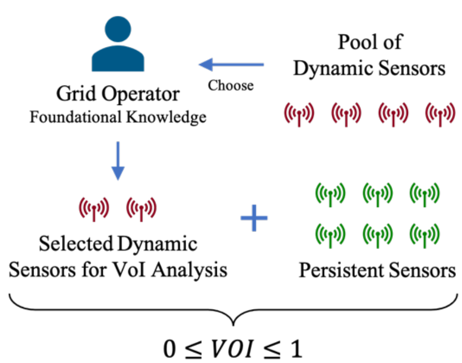

Fig. 1. The grid operator chooses from a pool of dynamic sensors that could be tasked in the future. The set of persistent and chosen dynamic sensors produces a VOI score to compare with other sensor modalities.

Intelligent systems such as microgrids task sensors and acquire data in real-time for RES energy generation forecasting through ML. However, adding or removing sensed information may be challenging due to the effect it can have on machine learning models, which can be very sensitive to such changes, compromising the grid's reliability. Under high uncertain conditions, there are opportunities to task different sets of sensors to keep or improve the accuracy of the predictions within a time horizon, even when the power system is affected by external factors. The selection of the best sensor tasking has been made by choosing sensors that contribute the most to the target variable, in this case, the power generated. Nevertheless, that approach does not incorporate grid operators' foundational knowledge, which can be detrimental to both the predictions and time-sensitive decision-making processes due to its computational complexity. To alleviate this issue, we introduce the concept of Value of Information (VoI) to measure the expected increase in utility that an ML model could obtain from considering additional sensors based on the grid operator's experience. Given a set of persistent sensors, i.e., existing or installed sensors, a VoI score can be computed for a set of dynamic sensors that a system operator could choose from to quantify the value of adding them to the set persistent sensors a specific time horizon (see Fig. 1). In this case, VoI is defined as the ML model's performance for a set of persistent and dynamic sensors for some metrics m considering the true and predicted values, which is given by

$$VoI = m(y_{true}, \hat{y}_{pred}). \quad (1)$$

The metric yields a normalized value between 0 and 1 for the convenience of comparison among different sensor modalities, and the one with the minimum VoI score is tasked for the associated time horizon. To the best of our knowledge, VoI has not been thoroughly studied in the context of power system applications, in particular, solar PV and wind energy.

This paper contributes to the field of ML by introducing VoI for the expected value of sensed information in the context of RES forecasting and a pipeline to help decision-making processes evaluate and prioritize sensor tasking. The proposed pipeline implements an algorithm for simulating the tasking of sensors considering foundational knowledge of grid operators, producing inferences utilizing several ML algorithms, including XGBoost, LightBoost, and CatBoost, and computing VoI scores. The simulation results demonstrate the effectiveness of the proposed pipeline to produce scores for different sensor modalities, allowing their evaluation, comparison, and tasking for different time horizons and seasons of the year.

LSTM-based short-term electrical load forecasting framework with improved input feature space

Abhishek Sharma
ECE Discipline (Power and Control)
PDPM-IIITDM Jabalpur, India
1812601@iiitdmj.ac.in

Sachin Kumar Jain
ECE Discipline (Power and Control)
PDPM-IIITDM Jabalpur, India
skjain@ieee.org

***Abstract*—This paper presents a Long short-term memory (LSTM) based framework for a block and an hour ahead forecasting. The lagged variables have been used as additional features, determined by studying the original series' correlogram. The lags with the highest autocorrelation have been chosen. The proposed framework has been tested on real data of different zones of the Madhya Pradesh State Load Dispatch Centre (MP-SLDC) in India. The results show that the proposed methodology outperforms the listed rival algorithms.**

***Keywords*— Deep learning, recurrent neural network, short-term load forecasting, time-series prediction.**

I. Methodology

This paper presents a methodology to forecast a 15-minute block-ahead and an hour-ahead load with several irregularities in the periodicities contained in the data. The raw historical data is first preprocessed to identify the lagged variables as the additional inputs using autocorrelation. These lagged variables help the LSTM [1] model to learn better based on the hidden representation of the input feature space, thus improving the forecasting accuracy as compared to deep RNN based method [2]-[3]. An encoder-decoder model without attention mechanism has been used to predict the four blocks for an hour-ahead forecast. Fig. 1 shows the complete flow of the data starting from preprocessing, feature engineering to prediction.

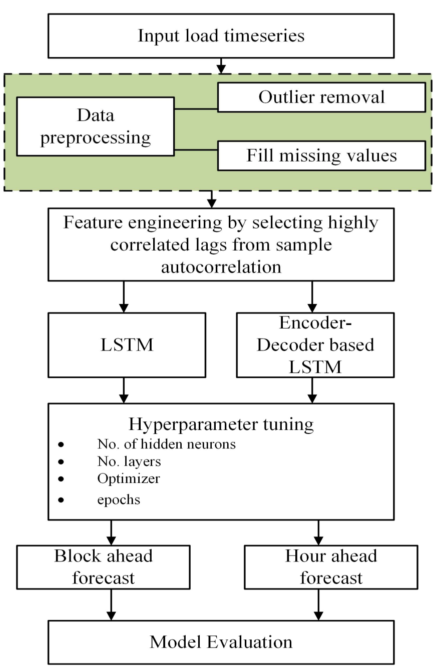

Fig. 1. Proposed methodology work-flow

II. Performance Validation and Conclusion

Three years of historical data (2017-2019) at the resolution of 15-minute block average load of three regions, viz. East, Central, and West of MP-SLDC have been used for the training and testing purpose. Performance of the proposed approach has been evaluated on the next four month's data for each zone separately. Root mean squared error (RMSE) and mean absolute percentage error (MAPE) has been considered as the performance parameters. The proposed method captures the patterns present in load data and maps it to a hidden space, which results in improved performance. Table I shows the forecasting accuracy for an-hour ahead model. The proposed methodology reports the lowest MAPE as compared to four other competitive techniques and performs consistently as the best among them.

TABLE I. Hour Ahead Forecast Summary

Zone	Metric	LSVM	QSVM	GPR	LSTM	Proposed
East Zone	Avg. RMSE (MW)	587.51	480.69	197.25	201.35	**70.36**
	Avg. MAPE (%)	10.21	10.11	6.22	4.84	**2.28**
Central Zone	Avg. RMSE (MW)	561.3	520.14	185.26	120.33	**72.78**
	Avg. MAPE (%)	13.64	9.35	5.49	4.80	**2.01**
West Zone	Avg. RMSE (MW)	611.08	499.14	210.97	172.49	**67.26**
	Avg. MAPE (%)	14.55	11.23	4.97	3.89	**1.87**

III. Conclusion

This paper evaluates the use of LSTM architecture with lagged variables as additional inputs. The lagged variables improve the LSTM model's learning, and the proposed method performs the best among LR (Linear Regression), LSVM (Linear Support Vector Machine), QSVM (Quadratic SVM) and exponential GPR (Gaussian process regression). This work can be extended to forecast a day-ahead load.

IV. References

[1] S. Hochreiter and J. Schmidhuber, "Long Short-Term Memory," *Neural Comput.*, vol. 9, no. 8, pp. 1735–1780, Nov. 1997.

[2] K. Chen, K. Chen, Q. Wang, Z. He, J. Hu, and J. He, "Short-Term Load Forecasting with Deep Residual Networks," *IEEE Trans. Smart Grid*, vol. 10, no. 4, pp. 3943–3952, Jul. 2019, doi: 10.1109/TSG.2018.2844307.

[3] S. Smyl, "A hybrid method of exponential smoothing and recurrent neural networks for time series forecasting," *Int. J. Forecast.*, vol. 36, no. 1, pp. 75–85, Jan. 2020, doi: 10.1016/j.ijforecast.2019.03.017.

Hierarchical Multi-timescale Framework for Operation of Dynamic Community Microgrid

Ashwin Shirsat, Valliappan Muthukaruppan, Rongxing Hu, Ning Lu, Mesut Baran, David Lubkeman, Wenyuan Tang

Department of Electrical and Computer Engineering

North Carolina State University

Raleigh, NC 27695, USA

{ashirsa, vmuthuk2, rhu5, nlu2, baran, dllubkem, wtang8}@ncsu.edu

***Abstract*—Distribution system integrated community microgrids (CMGs) can restore loads during extended outages. The CMG is challenged with limited resource availability, absence of a robust grid-support, and demand-supply uncertainty. To address these challenges, this paper proposes a three-stage hierarchical multi-timescale framework for scheduling and real-time (RT) dispatch of CMGs. The CMG's ability to dynamically expand its boundary to support the neighboring grid sections is also considered. The first stage solves a stochastic day-ahead (DA) scheduling problem to obtain referral plans for optimal resource rationing. The intermediate near real-time scheduling stage updates the DA schedule closer to the dispatch time, followed by the RT dispatch stage. The proposed methodology is validated via numerical simulations on a modified IEEE 123-bus system, which shows superior performance in terms of RT load supplied under different forecast error cases, outage duration scenarios, and against the traditionally used two-stage approach.**

I. Introduction

The distribution grid resiliency needs to be enhanced to withstand, operate, and recover from disruptions caused by extreme events such as hurricanes and wildfires. Post outage, a resilient grid uses modern automation techniques, algorithms, and information-communication technology to restore loads. Conventional system restoration strategies use the upstream transmission system along with distribution network reconfiguration post outage. However, such strategies are not effective at times when extreme events disrupt the transmission grid. To address this challenge, community microgrids (CMGs) have proved to be very promising. During such extended outages, the CMGs can operate in an islanded manner and ensure continued operation for its local loads. Further, they can also supply some part of the distribution grid by expanding their boundary to accommodate the neighboring nodes.

The existing literature covers various aspects of MG energy management. However, a holistic approach for proactive scheduling and dispatch of MGs during emergencies emphasizing uncertainty mitigation, critical load priority, optimal resource allocation for self-sustained extended duration operation, and MG support expansion to the neighboring grid has not been clearly addressed. The existing literature's operational objective emphasizes on cost minimization, which takes a lower priority during emergencies.

To address the above limitations, the contributions of our paper are summarized as follows:

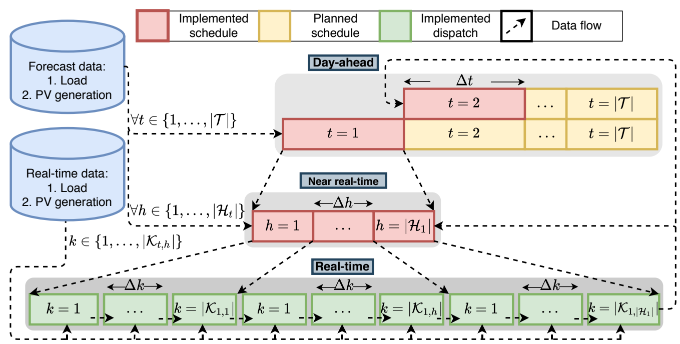

Fig. 1. Schematic layout of the proposed HMTS framework.

1) A three-stage hierarchical multi-timescale (HMTS) model, as shown in Fig. 1, for proactive scheduling and RT dispatch of a CMG having a high penetration of residential behind-the-meter (BTM) PV generators is proposed.
2) A CMG with dynamic boundary is considered, i.e., the CMG can dynamically expand its boundary to support neighboring system nodes. To incorporate this in the scheduling stage, a modified set of constraints is proposed to optimally decide the CMG boundary expansion.
3) The objectives of the proposed approach is focused on optimal resource allocation to ensure resource availability at all times, mitigate the impact of forecasting errors, prioritize service to critical loads, and provide reliable grid-forming support.

II. Results

Table I shows the critical (CL) and non-critical (NCL) load supplied under different forecast error cases using the proposed HMTS and the conventionally used two-stage approach. The results demonstrate the superiority of the HMTS approach.

TABLE I

Percent Load Supplied

Case	Base	A	B	C	D	E	F
	HMTS						
CL (%)	100	99.80	99.73	100	98.26	100	99.83
NCL (%)	69.58	49.61	33.72	98.13	37.49	97.71	80.58
	Two-stage						
CL (%)	95.36	91.17	79.21	100	79.21	100	98.32
NCL (%)	43.71	39.61	28.45	52.91	28.45	52.91	45.81

Partitioned Dynamic Modeling of Inverter with Grid Support Functions

Sunil Subedi†, *Graduate Student Member, IEEE* and Timothy M. Hansen, *Senior Member, IEEE*
South Dakota State University, Brookings, South Dakota, USA
Email: †sunil.subedi@jacks.sdstate.edu

***Abstract*—With the advancement in technology and standards, traditional converters are being replaced with new smart grid support functions (GSFs) IEEE 1847-2018 standard converter to support voltage and frequency control. Power system dynamics vary with different modes of operation and thus, new modeling methods are required for proper system planning, operation, and dispatch. This work presents a data-driven approach for partitioned dynamic modeling of inverters to speed up simulation and reduce computational complexity within acceptable accuracy. We tested and validated the proposed method for voltage support (Volt-var/watt) on a two-bus system considering dynamic loads on the residential home.**

I. Introduction

The modern power system is experiencing a rapid increase in the integration of inverter-based distributed energy resources like photovoltaic (PV) and wind. These converters incorporate grid support functions (GSFs) to support the voltage and frequency of the grid. However, these GSFs introduce stochastic dynamics and non-linearity, which becomes a major challenge in power system stability and control. Deriving detailed dynamics becomes challenging and computationally expensive as underlying models changes in size with proprietary. A generic, scalable, and robust framework is required to speed up the dynamic simulation of converter-based power systems by matching the appropriate level of complexity.

II. Proposed Model

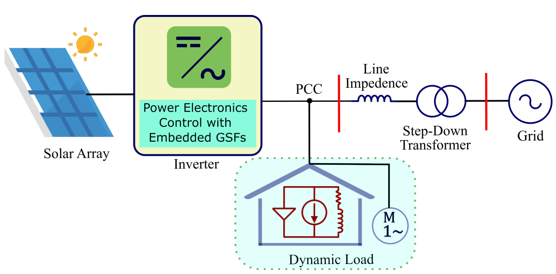

Fig. 1: Simulation setup with GSFs inverter and dynamic load.

A two-bus single house simulation model is created based on a 12-house benchmark model [1]. Inverter with GSFs is connected in a residential home with ZIP-load [2] and dynamic induction motor. A dynamic load profile is then generated from the simulation using load data from queue model [2]. A data-driven approach is applied utilizing the root mean square (RMS) voltage as input and RMS current as output to obtain the transfer function (tf) models.

III. Key Figures

Non-linear modes of operation (e.g., Volt-var/watt) cannot be accurately represented by a single linearized tf model. Thus,

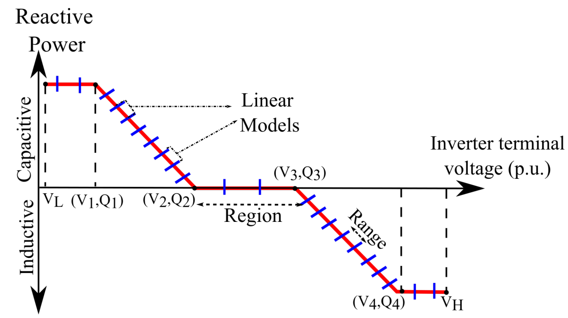

Fig. 2: Partitioning non-linear inverter's mode of operation into several smaller voltage range and developing linear tf models for these different range.

the modes of operations are divided into several ranges based on voltage magnitude. First, a step signal with a divided range of magnitude is used to train the models and the best model for the range is selected. Multiple linear tf models developed are then finally aggregated by switching between these models to capture overall dynamics. Fig. 2 shows the droop curve of volt-var mode operating at different regions and ranges.

IV. Key Results

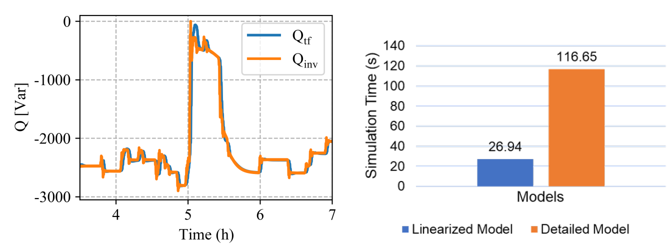

Fig. 3: a) Verification of reactive power and b) Speed comparison of the aggregated linearized model and the actual inverter model.

The generated load profile is used to compare the accuracy and speed of the detailed and linearized inverter model. Fig. 3 shows that the aggregated linearized model was a faster, computationally tractable, and good approximation for the detail system dynamics.

References

[1] R. Tonkoski, D. Turcotte, and T. H. M. EL-Fouly, "Impact of high PV penetration on voltage profiles in residential neighborhoods," *IEEE Transactions on Sustainable Energy*, vol. 3, no. 3, pp. 518–527, 2012.

[2] F. B. dos Reis, K. Duwadi, R. Fourney, R. Tonkoski, T. M. Hansen, M. A. I. Khan, and S. Paudyal, "Impact of residential load models for overvoltage prevention studies in PV-rich LV grids," in *2019 IEEE Milan PowerTech*, 2019, pp. 1–6.

Cyberattack Resilient Control of Microgrids Equipped with Renewable Energy

Tambiara Tabassum
Florida Polytechnic University
Email: ttabassum9993@floridapoly.edu

Dr. Mohammad Reza Khalghani
Member, IEEE
Florida Polytechnic University
Email: mkhalghani@floridapoly.edu

Dr. Onur Toker
Florida Polytechnic University
Email: otoker@floridapoly.edu

***Abstract*—The microgrid is a small power grid in which distributed generation (DG) units and renewable energy sources (RES) serve as the microgrid's prime mover. Microgrids are capable of providing smart and efficient charging and discharging of electric vehicles. Because of the volatile nature of DG systems, electric vehicles, and grid load, there is a considerable amount of uncertainty with the endless scopes of renewable energy integrated microgrids. These irregularities can impose an immeasurable effect on grid performance and can make the system even unstable. Therefore, communication networks and cyber interfaces are inserted into modern grids to increase their reliability, efficiency, and controllability. These cyber-physical grids are vulnerable to cyber disruptions that can degrade the system's performance and stability. It is critical that these natural grid uncertainties and cyber disturbances are detected and their adverse effects are mitigated. In this abstract, a secondary feedback control approach is proposed to address both of these unwanted entities.**

***Index Terms*—Microgrid, Uncertainties, Cyber Disruptions, Robust stability, Time-varying uncertainty, Optimal Control, Linear matrix inequality (LMI).**

I. Introduction

Smart grids are critical to the green energy revolutions success. They use a variety of technical advancements, such as edge cloud computing and artificial intelligence (AI), as well as sensors and smart meters, to better incorporate the growing amount of decentralized and intermittent renewable energy flows.

Growing the share of green energy in the modern grids, as well as retaining customer satisfaction would be impossible without the versatility of smart energy technology. The grids digitization, combined with renewable energy infrastructure including solar and wind farms, would help to improve the efficiency, controllability, and protection of vital and strategic assets while also increasing reliability and resilience..

The greater the integration of connected Internet of Things (IoT) technology into the energy network, however, the greater the possibility of cyber attacks. Fast data exchange are required to move through highly integrated communication networks, which are often enabled by a combination of modern and legacy infrastructure, will expose smart grids to vulnerabilities, necessitating the urgent need for resilient and efficient control strategy.

Cyber attacks on modern grids can take a variety of forms. A denial-of-service attack, for example, may involve an attacker hacking into grids and blocking staff access while gaining power. False data can be injected into information flows, creating a false narrative of events resulting in bad decisions.

The aim of load frequency control (LFC) is to keep the microgrids power balance such that the frequency deviations from its nominal value within prescribed bounds. The most basic control technique includes primary, secondary and tertiary control. Secondary control, which is this abstracts focus, compensates frequency deviations after incorporating primary control. Secondary control acts as supervisory control and needs cyber interfaces and measurements. The microgrid is vulnerable to all forms of cyber intrusions because of the cyber-interface embedded in secondary control. Hence we need to design a resilient approach for secondary control of microgrids. We will design a resilient controller for microgrids that operates based on robust control theory.

Event Identification Framework Based on Modal Analysis of Phasor Measurement Unit Data

Nima T.Bazargani, Gautam Dasarathy, Oliver Kosut, and Lalitha Sankar
School of Electrical, Computer and Energy Engineering
Arizona State University
Tempe, AZ 85287

***Abstract*—Considering the importance of real-time identification of power system events, we propose a novel machine learning framework for event identification by characterizing event signatures based on their modal information that can be directly extracted from phasor measurement units (PMUs). Combining such physics-based feature extraction methods with machine learning methods to distinguish between feature patterns to identify different events is the key focus of this study. The key challenges in this context are understanding if there are specific underlying patterns and set of features that can help identify an event. Moreover, using various measurements obtained from multiple PMUs to extract features will result in the high-dimensionality problem which may greatly degrade the performance of many machine learning algorithms. Hence, various filter methods for feature selection are implemented in order to choose the best subset of features. Then, the performance of two well known classifiers - support vector machine with radial basis function (RBF) kernels and logistic regression - are compared based on the low-dimensional feature space. Finally, we used a bootstrap re-sampling technique for a fair evaluation of each model accuracy. The performance of the proposed framework is tested on real PMU data collected from nearly 500 PMU.**

I. Introduction

Electric power systems are prone to a variety of events such as line trips and generation loss that can potentially limit grid resilience. Real-time identification of such events using observed patterns in measurement data is crucial to take suitable control actions and ensure reliability. However, power systems are inherently nonlinear with complex spatial-temporal dependencies; as a result, in many cases, it is not possible to develop accurate and sufficiently low order dynamical models that can be used to identify each distinct event. This has made real time identification of these events a challenging task.

The aim of this study is to identify various types of events, such as line trip and generation loss, by extracting relevant features from PMU data based on the domain knowledge. Specifically, we assume that the PMU data streams after an event consists of a superposition of several dynamic modes — thus, the features will be the frequency and damping ratio of these modes, as well as the residual coefficients indicating the quantity of each mode present in each data stream. Considering robustness of matrix pencil method (MPM) against noise compared with other modal analysis techniques (i.e. Prony's method [1]), this method is used as the main tool for modal analysis. The overview of our proposed framework is shown in Fig. 1. After extracting features from PMU data streams via mode decomposition, the next step is to select which of these features are the most relevant. This step is necessary for two main reasons: limited number of labeled historical events and relatively large number of features which can be obtained from modal analysis. To reduce features to a more manageable number, we consider various filter methods for feature selection. Due to the limited number of historical events and to avoid overfitting problem, we will rely on a well-known approach in machine learning: bootstrapping: this is a technique of sampling with replacement to create multiple datasets from the original dataset thereby attempting to learn many noisy models that can then be averaged in a meaningful manner. The performance of our proposed framework is tested on the real dataset obtained from 70 labeled events over three year of PMU data. Our simulation results indicate that our framework is promising for identifying generation loss and line trip events. Simulation results in terms of average area under curve of receiver operator characteristic are shown in Table I. F, S, M, P, and K are various measures for feature selection and represent F-test, sure independence screening, mutual information, Pearson and Kendall correlation, respectively.

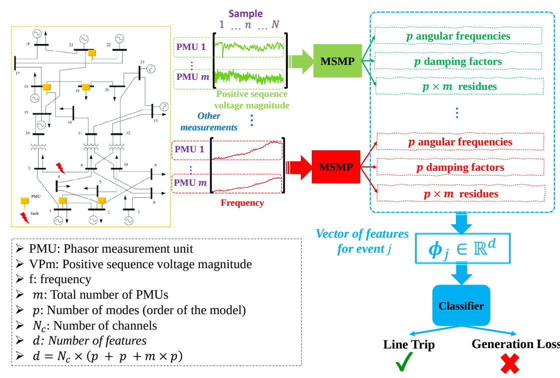

Fig. 1. Overview of the proposed event identification framework

TABLE I
PERFORMANCE OF EACH CLASSIFIER

	Filter Method				
	F	S	M	P	K
Logistic regression	0.98	0.93	0.92	0.9	0.88
SVM with RBF kernel	0.96	0.94	0.91	0.92	0.85

References

[1] L. L. Grant and M. L. Crow, "Comparison of matrix pencil and prony methods for power system modal analysis of noisy signals," in *2011 North American Power Symposium*, 2011, pp. 1–7.

Reliability Analysis of the Control and Automation Systems in Electrical Substations

João Tarquínio, Andrés A. Zúñiga and Paulo José da Costa Branco
Department of Electrical and Computer Enginering,
Instituto Superior Técnico, University of Lisbon
Lisbon, Portugal
Email: joao.tarquinio@tecnico.ulisboa.pt, andres.zuniga@tecnico.ulisboa.pt, pbranco@tecnico.ulisboa.pt

***Abstract* — This work shows a detailed reliability analysis of the control, automation and communication equipment in an IEC61850 based digital electrical substation considering four different communication architectures. The method used to perform the substation's availability analysis consists in a Markov-Monte Carlo algorithm. Moreover, a quantitative benefit–cost analysis throughout the substation's life cycle is conducted to conclude about the economic feasibility of each architecture, allowing more objective decisions to be taken when considering the reliability requirements for electric power distribution systems.**

Keywords— Substation Automation Systems, Reliability, Markov Chain, Monte Carlo simulation, IEC61850.

I. Introduction

In the context of smart grids, the increase in complexity, growing demand and requirement for greater grid reliability, security and efficiency continue to highlight the need to implement Substation Automation Systems (SAS) [1]. These systems provide automation functions for monitoring, protection and control within substations. Requirements for better electricity availability and the evolution of the electric generation are the most significant factors for the progress of substation automation, increasing the responsibility from electricity distribution companies to offer better electricity quality. This implies a deeper study on the reliability of control and automation equipment, as well as an economic evaluation of its implementation in conventional substations.

The application of the IEC-61850 in SAS brings significant changes to its monitoring, communication, control and protection systems, providing more flexibility and a better performance of SAS architectures [2]. The main objective of this standard is to facilitate interoperability, enabling logical configuration of the SAS by connecting various types of equipment from different manufacturers or different generations through a Local Area Network (LAN) [3].

II. Reliability Analysis

In this work, an electrical substation supplying four equivalent loads is given as an example. The Markov Chain representation of the substation is shown in Fig. 1 and considers four operational states corresponding to the number of loads supplied by the substation. The states' description is as follows: (1) S1 – all loads supplied, (2) S2 – 3 loads supplied, (3) S3 – 2 loads supplied, and (4) S4 – no loads supplied.

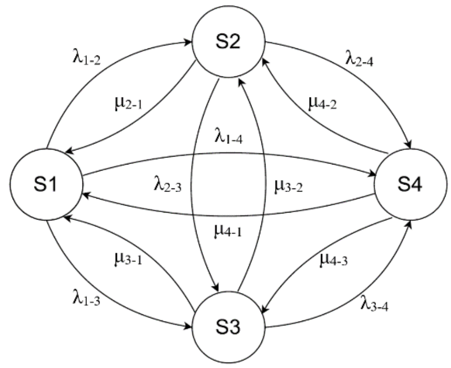

Fig. 1. Markov Chain of the substation.

In order to compute the transition rates (λ and μ) between states, a reliability block diagram (RBD) was developed for each faulty state. The RBDs only consider circuit breaker (CB) failures, assuming that CBs have only two possible operational failures: (1) miss operation, and (2) fail to operate. Since it is intended to evaluate the impact of SAS equipment in digital substations, a detailed analysis of their numerous failure causes was performed for all equipment considered, attributing an occurrence probability to each failure cause. Then, all failures causes were assumed as a possible trigger for one of the two CB failures considered. Thus, it was possible to associate SAS equipment failure to the substation's states, which impact depends on the communication architecture used to connect all SAS equipment. In order to simulate the behaviour of this components throughout the substation's life cycle, and hence computing its availability, the Monte Carlo simulation method was used, allowing the algorithm to behave as most as possible to a real substation in operation.

Additionally, the communication architectures considered for the SAS were compared in terms of their initial investment, preventive maintenance, corrective maintenance and penalties for energy not supplied considering the regulatory framework. The preventive maintenance frequency for each equipment is established according to an importance measure, which indicates how critical the failure of the equipment is to the substation's proper operation. Results show that as redundancy in communication links and equipment increases with each architecture, the greater the substation's availability. Similarly, despite the increase in investment, the overall expenses throughout the substation's life cycle are compensated, as indicated by the net present value (NPV) and the internal rate of return (IRR).

References

[1] K. Moslehi and R. Kumar, Smart Grid - A Reliability Perspective. IEEE Transactions on Smart Grid, 1(1), 57–64. https://doi.org/10.1109/TSG.2010.2046346, 2010.

[2] N. Liu, M. Panteli, and P. A. Crossley, Reliability evaluation of a substation automation system communication network based on IEC 61850. 12th IET International Conference on Developments in Power System Protection, DPSP 2014, 1–6., 2014.

[3] S. Roostaee, S. Mehfuz, and M. S. Thomas, Reliability Comparisson of Various Power Substation Automation based on IEC61850. International Journal Series Engineering Science, 3, 15–26., 20

Stakeholder Decision Tool for University Campus Microgrid with Solar Farm Integration

Patrick Wilk [#1], Christopher Contos[#1], Dr. Jie Li [#1]

[#1]*Electrical & Computer Engineering, Rowan University*

[1] wilkp0@students.rowan.edu

Abstract—**This study involves the development of a stakeholder decision tool for assessing the technical feasibility and financial viability of upgrading a university's power system into a campus microgrid. The novel approach uses quantitative engineering and economic modelling to evaluate the performance of various system designs and business models. Simulation results show that with a proposed photovoltaic (PV) farm and existing combined heating and power generators, the university can supply its critical loads in islanded mode and yield financial benefits while grid connected. In addition to the long-term performance feasibility, an hourly economic dispatch (ED) model was developed to identify the optimal day-to-day campus energy source configuration with minimized overall utility cost and emissions. The onsite generators, building loads, feeder ratings, simulated PV farm, as well as the campus grid were modelled in MATLAB for power flow analyses. A LabVIEW user-interface was developed to provide stakeholders with a visualization tool that displays essential system information for decision making.**

I. Methodology

A. PV Farm Planning and Integration

The purpose of executing the solar PV farm planning and integration analysis was to provide administration with quantitative results for making data-driven decisions.

1) PV Farm Planning

The PV farm planning accounts for the capital costs of solar construction, recurring costs for operations and maintenance, as well as revenue from federal and state renewable incentives and a power purchase agreement (PPA) with a local utility. The lifetime of the solar farm was assumed to be a conservative 15 years, aligning with the limitations on the NJ Transition Renewable Energy Credits program. For the financial modelling, a PPA was assumed as the means for selling electric energy generated by the PV farm back to the utility grid. The highest net profit of $36,654,564.60 USD was achieved using a loan term of 10 years and annual interest rate of 2.5%.

2) PV Farm Integration into Campus Microgrid

The PV farm was integrated into the campus microgrid model through net metering. That is, electricity generated by the PV farm is used to compensate for the university energy consumption, with surplus fed back to the grid. This process can be summarized as earning energy credit, at an assumed $0.05 per kWh, with the local utility company. Using fiscal year 2019 historical energy consumption data, the Campus's annual utility cost $5,081,206.45 could be reduced by $1,244,339.20.

B. Economic Dispatch of Campus Central Utility Plant

The ED provides campus microgrid operators insight to the optimal day-to-day configuration of campus energy sources. Historical utility electricity cost and campus load curves were used to optimize the coordination between the university's Central Utility Plant (CUP) assets and the electric energy purchased from the local utility grid. The CUP consists of two combined heat and power generators and 3 boilers, in addition to the modelled PV farm. The ED problem coordinated the supply of electric and thermal energy generation to meet all campus demands while minimizing the campus utility cost and CO_2 emissions. Simulation results showed that most of the solar production is during the utility on-peak hours, therefore effectively flattening the campus electric load curve and decreasing electric energy purchased from the utility resulting in reduced campus utility costs and energy-related emissions.

II. Key Results

Observing a typical day in October 2019, compared to the current normal campus CUP operation, the ED model decreased the total cost by 24.21%, as shown in Table I.

TABLE I. COST COMPARISON

Cost Comparison	Emission Cost	CUP Fuel Cost	Utility Grid Cost	Total Cost
Retrospective	$11,704.88	$5,229.02	$5,536.91	$22,470.81
ED Simulated	$8,957.80	$6,919.73	$1,152.59	$17,030.12

LabVIEW was used to visualize the campus microgrid's ED and power flow results, allowing user interaction with the microgrid in both grid-connected and islanded modes. The proposed campus microgrid system design and business models suggest engineering and economic viability of upgrading the university's power system into a campus microgrid.

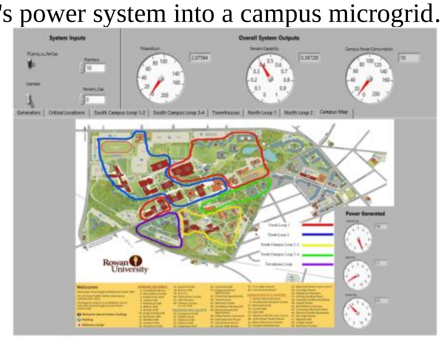

Fig. 1. LabVIEW Microgrid Panel Design

Voltage Control for Three-phase Battery Inverter Connected to Unbalanced Distribution Networks

Bei Xu, Victor Paduani, Ning Lu
Department of Electrical and Computer Engineering
North Carolina State University, Raleigh, NC
{bxu8, vdaldeg, nlu2}@ncsu.edu

***Abstract*—This poster presents a control strategy for three-phase battery-inverters connected to distribution grids operating under unbalanced load conditions. The method achieves balanced three-phase output voltages by compensating the voltage distortions resulted from negative sequence currents with a controller in the stationary reference frame. Moreover, a grounding transformer is used to filter the zero sequence current caused by single-phase unbalanced loads, which can further assist the inverter control strategy when dealing with very unbalanced load conditions. Simulation results reveal that the proposed control strategy can meet grid standards for maximum voltage unbalance under most unbalanced load conditions.**

***Index Terms*—Three-phase battery inverter, grounding transformer, unbalanced load, voltage control.**

I. Introduction

Due to the growing trend in the integration of battery-energy-storage systems (BESS) to distribution grids, superb grid-support functionalities are developed for three-phase inverters. When a BESS operates in grid-forming mode to regulate voltage and frequency, it may present serious power quality issues due to unbalanced loads. That is because unbalanced three-phase currents result in unbalanced voltage conditions due to the non-zero output impedance of inverters. Thus, to achieve balanced three-phase voltages in grids operating under unbalanced loads, here we present a strategy for maintaining maximum voltage unbalance within grid standards (3%).

II. Key Technologies and Results

The common structure of a three-phase battery inverter is shown in Fig. 1. It consists of a three half-bridge, an LC filter, and a Δ-Yg (or Y-Yg) isolation transformer. According to the superimpose theorem, the unsymmetrical output voltage, (V_{PCC}), in unbalanced operations, is the sum of response when positive, negative, and zero sequence currents are applied to the inverter, respectively. By filtering the zero sequence current component using a grounding transformer, the control system of the inverter only needs to compensate for the unbalances caused by the negative sequence current. Thus, a grounding transformer is connected to its output so that the zero sequence voltage can be reduced.

A droop-based hierarchical control structure was adopted for the battery inverter as shown in Fig. 2. In order to realize negative sequence component regulation, the inner current and voltage control loop should be based on the stationary reference frame ($\alpha\beta$-axis) instead of the synchronous reference

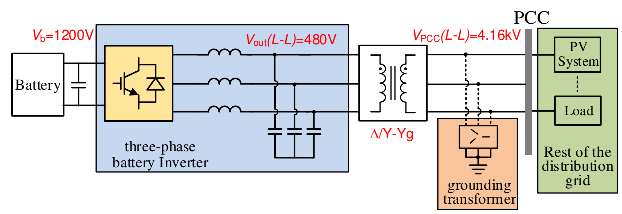

Fig. 1: The generic topology of the three-phase battery inverter.

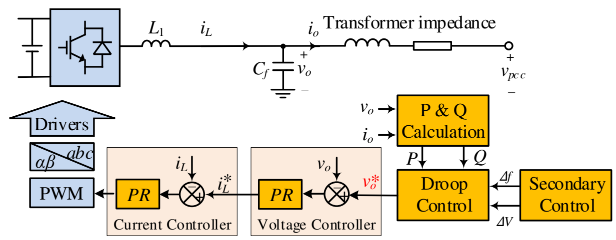

Fig. 2: Control diagram for the three-phase inverter.

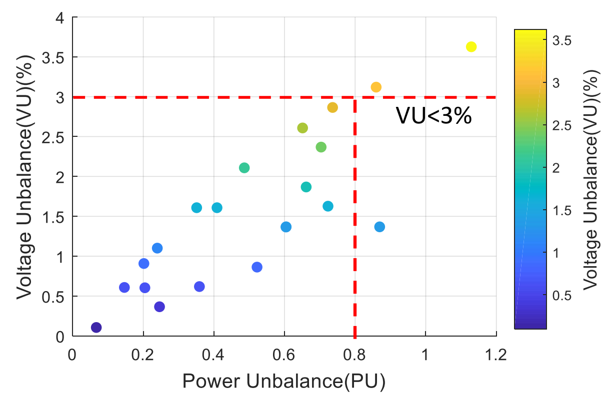

Fig. 3: Voltage regulation capability of the three-phase inverter.

frame (dq-axis). This is because the positive sequence component in dq coordinates is a DC value, while the negative sequence component is an AC value with twice the grid's nominal frequency (120 Hz), which cannot be controlled via PI controllers.

An electromagnetic transient (EMT) simulation testbed of a microgrid was developed in OPAL-RT/eMEGASIM to validate the proposed strategy. Fig. 3 presents the relationship between power unbalance and voltage unbalance factor. The results show that voltage unbalance can be regulated within 3% when the power unbalance is limited within 80%, which could be satisfied in most applications.

Data-driven Global Sensitivity Analysis of Three-Phase Distribution System with PVs

Ketian Ye, Junbo Zhao, Can Huang, Nan Duan, Fei Ding, Rui Yang

***Abstract*—Global sensitivity analysis (GSA) of distribution system with respect to stochastic PV variations plays an important role in designing optimal voltage control schemes. This paper proposes a Gaussian process enabled data-driven GSA method. The key idea is to develop a surrogate model that captures the hidden global relationship between input and output and to assess the global sensitivity using Sobol indices.**

***Index Terms*—Distribution system analysis, global sensitivity analysis, Sobol indices, Gaussian process, PVs.**

I. Introduction

With the increased penetration of stochastic and uncertain solar PVs into the distribution systems, there is an emergent concern about the voltage security. Sensitivity analysis of voltage to uncertain power injections allows us to effectively quantify these effects. Sobol indices (SI) are widely used in the variance-based analysis [1]. The main idea of SI is to decompose the model into summands that satisfy the orthogonality condition. Then, the influence of the variability of the input on the model response can be conveniently quantified [1]. Note that the Monte Carlo (MC) simulations are usually used for SI calculation, which is time-consuming. To deal with the computational burden of MC-based SI calculations, reduced order model for the original one is developed. This can be achieved using the surrogate modeling techniques. This paper proposes a data-driven Gaussian process (GP) based framework for GSA of distribution system.

II. Methodology

A. Problem Statement

Let $\boldsymbol{y} = \mathcal{M}(\boldsymbol{x})$ the model with random input vector $\boldsymbol{x}$ and its response $\boldsymbol{y}$. In the three-phase distribution systems, the uncertain inputs may include PV injections and loads while the outputs are typically bus voltage magnitudes V, voltage angles θ, line power flows P_f, etc. Sensitivity analysis aims to quantify how the power flow model response is affected by each uncertain PV input and their combinations.

B. Sobol Indices

Based on the idea of decomposing the model with respect to variance, the analysis of variance (ANOVA)-representation of $\mathcal{M}(\boldsymbol{x})$ is defined as:

$$\mathcal{M}(x_1, \ldots, x_d) = \mathcal{M}_0 + \sum_{i=1}^{d} \mathcal{M}_i(x_i) + \sum_{1 \le i < j \le d} \mathcal{M}_{ij}(x_i, x_j) + \cdots + \mathcal{M}_{1,\ldots,d}(x_1, \ldots, x_d) \quad (1)$$

under the condition that $\int_0^1 \mathcal{M}_{i_1,\ldots,i_s}(x_{i_1}, \ldots, x_{i_s})\, dx_{i_k} = 0$ for $1 \le k \le s, 1 \le s \le d$. Using the orthogonality condition, the variance of model response can be decomposed in the same way: $V = \sum_{i=1}^{d} V_i + \sum_{i<j}^{d} V_{ij} + \cdots + V_{1,\ldots,d}$. Then, the Sobol indices are defined as $S_I = V_I / V$, where $I \subset \{1, \ldots, d\}$. The calculation of Sobol indices can be achieved via MC-based approach.

C. Data-Driven Surrogate Model

GP modeling assumes that the original model is an observation of a Gaussian process (GP) [2]: $\mathcal{M}_{kr}(\boldsymbol{x}) = m(\boldsymbol{x}) + Z(\boldsymbol{x}; \sigma^2, \boldsymbol{\theta})$, where $m(\boldsymbol{x}) = \boldsymbol{\beta}^T \boldsymbol{f}(\boldsymbol{x})$ represents the mean function or the trend; $Z(\boldsymbol{x}; \sigma^2, \boldsymbol{\theta})$ is a centered GP with zero mean, variance σ^2, and covariance kernel function $k(\boldsymbol{x}, \boldsymbol{x'}; \boldsymbol{\theta})$. $\boldsymbol{f}(\boldsymbol{x})$ is typically prescribed while parameters $\boldsymbol{\beta}, \sigma^2$, and $\boldsymbol{\theta}$ need to be estimated, such as via the maximum likelihood (ML) estimator.

III. Experiment Results

Numerical results are carried out on the modified IEEE 37-bus system considering PVs. The input consists of six random variables including 3 loads and 3 PVs at nodes $[731b, 733a, 735c]$ and $[731b, 733a, 735c]$, respectively. Note that a, b and c are different phases. The model-based PCE [1] and the proposed data-driven methods are compared with the benchmark that uses the MC simulations. The root mean square error (RMSE) is used to quantify the model and Sobol indices calculation accuracy. Fig. 1 verifies the performance of two methods and demonstrates the advantage of GP when handling noisy observations.

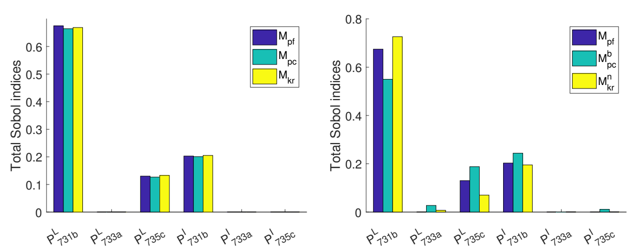

(a) Noise free observations (b) Noisy observations

Fig. 1. Sobol indices result of V_{731c} for different methods.

References

[1] F. Ni, *et al.*, "Variance-based global sensitivity analysis for power systems," *IEEE Trans. Power Syst.*, vol. 33, no. 2, pp. 1670-1682, 2018.
[2] C. Rasmussen and Christopher K. I. Williams, *Gaussian processes for machine learning*, The MIT Press, 2006.

A Distributionally Robust Optimization Approach to Unit Commitment in Microgrids

Ogun Yurdakul, Fikret Sivrikaya, and Sahin Albayrak
Department of Electrical Engineering and Computer Science
Technical University of Berlin, Berlin, Germany
Email: {yurdakul, fikret.sivrikaya, sahin.albayrak}@tu-berlin.de

***Abstract*—This paper proposes a distributionally robust unit commitment approach for microgrids under net load and electricity market price uncertainty. The key thrust of the proposed approach is to leverage the Kullback-Leibler divergence to construct an ambiguity set of probability distributions and formulate an optimization problem that minimizes the expected cost brought forth by the worst-case distribution in the ambiguity set. The proposed approach effectively exploits historical data and capitalizes on the k-means clustering algorithm—in conjunction with the soft dynamic time warping score—to form the nominal probability distribution and its associated support. A two-level decomposition method is developed to enable the efficient solution of the devised problem. We carry out representative studies and quantify the relative merits of the proposed approach vis-à-vis a stochastic optimization-based model under different divergence tolerance values.**

***Index Terms*—distributionally robust optimization, microgrids, unit commitment**

I. Introduction

The deepening penetration of variable energy resources creates a dire need for short-term planning approaches that can effectively tackle the uncertainty in net load and electricity prices. This work proposes a distributionally robust optimization (*DRO*) approach to microgrid unit commitment (*UC*) under net load and electricity market price uncertainty. Our approach effectively exploits historical observations in conjunction with machine learning models to construct scenarios, and it leverages the Kullback-Leibler (*KL*) divergence to construct an ambiguity set of probability distributions. The proposed approach eliminates the need to commit to one prespecified probability distribution and hedges optimal decisions against adopting a misrepresenting probability distribution.

II. Proposed Approach

The proposed approach comprises three key pillars, *viz.*: setting up the nominal probability distribution, constructing the ambiguity set, and working out a method based on Benders' decomposition to efficiently solve the devised *DRO* problem.

To set up the nominal probability distribution, we utilize daily historical net load and electricity market price data and leverage the k-means clustering algorithm jointly with the soft dynamic time warping score to partition the multidimensional time-series data points to multidimensional clusters. For each constructed cluster, we utilize the cluster centroid to represent a realization and assign its probability by dividing the number of data points assigned to that cluster by the total number of data points.

We next leverage the *KL* divergence to construct an ambiguity set of probability distributions around the nominal probability distribution, where we adjust the size (and, in effect, the degree of conservatism) of the ambiguity set by assigning different values for divergence tolerance. The proposed approach ensures that all probability distributions in the ambiguity set be assessed and the optimal first-stage decisions be taken based on the expected cost brought forth by the worst-case distribution. To solve the formulated *DRO* problem, we work out its tractable reformulation and put forward an algorithm based on Benders' decomposition that enables its solution by off-the-shelf solvers.

III. Representative Results

To evaluate our approach, we carried out case studies involving a microgrid with an integrated *PV* panel and diesel generator, where we used historical measurements collected in a house in New York and the locational marginal prices at the N.Y.C. bus in the New York Independent System Operator network. Some representative results from the case studies conducted are depicted in Fig. 1, which shows that the out-of-sample cost under the proposed approach (RKL − MUC) is less than or equal to that under a stochastic *UC* (SUC) approach for each divergence tolerance value. These results illustrate the relative merits of our approach and bring out the benefit of taking into account additional probability distributions other than the nominal probability distribution.

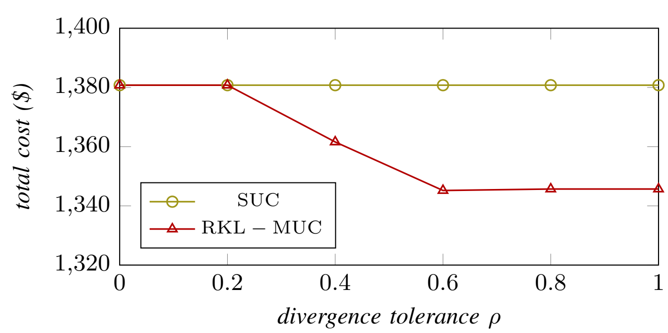

Fig. 1. Out-of-sample performances under RKL − MUC and SUC

This work was supported in part by the Research Council of Norway under the "LUCS" project, and by the German Federal Ministry for Economic Affairs and Energy under Grant 03EI6004B.

Operation of a CAES Facility Under Price Uncertainties Using Robust Optimization

1st M. F. Zambroni de Souza
Electrical and Computing Engineering
University of Waterloo
Waterloo, Canada
m6ferrei@uwaterloo.ca

2nd Kankar Bhattacharya
Electrical and Computing Engineering
University of Waterloo
Waterloo, Canada
kankar.bhattacharya@uwaterloo.ca

3rd Claudio A. Canizares
Electrical and Computing Engineering
University of Waterloo
Waterloo, Canada
ccanizar@uwaterloo.ca

***Abstract*—This study proposes a robust optimization model to maximize the profit of a price-taker Compressed Air Energy Storage (CAES) plant under price uncertainty. In order to have a more realistic representation, the thermodynamic characteristics of the CAES plant are considered. The model takes the point of view of the plant owner, determining its optimal operating schedule, while participating in the energy, spinning, and idle reserve markets. The model is tested for a CAES plant proposed in the literature, using historical data of hourly energy and reserve prices for Ontario, Canada. Different ranges of price uncertainties are considered in the robust optimization model to evaluate how they would affect the daily schedule and profit of the plant. The results are validated by a comparison with Monte Carlo simulations, demonstrating the features of the proposed model.**

***Index Terms*—Compressed Air Energy Storage (CAES), investor, modeling, price uncertainty, robust optimization.**

I. CAES Model

Large-scale Energy Storage Systems, such as CAES, present physical limitations. Thus, to ensure reliable operation and profit to the investors, self-scheduling models are developed to determine the optimum daily schedule of the plant based on the day-ahead electricity prices forecast. CAES technology presents large energy density; hence, it provides energy management services to the grid, participating in the energy, spinning and idle reserve markets. For this study, the facility is assumed to be a price-taker, and the objective function is an MILP expressed as follows:

$$\max_{P_t^X} \sum_{t}^{T} \left[f(P_t^X) - OC_t \right] \tag{1}$$

where P_t^X denotes the power dispatch, $f(P_t^X)$ the revenue and OC_t the operational cost.

A CAES plant is mainly composed of: motor, compressor, cavern to store the air, high pressure and low pressure turbines. To have an accurate representation of the CAES plant its thermodynamic characteristics are considered in the model. As the State of Charge of the plant increases, so does the pressure inside the cavern, making it harder to store more air inside, decreasing the charging Air Flow Rate (AFR), as depicted in Fig. 1(a). The efficiency of a high pressure turbine decreases when operating below its rated power. Thus, a greater AFR is necessary to generate one unit of power, and a greater AFR implies in a higher fuel rate, i.e., a higher Heat Rate, as depicted in Fig. 1(b).

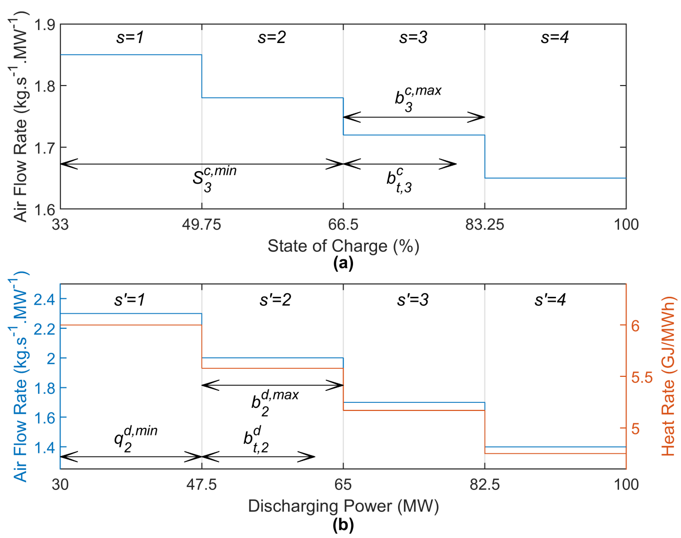

Fig. 1. (a) Charging AFR vs SOC, and (b) discharging AFR and HR vs discharging power

II. Robust Optimization

Electricity prices are subject to uncertainties. Therefore, to represent these uncertainties, Robust Optimization is employed to protect the plant against the worst case scenario. Thus, the objective function is represented as follows:

$$\max_{P_t^X} \min_{\Delta\pi_t^Y} \sum_{t}^{T} \left[f(P_t^X) - OC_t \right] \tag{2}$$

where the function is maximized in terms of the power dispatch and minimized in terms of the price uncertainty ($\Delta\pi_t^Y$).

Taking the dual of (2) the problem becomes an MILP. The main advantage of this method is that the range of uncertainty and level of conservatism in the model can be adjusted by the operator. Thus, based on a trade-off between these parameters, a set of schedules can be obtained so that the operator can choose the one that provides a reasonable profit while also ensuring a certain protection against uncertainties.

Cyber-Physical Energy Systems: The Need for Security Evaluation

Ioannis Zografopoulos, *Graduate Student Member, IEEE*, and Charalambos Konstantinou, *Senior Member, IEEE*

***Abstract*—In this work, we present a security framework for cyber-physical energy system investigations. The interconnection and dependencies between the cyber and physical counterparts of energy systems are modeled and evaluated leveraging the real-time simulation capabilities of cyber-physical testbeds. The practicality and modularity of our framework can be harnessed for studies examining diverse cyber-attack scenarios.**

***Index Terms*—Cyberattacks, security assessment, impact analysis, integrated power systems.**

I. Cyber-Security Framework Overview

Electric power systems (EPS) are a principal pillar of the critical infrastructure and thus their security is of utmost importance from a socio-economical perspective. Recently, the shift towards flexible, efficient, and distributed power system architectures leveraging information and communication technologies significantly increases the power grid's threat surface. Potential attack entry points include distributed energy resources such as solar/wind generation and/or storage systems, as well as internet connected devices, e.g., controllable loads, smart meters, IoT devices, electric vehicles, etc.

Power system cyber-security studies can identify vulnerabilities, malicious behavior, and avert or interrupt the propagation of attacks before they become system-wide threats. However, security studies require high-fidelity system models – factoring the interconnection, cyber and physical components – and computational resources to systematically evaluate the behavior of complex grid architectures (e.g., integrated transmission and distribution) under varying operational scenarios [1].

In this work, we propose a framework, which supports cyber-security investigations leveraging threat and simulation resource modeling, synergistically with simulation-aided risk assessment, performed in cyber-physical system (CPS) testbed real-time environments [2]. An overview of the cyber-security framework and its corresponding components is illustrated in Fig. 1. The four distinct components of the described framework include, *(i)* the threat modeling methodology, *(ii)* the essential resources for the CPS simulation, *(iii)* the evaluation metrics for the system performance characterization, and *(iv)* the risk assessment for cyber-attack impact calculations.

The threat modeling methodology is comprised of the adversary and attack models. The adversary model captures the attacker characteristics such as adversarial knowledge, access resources, etc., while the attack model accounts for the details of the investigated attack, e.g., frequency, targeted asset, techniques, etc. Thus, comprehensive attack evaluation can be performed without overlooking the adversarial intentions or potential malicious attack consequences.

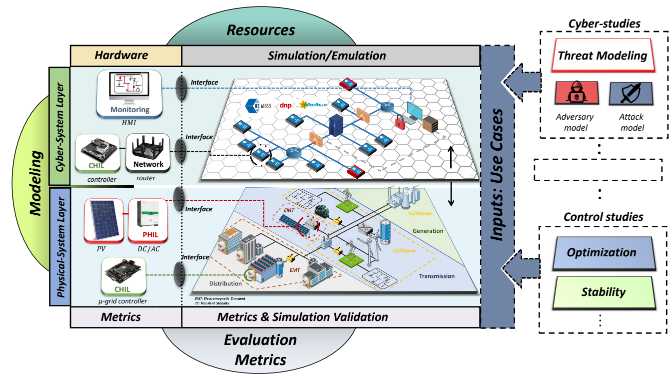

Fig. 1. Cyber-physical energy system (CPS) framework: the cyber- and physical-system layers, i.e., threat modeling, simulation resources, and evaluation metrics, needed for cyber-physical security studies.

A vital part of the framework considers the requisite resources for the modeling, simulation, and evaluation of CPS. The resources are essential for various cyber-security studies, involving the cyber, physical, or both domains, and account for the interconnections between the mentioned domains. Additionally, combined with the system modeling and simulation, the identification of evaluation metrics is leveraged to assess the system performance with respect to specific objectives (e.g., attacks, faults, frequency/voltage stability, etc.).

The risk assessment methodology integrates the adversary and attack information analyzed during the threat modeling definition. In more detail, the risk scores vary depending on the adversary capabilities, the effectiveness of an attack, the targeted system elements, and the importance of the system process that an attacker aims to compromise. As a result, different scores are evaluated (denoting the potential impact) enabling one-to-one comparisons and threat prioritization.

Our systematic cyber-security framework can pave the way for threat modeling, simulating, system performance evaluation, and impact assessment of attacks aimed at different system assets, following diverse attack paths or aiming to affect distinct system objectives. The proposed framework encourages comprehensive security analyses and can assist in developing secure end resilient future energy systems.

References

[1] I. Zografopoulos, C. Konstantinou, N. G. Tsoutsos, D. Zhu, and R. Broadwater, "Security assessment and impact analysis of cyberattacks in integrated t&d power systems," *arXiv preprint arXiv:2102.03215*, 2021.

[2] I. Zografopoulos, J. Ospina, X. Liu, and C. Konstantinou, "Cyber-physical energy systems security: Threat modeling, risk assessment, resources, metrics, and case studies," *IEEE Access*, vol. 9, pp. 29 775–29 818, 2021.